DETECTION OF FOREST MORTALITY FROM THE 2011 TEXAS DROUGHT AND EXAMINATION OF ENVIRONMENTAL DRIVERS

A Dissertation

by

ROSALEEN GRACE MARCH

Submitted to the Office of Graduate and Professional Studies of
Texas A&M University
in partial fulfillment of the requirements for the degree of

DOCTOR OF PHILOSOPHY

Chair of Committee,	Georgianne W. Moore
Co-Chair of Committee,	Robert A. Washington-Allen
Committee Members,	A. Michelle Lawing
	Charles W. Lafon
Head of Department,	Kathleen Kavanagh

May 2016

Major Subject: Ecosystem Science and Management

Copyright 2016 Rosaleen G. March

ABSTRACT

Climate change projections have predicted more frequent and severe droughts that may lead to major loss of trees and subsequent range shifts. Drought-induced tree mortality leaves both dead & live trees intermixed that remain standing rather than leaving clearings that result from acute disturbances such as fire. Thus this disturbance is difficult to detect at a regional scale, but is a harbinger of range shifts so its detection is high priority. During the summer of 2011, the southwestern US including Texas was impacted by an extreme drought. Statewide tree mortality was observed and thus provided an opportunity to test the efficacy of moderate to coarse resolution remotely-sensed indicators to detect, map and enumerate drought-induced tree mortality. Calibration models of 250-m ΔNDVI and 1-km VegDRI with 599 field data plots of tree mortality were developed to produce predictive maps. ΔNDVI, ΔPV, and NPV mortality indices were derived from 30-m Landsat 7 and compared to each other and 250-m ΔNDVI. ΔNDVI predicted tree mortality best (Khat = 0.15), with an estimate of 9% mortality that was primarily concentrated in East and Central Texas. However at 30-m resolution for East Texas, ΔPV matched the validation data best (Khat = 0.21).

Maximum entropy models were used with the field data to test the relative importance of 2011 drought conditions versus historical climate drivers of the distribution of drought-induced tree mortality. 2011 drought conditions explained 57% of the resulting model (AUC = 0.84) and bioclimate variables explained 43%. Mean annual precipitation explained 17% of tree mortality, followed by 2011 isothermality

(16%). Models were run to test the contribution of edaphic, biotic, and climatic factors toward explaining dead tree distribution, and also test of effects of scale and location (East vs. Central Texas). Climate was the highest contributor at the state scale (42%) and also in Central Texas (48%). In East Texas, edaphic factors were the major driver (47%). As drought frequency and intensity increase as predicted, a refinement of detection techniques and understanding of the drivers of tree mortality are needed to understand and predict the nature of drought consequences for forests.

ACKNOWLEDGEMENTS

First and foremost I would like to acknowledge my co-chairs, Dr. Moore and Dr. Washington-Allen for showing me how to be a researcher and scholar, and entrusting me with this research. Thanks to Dr. Moore for not only lighting my way through this journey but helping me navigate the graduate student process to completion, especially when my situation made it tricky. Thanks to Dr. Washington-Allen for seeing my potential, and for all his bright ideas that made this project unique. I would like to thank my committee, Dr. Lawing and Dr. Lafon, for their expertise and insight that was instrumental to the success of this project. Thank you to my labmates, for taking the time to look through drafts, listen to ideas, and provide helpful input.

I would like to acknowledge two fellowships: The USDA National Needs Fellowship from the US Forest Service to Texas A&M University and the Tom Slick Senior Graduate Fellowship from the College of Agriculture and Life Sciences, Texas A&M University. Also, the Texas A&M University Forest Service, College Station, TX for a research grant that supported this project. I would also like to thank Drs. Hargrove and Christie of USFS Asheville ForWarn project for access to processed eMODIS data and Karin Callahan of the National Drought Mitigation Center (NDMC) for access to VegDRI data. Lastly I would like to thank my husband Travis for his unyielding support and sacrifice that has allowed me to endeavor and succeed.

NOMENCLATURE

AVHRR	Advanced Very High Resolution Radiometer
CALMIT	Center for Advanced Land Management Information Technologies
CLASlite	Carnegie Landsat Analysis System “lite” software package
DI	Disturbance Index
EFETAC	Eastern Forest Environmental Threat Assessment Center
ETM+	Enhanced Thematic Mapper Plus
EVI	Enhanced Vegetation Index
FPAR	Fraction of Photosynthetically Active Radiation
GDI	Global Disturbance Index
LST	Land Surface Temperature
Maxent	Maximum Entropy (modeling)
MODIS	Moderate Resolution Imaging Spectroradiometer
MSS	(Landsat) Multispectral Scanner
NDMC	National Drought Mitigation Center
NDVI	Normalized Difference Vegetation Index
NIR	Near Infrared
NPP	Net Primary Productivity
NPV	Nonphotosynthetic Vegetation
NRCS	Natural Resources Conservation Service

OLI	Operational Line Imager
PDSI	Palmer Drought Severity Index
PV	Photosynthetic Vegetation
R	Red
SMA	Spectral Mixture Analysis
SSURGO	Soil Survey Geographic Database
STATSGO	State Soil Geographic Database
TFS	Texas A&M Forest Service
TIRS	Thermal Infrared system
TM	(Landsat) Thematic Mapper
VegDRI	Vegetation Drought Response Index
ΔNDVI	Normalized Difference Vegetation Index change
ΔPV	Photosynthetic Vegetation change

TABLE OF CONTENTS

Page

ABSTRACT ii

ACKNOWLEDGEMENTS iv

NOMENCLATURE v

LIST OF FIGURES ix

LIST OF TABLES xiii

1. INTRODUCTION AND LITERATURE REVIEW 1

1.1. The global trend of drought mortality 1
1.2. The 2011 Texas Drought 3
1.3. Approaches for estimating ecologic effects of drought 4
1.4. Dissertation overview 5

2. MODELLING DROUGHT-RELATED TREE MORTALITY WITH MODERATE TO LOW RESOLUTION IMAGERY 7

2.1. Introduction 7
2.2 Methods 13
2.2.1. Field data collection 13
2.2.2. Data acquisition and processing of ΔNDVI and VegDRI 15
2.2.3. Landsat ΔNDVI and ΔNPV processing 23
2.3. Results 27
2.3.1. Continuous estimation with NDVI change and VegDRI 27
2.3.2. Index-based binary classifications, sensitivity, and detection thresholds 31
2.3.3. Landsat indices 38
2.4. Discussion 43
2.5. Conclusions 47

3. THE CONTRIBUTION OF CLIMACTIC AND DROUGHT CONDITIONS TO DROUGHT-RELATED TREE MORTALITY 48

3.1. Introduction 48
3.1.1. Ecological description of Texas 48
3.1.2. Drought adaptation 53

Page

3.1.3. Species distribution models 56
3.1.4. Climatic factors and ecological niche modeling 58
3.2. Methods 62
3.2.1. Occurrence data 62
3.2.2. Bioclimate variables 62
3.2.3. 2011 variables 64
3.2.4. Analysis 65
3.3. Results 69
3.3.1. Correlation results and variables used 69
3.3.2. Bioclimate and 2011 variables modeled in isolation 70
3.3.3. Relative contributions of bioclimate and 2011 variables 71
3.4. Discussion 77

4. THE RELATIVE CONTRIBUTION OF CLIMATIC, EDAPHIC, AND BIOTIC DRIVERS TO RISK OF TREE MORTALITY FROM DROUGHT 83

4.1. Introduction 83
4.1.1. Forest density and forest type 85
4.1.2. Soils 86
4.1.3. Topography 87
4.1.4. Possible effects of scale and location 88
4.2. Methods 89
4.2.1 Data 89
4.2.2. Analysis 91
4.3. Results 94
4.3.1. Statewide models 94
4.3.2. Local models 103
4.4. Discussion 116

5. CONCLUSIONS 124

REFERENCES 128

LIST OF FIGURES

Page

Fig. 1. FIA Regions and distribution of field plot locations. 14

Fig. 2. FIA maps (Wilson et al 2012) depicting a) forest proportion and b) forest density 17

Fig. 3. Original maps of a) dNDVI and b) VegDRI 18

Fig. 4. General methods for mapping mortality with ΔNDVI and VegDRI 19

Fig. 5. Flow chart showing the location of calibration plots used to create each model, and the area of application 20

Fig. 6. Location of Landsat 7 ETM+ time series images 23

Fig. 7. Results of image gap filling on near infrared color composite 25

Fig. 8. Negative exponential regression models and scatter plots using NDVI change as an independent variable to estimate percent dead in plots within a) All Forested area, b) high density and forest proportion, c) West Texas, and d) East Texas; and e) regression model and scatter plot using VegDRI as an independent variable to estimate percent dead in plots within 75% forest proportion 29

Fig. 9. Predicted vs. observed plots for validation data for ΔNDVI calibration models located in a) All Forest, b) high density forest, c) West Texas, and d) East Texas; and e)VegDRI in 75% forest 30

Fig. 10. a) All Forest model-based classification and b) ΔNDVI index-based classification 33

Fig. 11. Resulting maps of percent dead trees from modeling ΔNDVI with percent dead in plots within all forested area 36

Fig. 12. Resulting maps of percent dead trees from modeling ΔNDVI with percent dead in plots within high density and forest proportion 36

Fig. 13. Resulting maps of percent dead trees from modeling ΔNDVI with percent dead in plots within West Texas 37

Page

Fig. 14. Resulting maps of percent dead trees from modeling ΔNDVI with percent dead in plots within East Texas 37

Fig. 15. Resulting map of percent dead from modeling VegDRI with percent dead in plots within 75% forest proportion 38

Fig. 16. Sub-pixel unmixing results of gap-filled images for a) May 2011 and b) June 2012 39

Fig. 17. Scatter plots of Landsat-derived index values with number dead in a plot 40

Fig. 18. Comparison of forest area distribution depicted between a) FIA forest proportion (≥50%) and b) Classification of June 2012 Landat ETM+ image using fractional cover of PV and S 41

Fig. 19. Zoomed-in view of Landsat fractional cover-derived forest loss (black) overlaid on the All Forest model mortality prediction and burned areas in 2011 (light blue) 42

Fig. 20. Vegetation regions of Texas from Gould et al. (1960) 49

Fig. 21. Conceptual diagram by Anderegg et al. (2013) describing the process by which water deficit translates to plant mortality. 56

Fig. 22. The 2011 climate variables model prediction probability response of dead trees as function of 2011 precipitation when keeping other variables at average value. 72

Fig. 23. The 2011 climate variables model prediction probability response of dead trees as function of 2011 isothermality when keeping other variables at average value 73

Fig. 24. The combined model prediction probability response of dead trees as function of annual precipitation when keeping all other variables at their average value 74

Fig. 25. The combined model prediction probability response of dead trees as function of 2011 isothermality when keeping other variables at average value. 75

Fig. 26. Spatial representation of Maxent model prediction of dead tree occurrence using bioclimatic and 2011 weather conditions. 76

Page

Fig. 27. Mean predicted probability of dead tree occurrence by FIA region 77

Fig. 28. Theoretical model of the biotic, edaphic, and climatic factors affecting tree mortality. Items in boxes are indirect factors that can be measured. 84

Fig. 29. Study area: forested non-burned areas of the state and two Landsat footprints in East and Central Texas. 93

Fig. 30. AUC of test data for Maxent models created with different variables 95

Fig. 31. Percent contributions of edaphic, biotic, and climatic variables to statewide Maxent models created using varying combinations of each 96

Fig. 32. Response of dead tree probability of occurrence to AWSrz in edaphic variable model when all other variables are held constant 97

Fig. 33. Response of dead tree probability of occurrence to forest density in edaphic and biotic variables model when all other variables are held constant. 98

Fig. 34. Response of dead tree probability of occurrence to annual precipitation in the edaphic, biotic, and climatic model when all other variables are held constant. 99

Fig. 35. Mean predicted probability of dead tree occurrence by FIA region for all three models. 100

Fig. 36. Predicted probability of dead tree occurrence with Maxent model using only edaphic variables 101

Fig. 37. Predicted probability of dead tree occurrence with Maxent model using edaphic and biotic variables. 102

Fig. 38. Predicted probability of dead tree occurrence with Maxent model using edaphic, biotic, and climatic variables. 103

Fig. 39. Percent contributions of edaphic, biotic, and climatic variables to the all-inclusive statewide, Central, and East Texas Maxent models 106

Fig. 40. Central Texas response of dead tree probability of occurrence to AWSrz in edaphic variable model when all other variables are held constant. 107

Page

Fig. 41. East Texas response of dead tree probability of occurrence to AWSrz in edaphic variable model when all other variables are held constant. 108

Fig. 42. Central Texas response of dead tree probability of occurrence to forest density in edaphic and biotic variables model when all other variables are held constant 109

Fig. 43. East Texas response of dead tree probability of occurrence to forest density in edaphic and biotic variables model when all other variables are held constant. 110

Fig. 44. Central Texas response of dead tree probability of occurrence to 2011 precipitation in edaphic, biotic, and climatic variables model when all other variables are held constant. 111

Fig. 45. East Texas response of dead tree probability of occurrence to forest density in edaphic, biotic, and climatic variables model when all other variables are held constant 112

Fig. 46. Maxent-predicted probability of dead tree occurrence in Central TX (left) and East TX (right) using only edaphic variables..... 113

Fig. 47. Maxent-predicted probability of dead tree occurrence in Central TX (left) and East TX (right) using edaphic and biotic variables. 114

Fig. 48. Maxent-predicted probability of dead tree occurrence in Central TX (left) and East TX (right) using edaphic, biotic, and climatic variables. 115

Fig. 49. Mean predicted probability of dead tree occurrence in Central and East TX for all three models 116

LIST OF TABLES

Page

Table 1. Spatial data and indices used to generate models of percent dead trees 16

Table 2. Results of model-estimated percent dead and model validation. 31

Table 3. Commission and Omission errors for model-based binary classifications 31

Table 4. Index-based binary classification accuracy and sensitivity analysis.....34

Table 5. Commission and Omission errors for index-based binary classifications with 1% dead and 6.2% dead thresholds.....34

Table 6. Accuracy statistics of binary Landsat derived index-based classification, and sensitivity calculated as the average dead on the "live side" (positive NDVI & PV change or < 25% NPV) and the "dead side" (negative NDVI & PV change or ≥ 25% NPV) 41

Table 7. Commission and Omission error for Landsat-derived index classifications.....42

Table 8. Nineteen bioclimatic variables derived from the WorldClim database 63

Table 9. Correlations between the 19 bioclimactic variables.....68

Table 10. Contribution rankings of models separated by variable type 71

Table 11. An estimate of relative contributions of environmental variables to the Maxent model 74

Table 12. Difference in percent contribution between the bioclimatic variable and corresponding 2011 variable.....75

Table 13. Spatial data on environmental drivers used as inputs to the Maxent model 90

Table 14. An estimate of relative contributions of environmental variables to the statewide Maxent models.....96

Table 15. An estimate of relative contributions of environmental variables to the Maxent models in Central Texas 104

Page

Table 16. An estimate of relative contributions of environmental variables to the Maxent models in East Texas 105

1. INTRODUCTION AND LITERATURE REVIEW

Global climate change is projected to produce warmer, longer, and more frequent droughts that have the potential to trigger widespread tree die-offs (Bernstein et al. 2007; Breshears et al. 2005). These predicted changes in climate suggest droughts may become more common and/or more intense in some regions of the world (Bernstein et al. 2007). Larger and more frequent drought-related tree mortality events can alter: biogeochemical cycling (McKinley et al. 2011; Moore et al. 2016), energy balance (Royer et al. 2011), and distributions of faunal and floral species within terrestrial ecosystems (Parmesan and Yohe 2003). Indirect effects can be just as or more devastating than the drought itself. For example, insect and pathogen outbreaks can be extensive, with bark beetle outbreaks being the most important agent of tree mortality; and wildfire risk greatly increases with drought (Vose 2016). Widespread tree die-offs have been observed across the western United States and this has been attributed to an increase in mortality rates due to regional warming in the past decade and consequent decreases in water availability (Breshears et al. 2005; van Mantgem et al. 2009).

1.1. The global trend of drought mortality

Future climate change is predicted to bring increases in mean temperature (2-4 °C globally), and altered precipitation regimes which will together produce an increase frequency and severity of drought events and conditions (Bernstein et al. 2007; Sterl et al. 2008). Understanding and forecasting how these changes will impact our ecosystems

is emerging as a major challenge for global change scientists (Allen et al. 2010; Boisvenue and Running 2006; Bonan 2008). Climate change effects on forests are of particular concern due to their direct value to society (e.g. timber and watershed protection) and as habitat for much of the earth's biodiversity. Recent die-offs have raised the alarm on the vulnerability of forests to changing climate and there has been an increase in the documentation of these events that may have a loose association with the increase of warming temperatures (Allen et al. 2010). Allen et al. (2010) compiled all recent major drought-related forest mortality events from 1970 to 2010, finding 88 events in each wooded continent across multiple forest types and climatic zones.

The mechanisms of drought-related mortality can be very complex as there can be multiple abiotic and biotic factors that interact, weakening and eventually causing death of a tree. These factors depend on the environmental and climatic conditions of the mortality event and each factor can have any range of contribution both direct and indirect to the death of a tree. Ecological and landscape variables such as soils, elevation, aspect, slope, and topographic position could potentially interact with density-dependent processes such as insect outbreaks, competition, or facilitation, which creates the spatial pattern of mortality that is ultimately produced (Allen et al. 2010; Fensham and Holman 1999; Lloret et al. 2004). However, if severe enough, the drought alone can drive extensive forest mortality independent of tree density (Allen et al. 2010; Floyd et al. 2009).

Other factors that weigh heavily into the vulnerability to mortality include species and associated life-history traits and tolerances, leading to differential rates

between co-occurring species. Size and age are a factor as well, with larger and/or older having been repeatedly found to be more vulnerable to drought-induced mortality (Moore et al. 2016; Mueller et al. 2005; Nepstad et al. 2007).

A source of complication for interpreting die-off events are lagged responses, where mortality can sometimes occur years after drought stress (Bigler et al. 2007; Pedersen 1998, 1999). Also, the ability of trees to respond to stress through adaptations such as reallocation of resources, modification of root structure, or dormancy, can lead to non-linear responses to drought stress in both space and time (Allen et al. 2010; Miao et al. 2009).

1.2. The 2011 Texas Drought

In October 2010, a La Niña event occurred resulting in record low rainfall and extreme drought in Texas until September 2011. This was the driest 12-month period recorded in Texas with statewide precipitation totaling 287 mm (Hoerling et al. 2013). This dearth of precipitation coincided with record high temperatures in the summer. The mean temperature for June through August, 30.4°C, was warmer than any previous single month in the instrumental record and 2.9°C above the long term mean (Hoerling et al. 2013). The combination of conditions ranked Texas in extreme to exceptional drought from June-September 2011 (Dawson 2011; NOAA National Centers for Environmental Information 2011). Severe drought continued throughout 50% or more of Texas forests in both 2012 and into 2013. The Palmer Drought Severity Index (PDSI, Alley 1984; Palmer 1965) is a standardized meteorological drought index used to

estimate relative dryness and spans from -10 (dry) to +10 (wet). The soil moisture algorithm uses a supply-and-demand concept of the water balance equation, using local temperature and precipitation inputs as well as available water content of the soil. PDSI in Texas was a record low of -7.93 in September 2011. The next lowest was -7.80 which occurred in September 1956 (Hoerling et al. 2013). For June through August 2011, PDSI was -5.37, the lowest value for those dates since 1789 (Dawson 2011; NOAA National Centers for Environmental Information 2011) (Figure 1). This drought has resulted in the death of an initial estimated 300 million trees.

1.3. Approaches for estimating ecologic effects of drought

Metrics derived from satellite imagery, e.g. , the normalized difference vegetation index (NDVI) have been used successfully to show and quantify change in vegetation condition in different ecosystems (Washington-Allen et al. 2006). Satellite remote sensing NDVI and similar indices have been used to detect ecological disturbances such as drought, fire, and hurricanes. The enhanced vegetation index (EVI) optimizes the vegetation signal with improved sensitivity in high biomass regions and reduces the canopy background signal and atmospheric influences (Huete et al. 2002). Mildrexler et al. (2007) created a Disturbance Index (DI) that is based on MODIS-derived land surface temperature (LST) and the EVI. By detecting changes in temperature and vegetative condition, The DI provides information on large-scale ecosystem disturbances such as disturbance location, area, intensity, and recovery. Archibald et al. (2009) assessed the environmental factors that are determinants of burnt

area using satellite-derived burned area maps, correlating burn area with other remotely sensed data on environmental factors such as land cover and topographic roughness.

Remote sensing has also helped to quantify number of trees impacted by a major hurricane (Chambers et al. 2007). Moore et al. (2016) generated regional-level estimates of dead trees from the 2011 drought using ForWarn's MODIS NDVI change product, exploitingan exponential relationship found between numbers of dead in the field plots and the NDVI change value. Results from this study found that about 6.2 million trees died from 2011 to 2012. Using the same data, the current study creates a continuous (per-pixel) estimation of mortality and explores and compares different ways of calibrating a tree mortality model.

1.4. Dissertation overview

This document explores questions related to both the detection and predictability of drought-related mortality. Chapter 2 examines a suite of indices derived from moderate- to coarse- resolution imagery and tests their ability to model and determine the biogeography of tree mortality from the 2011 Texas Drought. Objectives were to 1) Determine the mortality detection threshold for each index, 2) Assess the ability of each index to estimate tree mortality relative to that of Moore et al. (2016), and 3) Compare and contrast the strengths and weaknesses of each index.

Chapter 3 examines the relative role of long-term average climate conditions (environmental states) vs. time-of-drought weather conditions in determining drought-related mortality. A species distribution modeling approach was used to accomplish this

objective and also to determine which long-term and/or immediate condition best explains mortality patterns. Lastly, chapter 4 considers edaphic, biological, and climatic variables and weighs their relative contribution to drought mortality, examining the relationship of each important driver to dead tree prediction. It also examines contribution differences between scales and locations in different climate zones. Chapter 5 presents final conclusions for the study.

2. MODELLING DROUGHT-RELATED TREE MORTALITY WITH MODERATE TO LOW RESOLUTION IMAGERY

2.1. Introduction

Over the last several hundred years, significant areas of the southwestern United States have experienced intense and, in some cases, unprecedented drought that has led to widespread tree mortality (Allen et al. 2010; Breshears et al. 2005; Swetnam and Betancourt 2010). Texas and much of the southwestern US have been in an extended drought since 2000 (Hoerling et al. 2013; Overpeck and Udall 2010). In the recorded climate history of Texas, the 2011 drought was comparable in severity only to a drought that occurred in 1789 (PDSI value of -5.37) (Dawson 2011; NOAA National Centers for Environmental Information 2011). By mid-September of 2011, 88% of the state experienced 'exceptional' conditions, with the rest experiencing 'extreme' or 'severe' drought. Widespread tree mortality was observed by the general public and led to a request from the state legislature to the Texas A&M Forest Service for an estimate of the number of trees that were dead and dying from the drought (Moore et al. 2016). Consequently, this exceptional to extreme drought provided a rare opportunity to test different remote sensing methodologies for evaluating the regional (State-level) consequences of drought induced-tree mortality.

Satellite-based remote sensing technology provides an excellent means of quantifying patches of disturbance, and can also be used to measure biophysical characteristics of vegetation that are sensitive to drought including vegetation canopy

cover, biomass (Washington-Allen et al. 2006), and net primary productivity (NPP, Running and Zhao 2015). A commonly used remote sensing-based proxy for these measurements is the normalized difference vegetation index (NDVI, Rouse Jr et al. 1974) that is approximately equal to the fraction of photosynthetically active radiation (FPAR, Running et al. 2004). NDVI is calculated from the surface reflectance of red (R) and near infra-red (NIR) radiation as:

$$NDVI = NIR - red / NIR + red$$

NDVI as indicator of vegetation sensitivity including mortality to drought was illustrated in Breshears et al. (2005) where in 2002 and 2003 areas of drought-induced mortality in piñion pine (*Pinus edulis*) were delineated in a four state region of the US southwest using 1 km^2 mean late May to June NDVI that was derived from the National Oceanic and Atmospheric Administration Advanced Very High Resolution Radiometer (NOAA AVHRR). High-resolution aerial photographs of stand-level mortality were used to verify areas of drought mortality in the satellite imagery. AVHRR data has been available since 1978, with 4 (TIROS-N) to 6 (NOAA-15, AVHRR/3) spectral bands or channels at ~1.1-km pixel resolution. AVHRR was designed as a weather sensor to specifically monitor clouds and surface temperatures. However, AVHRR sensors have been useful in other applications including the mapping and monitoring of global vegetation dynamics (e.g., Nemani et al. 2002; Pinzon and Tucker 2014) and drought dynamics using the Vegetation Drought Response Index (VegDRI, Brown et al. 2008).

VegDRI was designed to quantify the response of vegetation to drought by incorporating two AVHRR-derived observations of vegetation condition with the PDSI, the 36 week Standard Precipitation Index (SPI), climatic inputs, and other biophysical information such as land cover/land use type, soil characteristics, and ecological setting to monitor vegetation response to drought conditions (Brown et al. 2008). VegDRI maps were created by 1) processing data for eight variables across 776 weather station locations across the United States, 2) generating an empirically derived model by applying a supervised classification and regression-tree analysis to information in the database, and 3) applying the models to the geospatial data to produce a 1 km resolution map for the study area (Brown et al. 2008).

Drought-related tree mortality poses a particular challenge for remote sensing because unlike other catastrophic disturbances such as fire and hurricane damage where massive treefall or stand clearance is evident, the impacts from drought are rarely spatially discreet but rather are diffuse across a landscape as dead and dying trees remain standing. As a result, confirmatory visual detection of tree mortality requires that the spatial resolution of the image pixel be high enough to resolve individual dead tree canopies (e.g., Breshears et al. 2005). Although ideal, the acquisition of high-resolution imagery at the state and larger spatial scales is expensive and the processing and analysis of this dataset will also be time-consuming and computationally intensive making it more feasible for detection of disturbances that occur at small spatial scales. Therefore, remote sensing analysis of large-scale drought mortality must deal with a tradeoff

between the expense of data acquisition and processing, spatial resolution, spatial extent and in some cases, temporal extent and frequency.

The Moderate Resolution Imaging Spectroradiometer (MODIS) instruments aboard the Terra and Aqua satellite platforms provide global coverage with 36 spectral bands and pixel spatial resolutions of 250-m, 500-m, and 1-km. The MODIS sensor passes overhead daily, increasing the likelihood that there will be an unobscured view of an area of interest every few weeks. Daily passes also provide the ability to view within-season phenology of vegetation and therefore the ability to monitor possible disturbances making it useful for forest health monitoring (Lutz et al. 2008). Many forest assessment programs utilize MODIS products including the Eastern Forest Environmental Threat Assessment Center (EFETAC, http://www.forestthreats.org) that uses an ongoing web-based early warning monitoring system called ForWarn to detect impacts to forests from hurricanes, wildfire, insect damage, and other disturbances (Hargrove Jr et al. 2009). Mildrexler et al. (2007) used a combination of the MODIS enhanced vegetation index (EVI) and land surface temperature (LST) products to develop a continental scale disturbance index (GDI) that detects the location, spatial extent, and duration of disturbances such as fire, insect epidemics, flooding, climate change, and land use.

At finer pixel resolutions varying from 15-m panchromatic to 120-m thermal, the series of Landsat satellites and sensors from 1-5, 7 and 8 (Multispectral Scanner (MSS) Thematic Mapper (TM), Enhanced Thematic Mapper (ETM+), Operational Line Imager (OLI), and Thermal Infrared system (TIRS) have been used extensively to monitor forest disturbances (e.g., Hansen et al. 2013, Macomber and Woodcock (1994). Macomber and

Woodcock (1994) used Landsat to examine drought-related tree mortality using an unsupervised classification method. Landsat is still the primary sensor used today and improved computational algorithms and hardware computing technologies are allowing processing of decadal time series of datasets at global spatial scales. Hansen et al. (2013) quantified global forest change using parallel computing to process over 650,000 Landsat scenes from 2000 to 2012. However, the higher spatial resolution of Landsat is a tradeoff with its temporal sampling interval of every 14 to 16-days, thus reducing the likelihood of obtaining cloud-free images, whereas the daily AVHRR & MODIS overpasses offer a higher likelihood of cloud-free observations for a larger area, albeit with coarser spectral resolution.

Studies examining change detection of vegetation at regional to continental scales using coarse resolution data are less prevalent than those using fine resolutions (Coppin et al. 2004). Coarse scale products have been used to look at changes in primary productivity (Zhao and Running 2010), large natural disturbances (Tansey et al. 2004), climate-driven phenology (Moody and Johnson 2001), and deforestation (Malingreau et al. 1989; Zhan et al. 2002). These studies use diverse techniques and use multi-date differencing (Kasischke and French 1995), logistic regression, multi-temporal change vector analysis (Lambin and Strahlers 1994), decision trees (Borak and Strahler 1996) principal components analysis (Eastman and Fulk 1993; Young and Wang 2001), and hybrid methods (Zhan et al. 2000).

Another alternative for detection of diffuse drought-induced tree mortality is a sub-pixel analysis method that would be able to detect the fraction of the spectral

response that is indicative of mortality within a pixel. Sub-pixel analyses use multivariate discriminant analysis statistical techniques including principle components analysis, multiple regression, and factor analyses or some other spectral mixture analysis (SMA) technique to generate fractional components of a pixel that correspond to ground objects that are either linearly or non-linearly combined. Linear unmixing assumes that the pixel-level spectral reflectance is the linear combination of endmember spectra or fractions; however, there are a number of endmember combinations that can produce a particular spectral signal (Asner et al. 2000). To account for this variability, Asner and Lobell (2000) developed the Automated Monte Carlo Unmixing (AutoMCU) algorithm that uses an iterative random selection of endmember reflectance combinations (Asner and Lobell 2000; Bateson et al. 2000). Huang et al. (2010) correlated change in PV with field measures of above ground biomass (AGB) to examine the effects of widespread piñon-juniper mortality on carbon stocks. Similarly, Huang and Anderegg (2012) used NPV derived from SMA analysis and field measures of above ground biomass (AGB) to estimate the carbon footprint of Aspen dieback.

The fractional components within a pixel of a forested ecosystem include photosynthetic vegetation (PV), non-photosynthetic vegetation (NPV), and bare ground. SMA can detect widespread as well as diffuse disturbance impacts (McDowell et al. 2014) because it is capable of detecting sub pixel cover. However, one of the problems associated with detecting NPV is the greening up of the understory following canopy dieback that results in underestimation of tree death. This impact can be mitigated with

SMA because canopy mortality can be quantified as an increase in NPV rather than an increase in PV (Adams et al. 1995; McDowell et al. 2014).

Consequently, using the 2011 drought as our experimental backdrop, I aimed to assess the ability of three vegetation indices, NDVI, VegDRI, and NPV, that were derived from publicly available moderate (Landsat) to coarse (AVHRR and MODIS) resolution satellite technology to detect diffuse tree mortality and determine which methods are most promising for use in regional to global detection of drought mortality. Extensive tree mortality field data collected after the 2011 drought allowed the following objectives to be addressed: 1) Determine the mortality detection threshold for each index, 2) Assess the ability of each index to estimate tree mortality relative to that of Moore et al. (2016), and 3) Compare and contrast the strengths and weaknesses of each index.

2.2 Methods

2.2.1. Field data collection

The Texas A&M Forest Service conducted a statewide rapid damage assessment of tree mortality during the summer of 2012 that resulted in the collection of 599 plots distributed across 10 regions in Texas: the Panhandle, Trans Pecos, North, Central, South, Brazos Valley, Southeast East, Southwest East, Northeast East, and Northwest East (Fig. 1). Within each region, two-stage unequal probability samples with replacement were conducted (Lohr 1999). A 10 km × 10 km grid was overlaid on a forest distribution map that was prepared using techniques developed by (Wilson et al.

2012) from Forest Inventory & Analysis (FIA) datasets for Texas (Wilson et al. unpublished data) creating a list of primary sample units (PSUs) of known forest area. PSUs were then selected with a probability proportional to forest area. In each sampled PSU, seven secondary sample units (SSUs) consisting of 0.16 ha circular plots were selected at random.

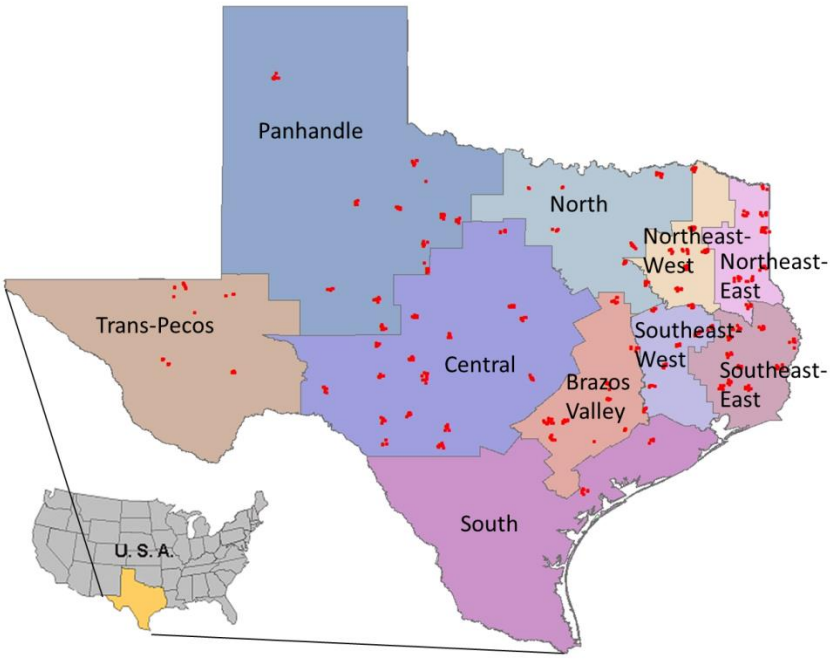

Fig. 1. FIA Regions and distribution of field plot locations.

This sampling procedure, described in Moore et al. (2015) recorded dead trees ≥12.7 cm in diameter, size (diameter), and identification to at least the genus level were recorded. Mortality from insects and disease was observed and noted, as were any other causes besides drought, if known. Because mortality from Hypoxylon canker (common

in *Quercus*) and Ips beetles (common in *Pinus*) is accelerated during drought, trees thus diagnosed were considered drought-killed. This dataset was used to both calibrate and validate the satellite remote sensing-based biophysical products used in the techniques described in this section.

2.2.2. Data acquisition and processing of ΔNDVI and VegDRI

The data sets used in this analysis are listed in Table 1. Only forested area was analyzed, which was defined using the FIA forest proportion map (Fig. 2a), creating a mask consisting of pixels with 50% or greater forest proportion. ΔNDVI data layers produced for the EFETAC ForWarn system (Hargrove Jr et al. 2009) were acquired to test its usefulness as a drought mortality index. ForWarn uses an 8-day MODIS-derived NDVI time series with a moving window that is 24 days long to increase the likelihood of a cloud- and smoke-free image. The image I analyzed was the percent change NDVI between April 30 and May 23 of 2012 (after the drought) window and the same window in 2011 (prior to the onset of acute mortality) (Fig. 3a). The growing season was selected in order to have leaf-out images to make tree death apparent in the forest area.

VegDRI was obtained from the National Drought Mitigation Center (NDMC) in the Center for Advanced Land Management Technologies (CALMIT) at the University of Nebraska-Lincoln. The image date analyzed was August 27, 2011 (Fig. 3b) because it coincided with the peak of the drought. Important components of the VegDRI index are the atmospheric drought indices, which are captured in real time during the drought

event itself. This image date best captured immediate tree mortality because it was taken within the growing season when deciduous trees should not have been dormant.

Table 1
Spatial data and indices used to generate models of percent dead trees.

Data	Units	Resolution (m)	Satellite	Source/attributes
Forest density	live trees > 5 in. DBH acre^{-1}	250	MODIS	FIA (Wilson et al 2012)
Forest proportion	Fraction forest per pixel	250	MODIS	FIA (Wilson et al 2012)
NPV and PV	% non photosynthetic vegetation and % Photosynthetic vegetation	30	Landsat	USGS Earth Explorer. Index derived from Landsat 7 TM using ClasLite (Asner et al 2009)
ΔNDVI	% change in NDVI from 2012 to 2011	232	MODIS	EFETAC ForWarn (Hargrove et al 2009)
	change in NDVI from 2011 to 2012	30	Landsat	USGS Earth Explorer. Index derived from Landsat 7 TM
VegDRI	model-derived index describing vegetative drought condition	1000	AVHRR	NDMC CALMIT at UN-Lincoln (Brown et al 2008)

The FIA density dataset (Fig. 2b) was used to account for live trees prior to the drought, which allowed the determination of the percent dead in each plot. Plot level estimates were then used to develop the best-fit model of percent mortality for each index, and this relationship was used to estimate continuous tree mortality throughout the state (Fig. 4). The total number of calibration plots differed for each because some plots fell within pixels with index values that were out of normal range. In each case, thirty percent of the plots were withheld for model validation.

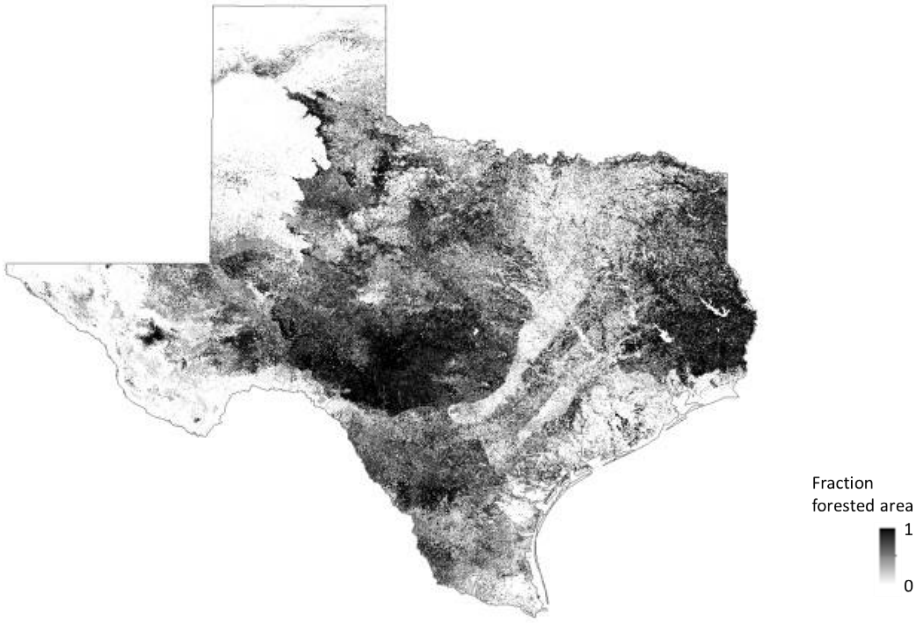

a.

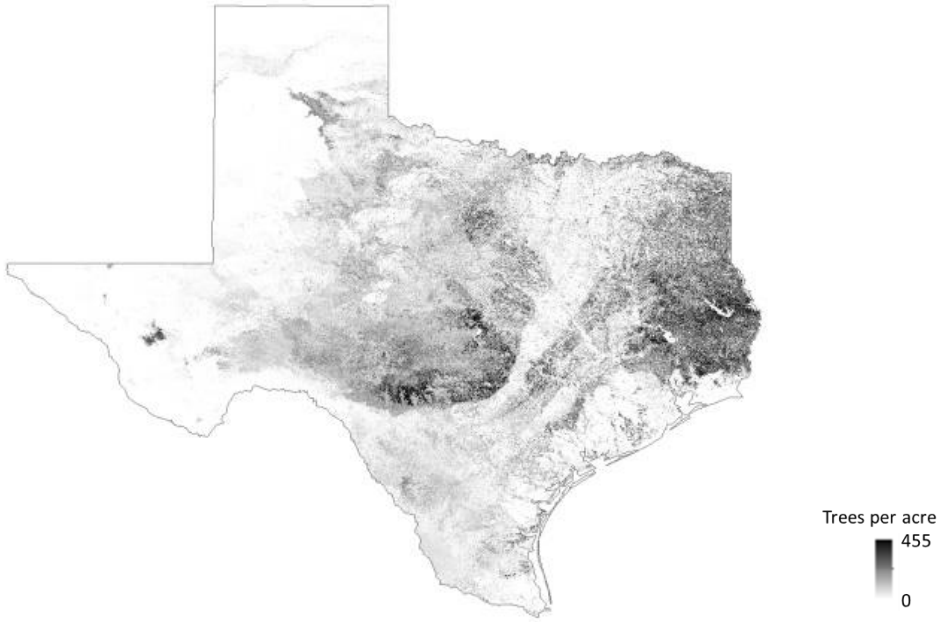

b.

Fig. 2. FIA maps (Wilson et al 2012) depicting a) forest proportion and b) forest density

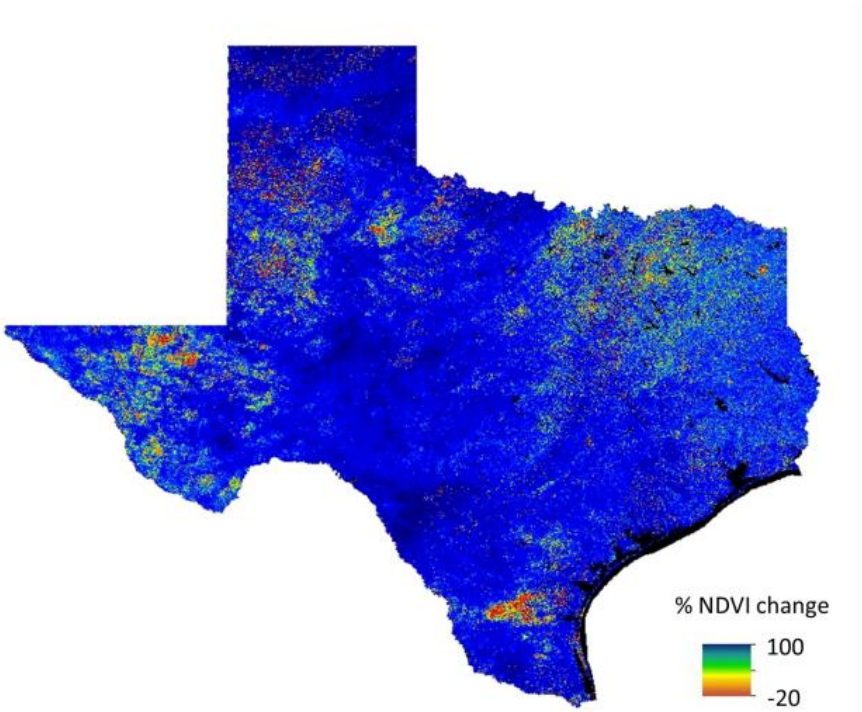

a.

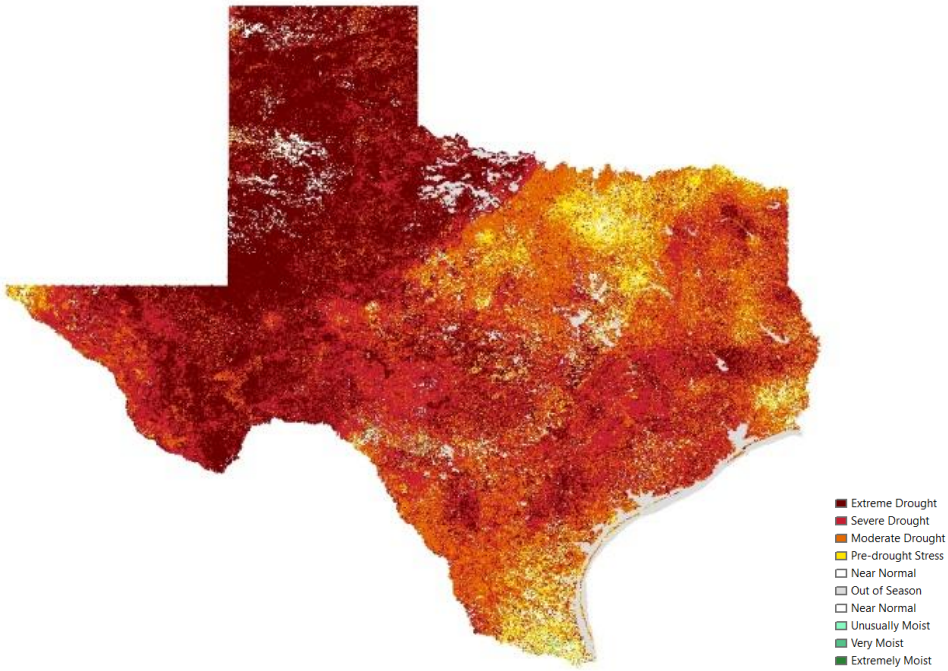

b.

Fig. 3. Original maps of a) dNDVI and b) VegDRI

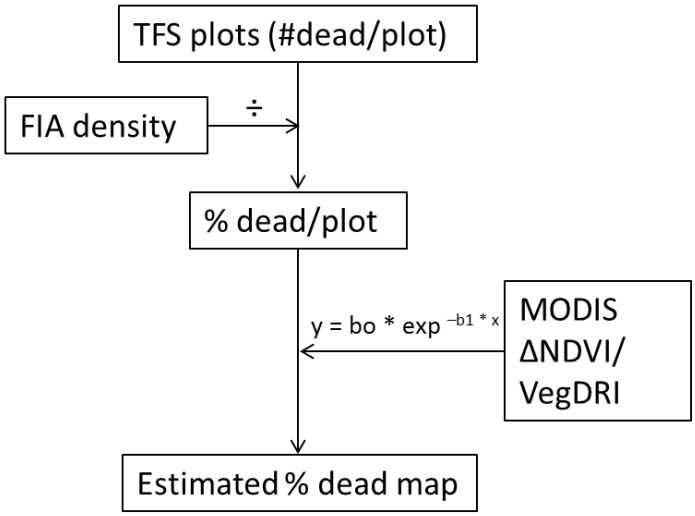

Fig. 4. General methods for mapping mortality with ΔNDVI and VegDRI.

Multiple variations of calibration plot locations were tested for model improvement (Fig. 5). I first regressed ΔNDVI with all usable field plots across the state (n=419). Plots were not used if the ΔNDVI value was highly negative (< -20), which corresponded with a large proportion of water in the particular pixel. Next I attempted to account for physiographic differences between East and West Texas by stratifying the calibration between the two areas, creating separate mortality models for each part of the state. Another strategy was used to test for model improvement, in which only plots located in high density forest were used for calibration. In this case the assumption was that sparse tree canopies masked mortality if understory greened up after the drought. Plots located in the overlap of 75% forest proportion and the upper 75th percentile of forest density were used for calibration. These totaled 85 plots located in East and

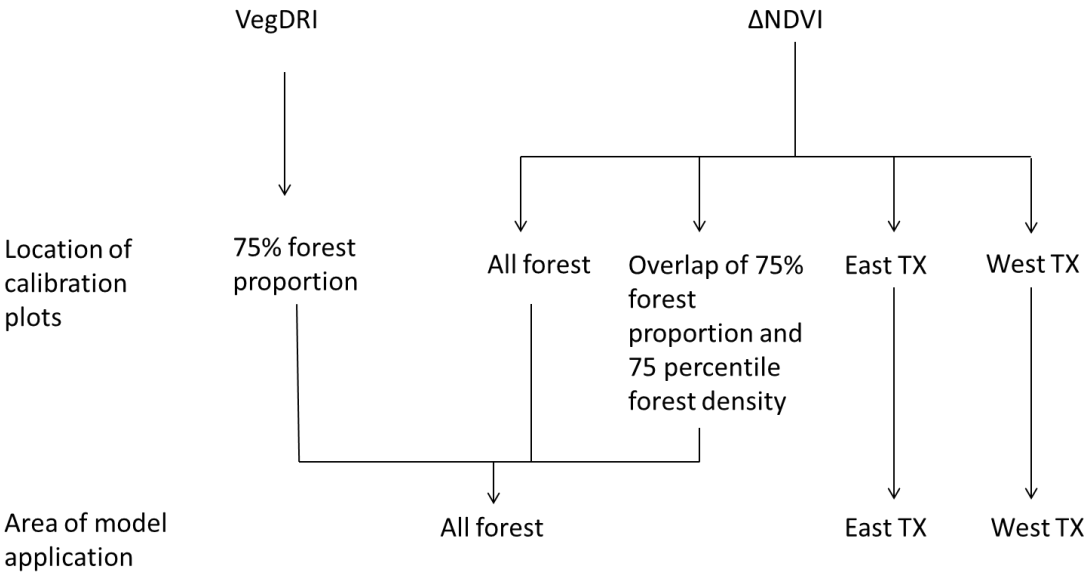

Fig. 5. Flow chart showing the location of calibration plots used to create each model, and the area of application.

Central Texas. Only one VegDRI model was examined in which calibration plots consisted of those within 75% or more forest proportion. To test the VegDRI model as a continuous dataset, I regressed the withheld validation data against the predicted percent dead tree values to get measures of agreement, evaluating the RMSE, which is the standard deviation of the differences between the predicted and observed values and the R^2 of the linear relationship, which explains the proportion of variability in the dataset that can be explained by the model. This value shows how well future outcomes can be predicted by the model and is more conducive for model comparison. These statistics were found using the R programming language (R Core Development Team).

Binary classification maps of predicted dead and no predicted dead were produced for each model variation, where the classification of each pixel was based on

the whether the respective model predicted 0 or greater than 0 percent dead. For these classifications, accuracy was quantified using overall % accuracy and the Kappa statistic (k-hat), which measures the improvement in classification over that of pure chance by accounting for omission and commission error (Congalton and Green 1998). The model-derived classifications were cross-validated using the validation plots.

For the ΔNDVI models, a different binary classification was assessed in which the NDVI change value determined the predicted presence (ΔNDVI < 0) or absence (ΔNDVI > 0) of dead trees. For these index-based classifications, no data was withheld for validation, but all of the plots within the calibration area were used for accuracy assessment. Two different thresholds were used for assessing the accuracy of the index-based classification: One in which an observed (field-derived) percent dead value of 1% or greater in the validation dataset indicated the presence of dead trees, and another threshold in which an observed 6.2% dead value indicated the presence of dead trees, based on the best-estimate of actual percent mortality from this drought event (Moore et al 2015). Everything below the thresholds indicated that no observed dead trees were present and included in the "live" category. The index-derived classifications were validated with a confusion matrix (Stehman 1997) using all of the available field plots as ground truth.

For each of the classifications, commission and omission errors are reported for the live and dead classes. Commission errors represent pixels that belong to another class that are incorrectly labeled as belonging to the class of interest. Errors of omission

are pixels that belong to the ground truth class but the classification failed to classify them into the correct class.

The detection threshold of each model was determined by the y-intercept of the model. This is the predicted percent of dead trees where ΔNDVI = 0, or the minimum percent of dead trees present in which the model correctly identifies the presence of dead trees, assuming that a negative change in NDVI occurs only if trees had died. A raising of the observed dead threshold for validating the index-based classifications was to acknowledge the high detection thresholds of each of the models (13-28% dead for ΔNDVI), and the fact that it was common for dead tree plots to fall within area with positive ΔNDVI values. The value of 6.2% was chosen because this is the overall estimated percent of drought-related tree mortality in Texas using design-based estimators as well as a similar calibrated remote sensing approach to obtain per-region estimates (Moore et al. 2016). Using this as a threshold should give an idea of the accuracy of that estimation.

Finally, I determined the sensitivity for each model that was derived, which in this case represents the response of percent dead trees to the change in the index. A similar statistical approach was performed by Reichmann and Sala (2014). The sensitivity of the models was determined by comparing the averages of percent dead observed in plots on both sides of a given threshold index value. Two dividing thresholds were used: one at a ΔNDVI of 0, where ideally there would be a large difference between the averages, and another at the x intercept where percent dead = 6.2%.

2.2.3. Landsat ΔNDVI and ΔNPV processing

A Landsat 7 Enhanced Thematic Mapper plus (ETM+) from May 7, 2011 and one from June 26, 2012 located in East Texas were acquired from Earth Explorer (http://earthexplorer.usgs.gov/) (Fig. 6). The dates were chosen to closely correspond with dates used for MODIS ΔNDVI and the most cloud-free image of the season was used. This particular scene was selected because that region was known to have relatively high levels of mortality and a relatively high extent of forest cover. All images

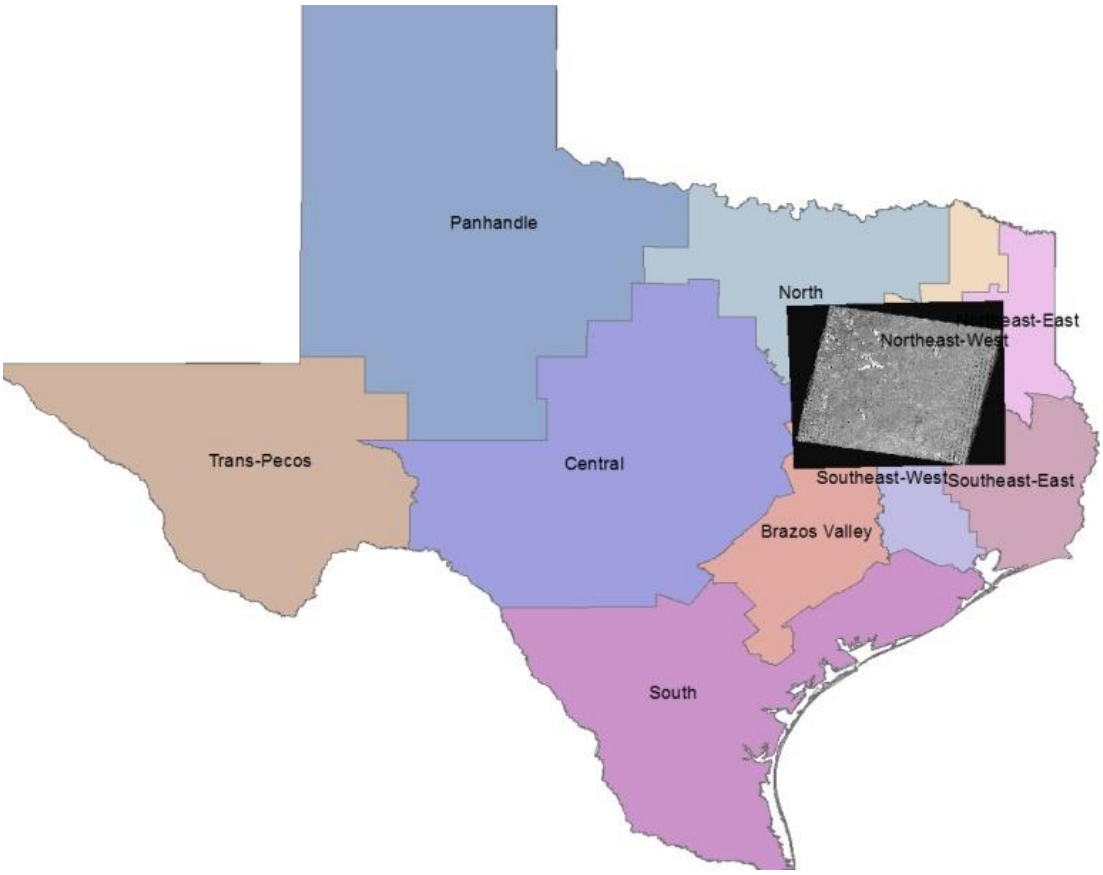

Fig. 6. Location of Landsat 7 ETM+ time series images.

were composited, stacked, and atmospherically corrected before further processing. In May 2003, the Landsat 7 ETM sensor scan line corrector (SLC) failure caused gaps throughout the scenes, resulting in approximately 22% data loss. As a result, less than half of the field plots that overlaid the scene location coincided with spectral data. A technique was developed by Scaramuzza et al. (2004) to fill gaps in one scene with data from another Landsat scene using a linear transform, adjusting the "filling" image based on the standard deviation and mean values of each band of the scene. This gap filling process was implemented using an add-on module in ENVI software (http://www.yale.edu/ceo) using cloud-free imagery as close in date as possible. The May 2011 image was filled with an image from April 5, 2011 and the June 2012 image was filled with an image from July 28, 2012 (Fig. 7), increasing the plot sample size from 33 to 84. Visual examination of the fill revealed that the land types were restored adequately in the gap-filled image.

Band math was used to create NDVIs for both images and to subtract the May 2011 NDVI from the June 2012 NDVI (Landsat 7 ΔNDVI). Two additional indices were derived: change in photosynthetic vegetation between 2011 and 2012 (ΔPV), and non-

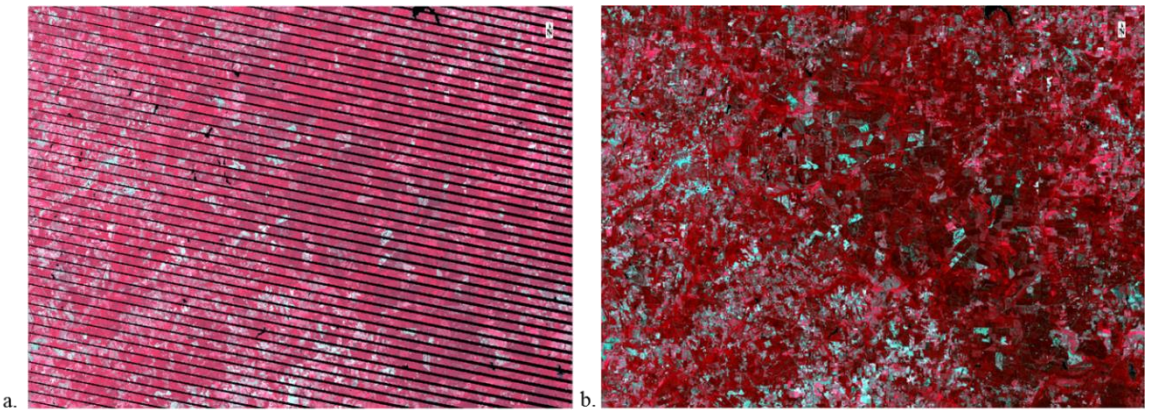

Fig. 7. Results of image gap filling on near infrared color composite. a) 26 June 2012 image b) Filled with 28 July 2012 image.

photosynthetic vegetation from the 2012 image (NPV). PV and NPV were calculated from the Landsat images using the Carnegie Landsat Analysis System (Claslite) (Asner 2009; CLASlite Team 2013), which performs a Spectral Mixture Analysis (SMA) using an automated Monte Carlo unmixing approach (Asner and Heidebrecht 2002) to deconvolute spectral profiles into sub-pixel fractional cover of PV, NPV, and bare soil.

Claslite can classify forest using the fractional cover, where a pixel is labeled forest if PV $\geq$ 80 AND S < 20. To get an idea of the accuracy of the forest classification, it was compared to the FIA forest proportion data used to classify forest in the coarse resolution imagery where a pixel was labeled forest when the proportion was 50% or greater. The software was used to detect forest change between the 2011 and 2012 as multi-image analysis is the most accurate approach for detection of forest change. The expressions below were derived from extensive field testing and validation to identify forest change (Asner et al. 2005; Oliveira et al. 2007)

A pixel was labeled as deforested if:

- (((PV1 – PV2) ≥ 25) [a pixel loses 25% or more of its PV fraction]
- OR ((S1 ≤ 5) AND ((S2 – S1) ≥ 15)) [S increase captures deforestation followed by early regrowth]
- OR ((PV2 < 80) AND ((NPV2 – NPV1) ≥ 20))) [a large spike in NPV signals deforestation. This encompasses deforestation caused by a lot of green vegetation dying.]

Where:

PV1 = 1st Image photosynthetic vegetation fraction

NPV1 = 1st Image non-photosynthetic vegetation fraction

S1 = 1st image bare substrate fraction

PV2 = 2nd image photosynthetic vegetation fraction

NPV2 = 2nd Image non-photosynthetic vegetation fraction

S2 = 2nd image bare substrate fraction

The decision tree for disturbance pixels is similar to deforestation regarding expected shifts in PV, S, and NPV values:

((((NPV2-NPV1) ≥ 10) AND ((PV1-PV2) > 10)) OR ((S1 ≤ 5) AND ((S2-S1) > 10) AND (S2 ≤ 15))).

The main difference between the deforestation and disturbance decision trees is that the thresholds for disturbance encompass many more pixels since disturbance is a more subtle form of forest loss. Drought mortality would be considered “disturbance”;

however, very few pixels were labeled as disturbance and Texas did not undergo expansive deforestation from 2011-2012.Deforestation and disturbance pixels were therefore combined and considered most likely to be drought-related tree mortality.

For Landsat ΔNDVI and ΔPV, the live and dead threshold was placed at a ΔNDVI value of 0. For NPV, a value of 25% or greater was chosen as the cutoff of where the sensor would expect to pick up at least 1 dead tree. As with the coarse-resolution imagery, the ability of each index to capture dead trees was tested by calculating a confusion matrix (Stehman 1997) for a binary classification of dead presence (dead) vs. non presence (live) in a pixel using all of plots present in the scene. A sensitivity analysis was performed to get an idea of the response of dead trees to each index, as described above in Section 2.2.

2.3. Results

2.3.1. Continuous estimation with NDVI change and VegDRI

The relationship between index value and observed mortality was best fit using a negative exponential decay model with highest mortality associated with lower index values. The fitted regression models for each index variation are shown in Fig. 8. The predicted vs. observed plots of the validation data shown in Fig. 9 indicated that all models tended to under predict mortality for plots with the greatest proportions of dead trees. Among the ΔNDVI models, high proportion forest ranked the highest, followed by East Texas, West Texas, then All Forest. High forest proportion ΔNDVI model had the highest R^2 value by far (0.3) despite the fact that it had the fewest validation plots.

VegDRI and East Texas ΔNDVI shared the same low value of 0.03 and West Texas ΔNDVI had a R^2 value of 0, showing that none of the variability is explained by the model. VegDRI had the lowest RMSE, however, the range of values is different from those of the ΔNDVI models making them incomparable. Considering the low R^2 value and an unrealistic predicted percent dead, this model ranks low compared to the others. There were inherent tradeoffs between estimating mortality over larger areas (with greater numbers of plots) and with a more conservative approach using fewer plots that only considered dense forest (Table 2). Nevertheless, the high forest proportion had high agreement, R^2, and the highest classification accuracy (k-hat = 0.31); however, it predicted the most unrealistic percent dead (49.9%). All the other models showed close to random (50%) overall accuracy and very low k-hat values (Table 2). The low k-hat values are due to the very high omission errors (> 75%) for the "live" class and high commission errors (> 45%) for the "dead" class for every model besides the high proportion and density forest model (Table 3), indicating a high overprediciton of pixels that contain dead trees. Conversely, the low commission errors of the live class and low omission of the dead class indicate that the majority of dead pixels were correctly identified.

a. y = 21.28 * exp(-0.05 * x)

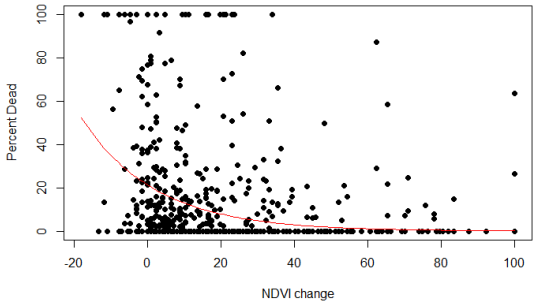

b. y = 12.66 * exp(-0.14 * x)

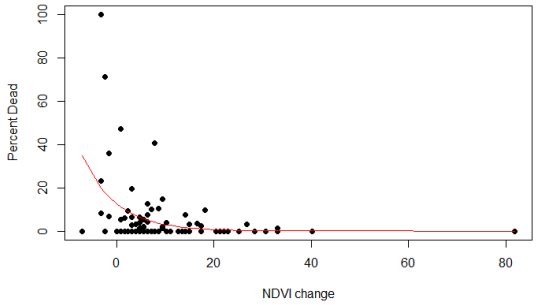

c. y = 27.81 * exp(-0.05 * x)

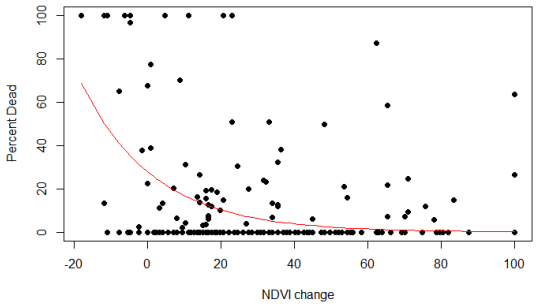

d. y = 19.59 * exp(-0.06 * x)

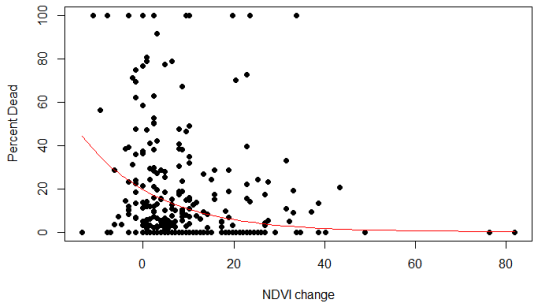

e. y = 1.28 * exp(-0.01 * x)

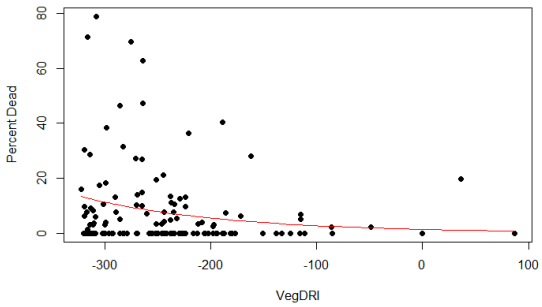

Fig. 8. Negative exponential regression models and scatter plots using NDVI change as an independent variable to estimate percent dead in plots within a) All Forested area, b) high density and forest proportion, c) West Texas, and d) East Texas; and e) regression model and scatter plot using VegDRI as an independent variable to estimate percent dead in plots within 75% forest proportion

a.

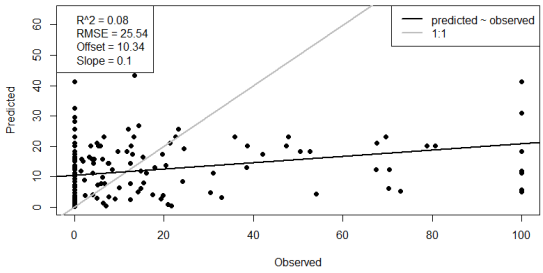

b.

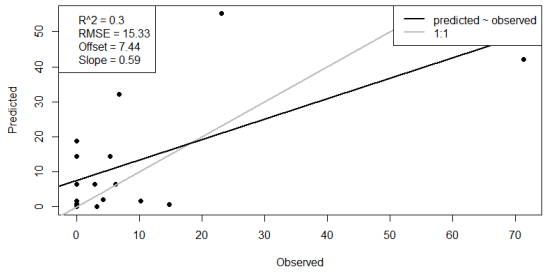

c.

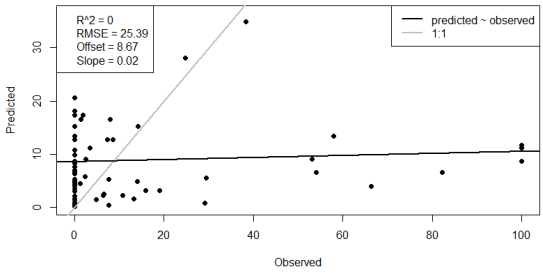

d.

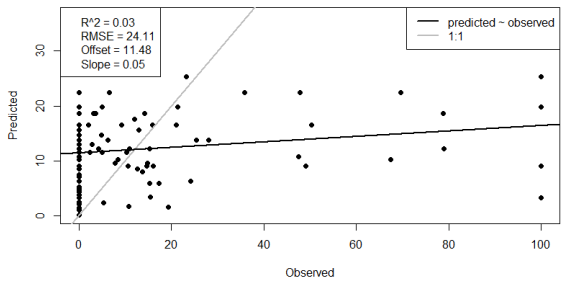

e.

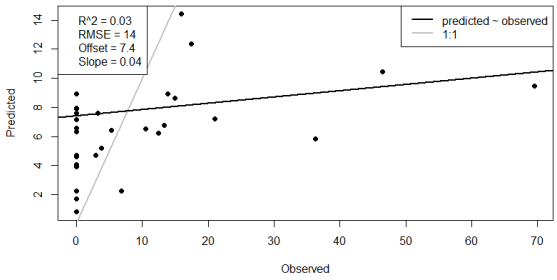

Fig. 9. Predicted vs. observed plots for validation data for ΔNDVI calibration models located in a) All Forest, b) high density forest, c) West Texas, and d) East Texas; and e)VegDRI in 75% forest

Table 2
Results of model-estimated percent dead and model validation. Note that higher density forests were predicted to have higher proportions of dead trees.

						predicted v. observed		model-based binary classification	
Index	Location of calibration plots	Calib. plots	Area of estimation (ha)	Estim. % dead	Valid. plots	R^2	RMSE	% accuracy	K-hat
MODIS ΔNDVI (250 m)	All plots	417	25,176,282	9.1	179	0.08	25.54	57.5	0.15
	East Texas	239	12,055,675	11.0	103	0.03	24.11	52.4	0.02
	West Texas	180	13,120,607	9.8	77	0.00	25.39	53.3	0.16
	High prop./dens. forest	60	25,176,282	49.9	25	0.30	15.33	64.0	0.31
Veg DRI (1000 m)	75% forest proportion	94	25,205,000	27.1	40	0.03	14.00	47.5	0.04

Table 3
Commission and Omission errors for model-based binary classifications.

Model	Class	Commission Error (%)	Omission Error (%)
All Forest	live	15.8	82.0
	dead	45.6	3.3
High proportion forest	live	20.0	46.7
	dead	46.7	20.0
East TX	live	0.0	98.0
	dead	48.0	0.0
West TX	live	15.4	75.6
	dead	53.1	6.3
VegDRI	live	0.0	95.5
	dead	53.8	0.0

2.3.2. Index-based binary classifications, sensitivity, and detection thresholds

Because of the high errors and over-prediction of the models (Fig. 10), additional classifications were done based on the index itself as the predictor of dead and live rather

than the model-derived values (Table 4). An index-based classification was not done based on VegDRI values because there was no clear or theoretical cut-off at which to separate dead and live. First a threshold was set at 1%, which is an extremely low detection limit, given noise and error. This was done to determine the lowest level of mortality that may be perceived by these indices. Using 1% as the threshold, overall accuracies were still only about 50% for All Forest and East Texas models, and around 61% for West Texas and high proportion forest. K-hats remained extremely low, not going above 0.13. This is partially due to the very high omission errors for the "dead" class, where all are over 83% (Table 5). However, increasing the threshold to 6.2%, corresponding with the reported estimate of actual mortality from this drought event (Moore et al 2015), raised all of the accuracy statistics. High proportion forest classification accuracy increased the most (34% overall, 172% for k-hat) while West Texas accuracy increased the least (about 6% for both overall and k-hat). Setting the threshold at 6.2%, the k-hats rose by 62% and 45% for East Texas and , respectively and commission errors generally decreased at this threshold. This suggests that these indices were modestly reliable at detecting mortality at levels similar to that observed in the 2011 Texas Drought.

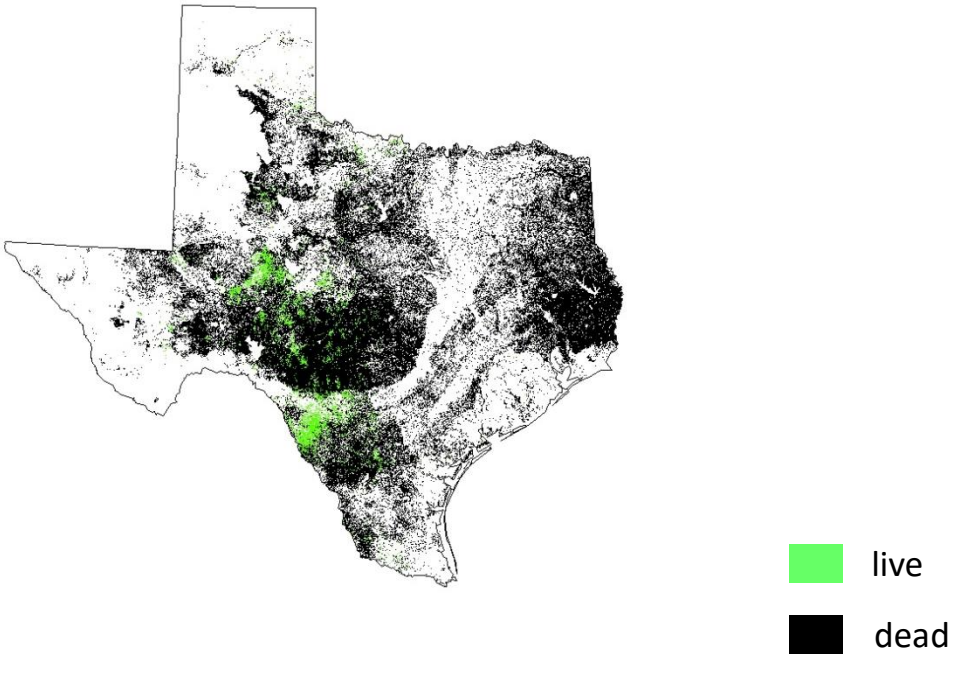

a.

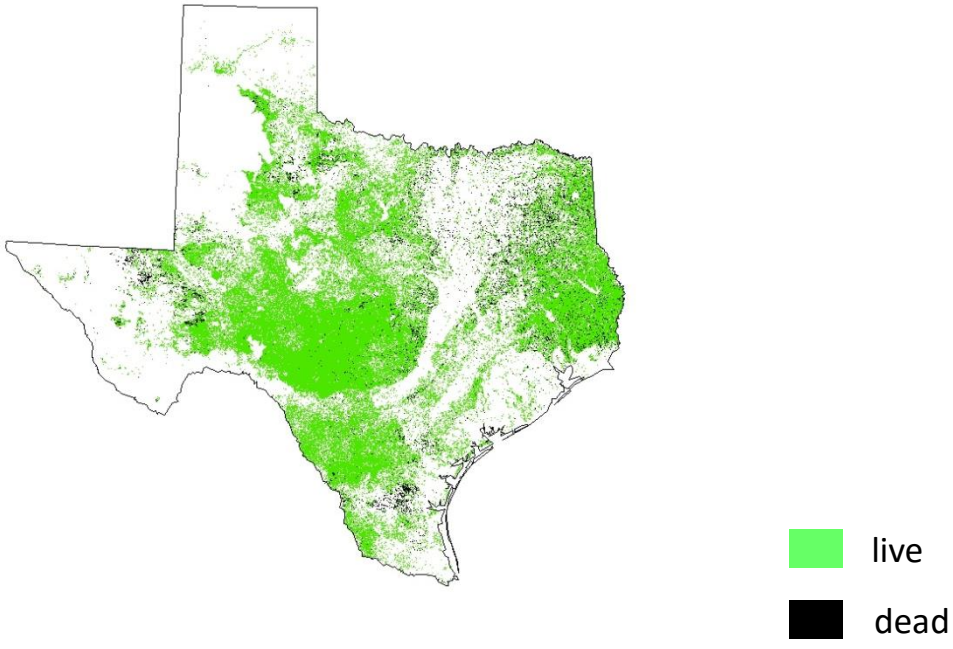

b.

Fig. 10. a) All Forest model-based classification and b) ΔNDVI index-based classification

Table 4
Index-based binary classification accuracy and sensitivity analysis. Overall accuracy and k-hat for two classifications: one using 1% as the threshold for constituting an observed "dead" pixel, and other using 6.2%. Sensitivity analysis is average % dead on "live" and "dead" sides with two thresholds: one using ΔNDVI of 0, and the other using the ΔNDVI value of the respective model corresponding to 6.2% dead.

		Accuracy				Sensitivity (Average % dead)				
		%		k-hat		"live" side		"dead" side		
		Threshold				Threshold				
Index	Location of calibration plots	1%	6.2%	1%	6.2%	0 ΔNDVI	6.2%	0 ΔNDVI	6.2%	Detection Threshold
ΔNDVI	All Forest	55.4	64.8	0.09	0.14	11.64	8.3	33.8	15.7	21.3
	ETX	51.5	63.7	0.10	0.17	12.17	13.9	30.8	14.3	19.6
	WTX	61.6	65.5	0.09	0.09	10.74	7.8	42.1	19.1	27.8
	high density	61.2	82.4	0.13	0.36	3.36	2.7	30.7	11.5	12.7
VegDRI	75% forest proportion	-	-	-	-	-	3.5	-	9.8	1.3

Table 5
Commission and Omission errors for index-based binary classifications with 1% dead and 6.2% dead thresholds.

		1% Threshold		6.2% Threshold	
Model	Class	Commission Error (%)	Omission Error (%)	Commission Error (%)	Omission Error (%)
All Forest	Live	46.5	4.9	35.6	4.9
	dead	26.8	86.0	32.1	83.5
ETX	Live	52.1	4.6	37.7	4.5
	dead	18.9	84.1	24.3	80.4
WTX	Live	38.1	6.6	15.8	82.0
	dead	41.2	85.9	45.6	3.3
high density	Live	40.3	4.2	16.9	3.0
	dead	25.0	83.8	25.0	68.4

While accuracy rose with the 6.2% dead threshold, sensitivity decreased (Table 4). The average difference between the average % dead between ΔNDVI > 0 ("live" side") and ΔNDVI < 0 ("dead" side) was 24.8%. When changing the dividing threshold from 0 to the corresponding ΔNDVI value at 6.2% dead, the average difference between the values dropped to 6.9% (this average includes VegDRI). Sensitivity was 31.4% greater in West Texas with the ΔNDVI 0 threshold and 11.3% greater with the 6.2 dead threshold. East Texas had the lowest sensitivity at both thresholds, improving by only 18.6 and 0.41%, respectively. Consistent with lower forest densities in drier regions, West Texas had the highest detection threshold (27.8% dead). VegDRI had the lowest (1.3 % dead) detection threshold, but this was likely due to the consistently low VegDRI across all plots. All Forest had the next highest threshold, followed by East Texas and high forest proportion.

Examining the relative mortality predictions spatially (Figs. 11 – 15), the NDVI change models all predict higher mortality in East Texas and in Central Texas northeast of the Balcones Escarpment. In the high density model prediction map, there were more extreme values (shown as colors at either end of the spectrum) although it showed the same patterns as the All Forest model. All the ΔNDVI models additionally showed high mortality in the West Texas mountain range and an area in south Texas and just south of the panhandle (Figs. 11 - 14). VegDRI predicts higher numbers overall (darker colors) (Fig. 15) and shows some differences in pattern compared to ΔNDVI. It does not predict high numbers northeast of the Escarpment, but seems to increase westward with long stretches of uniform high mortality prediction.

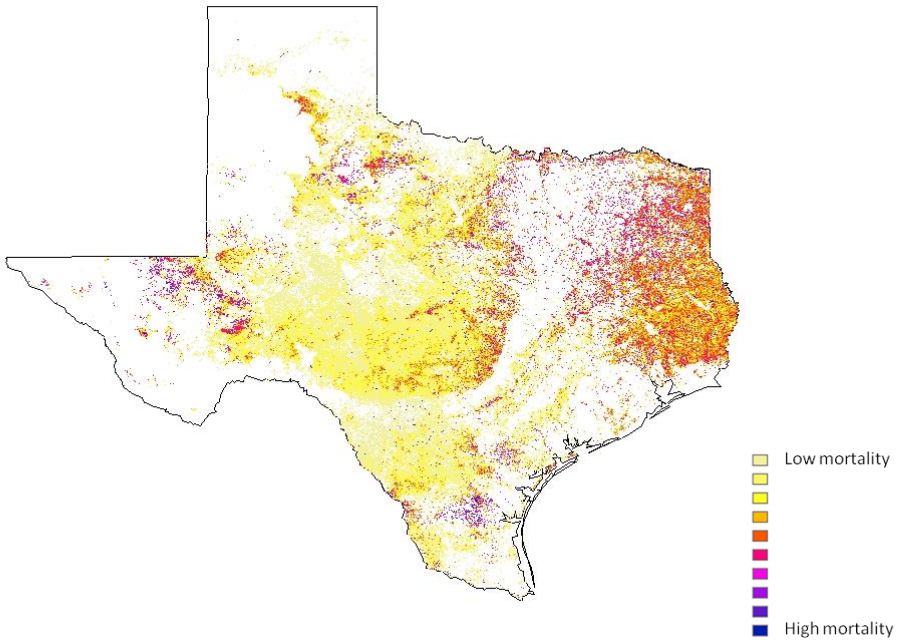

Fig. 11. Resulting maps of percent dead trees from modeling ΔNDVI with percent dead in plots within all forested area

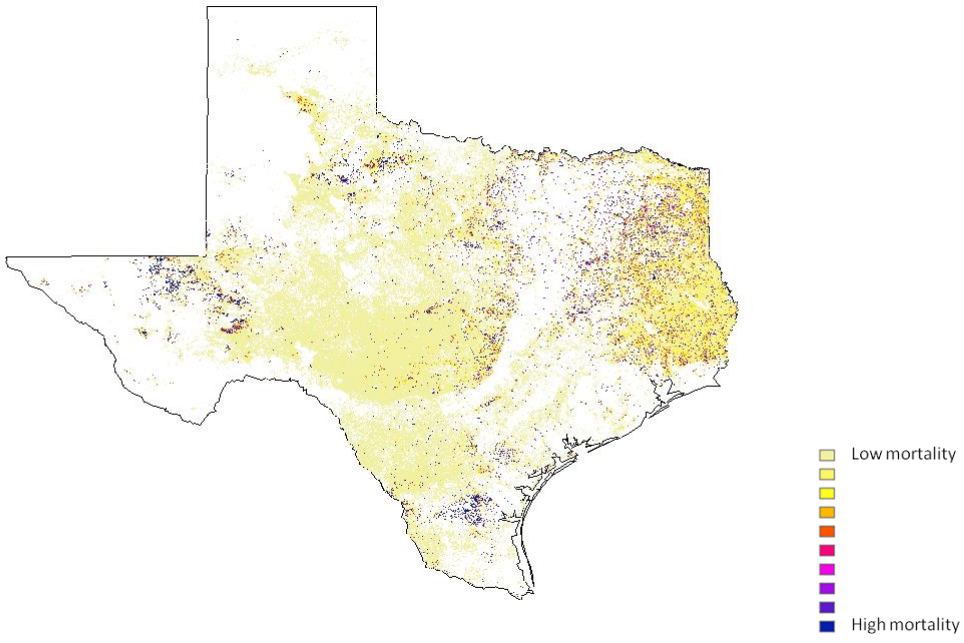

Fig. 12. Resulting maps of percent dead trees from modeling ΔNDVI with percent dead in plots within high density and forest proportion

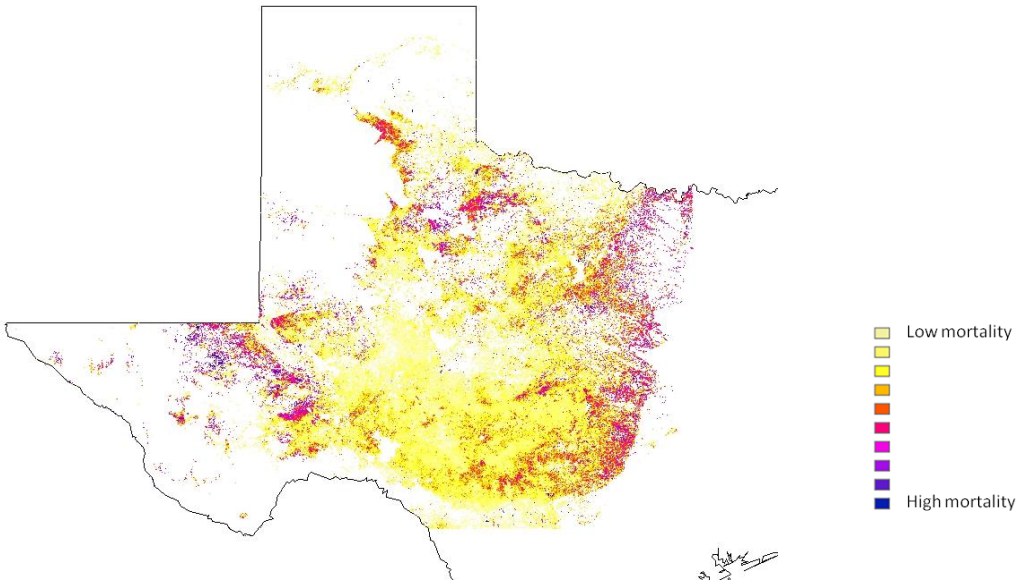

Fig. 13. Resulting maps of percent dead trees from modeling ΔNDVI with percent dead in plots within West Texas

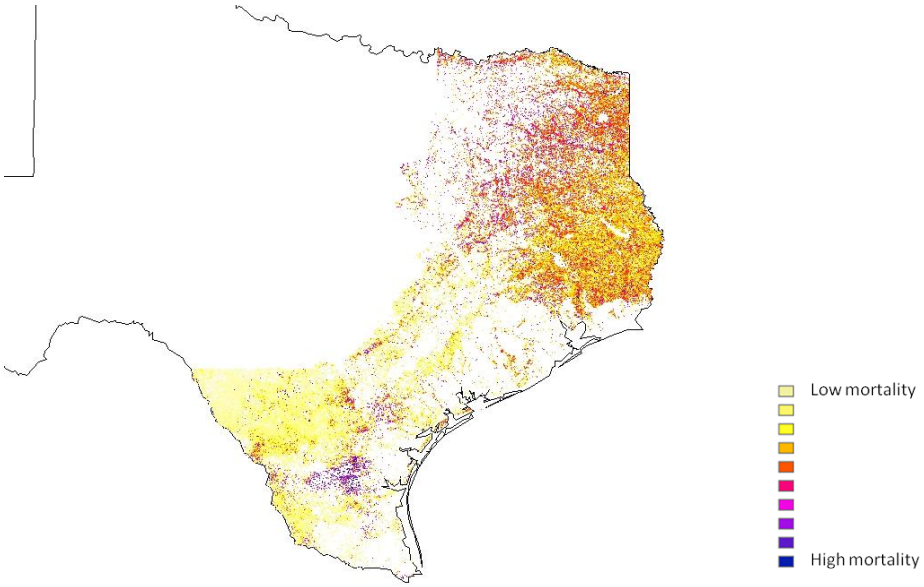

Fig. 14. Resulting maps of percent dead trees from modeling ΔNDVI with percent dead in plots within East Texas.

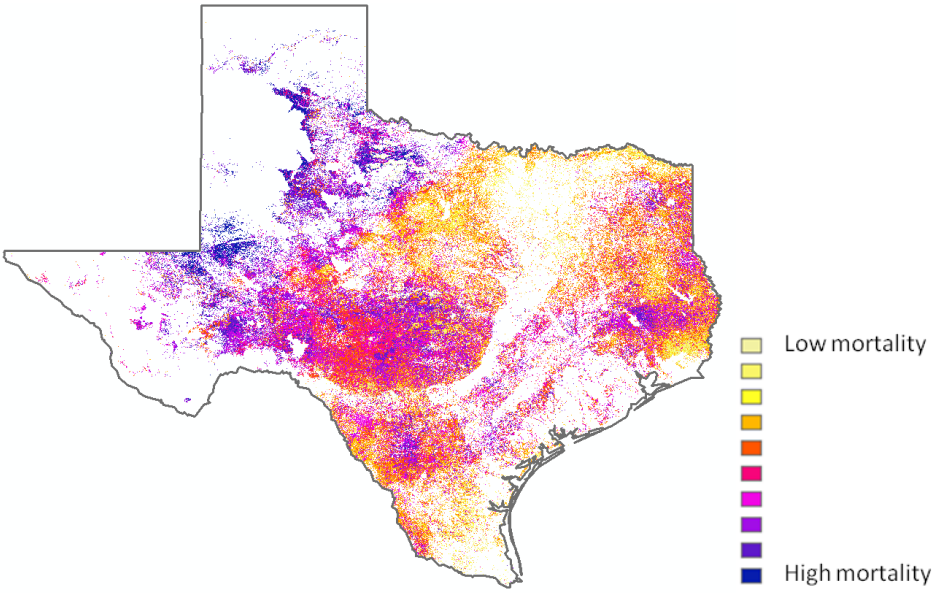

Fig. 15. Resulting map of percent dead from modeling VegDRI with percent dead in plots within 75% forest proportion.

2.3.3. Landsat indices

A visualization of the dominant cover type after undergoing spectral unmixing is seen in Fig. 16. When plotting the index values against the number dead per plot the Landsat-derived ΔNDVI and ΔPV (Fig. 17 a and b) show similar patterns, as would be expected. Both show a bell-shaped curve, where low numbers of dead are seen in the negative range, peaks at a value close to but less than 0, then drops precipitously as values increase. NPV does not follow the expected positive relationship (Fig. 17 c), but instead is slightly negative. Because of the small sample size and the weak and unexpected relationships to the field data, the data was not used to calibrate models of mortality in the image as with the coarse resolution imagery. Rather, the indices were used for classification of dead trees and fractional cover was used to predict potential

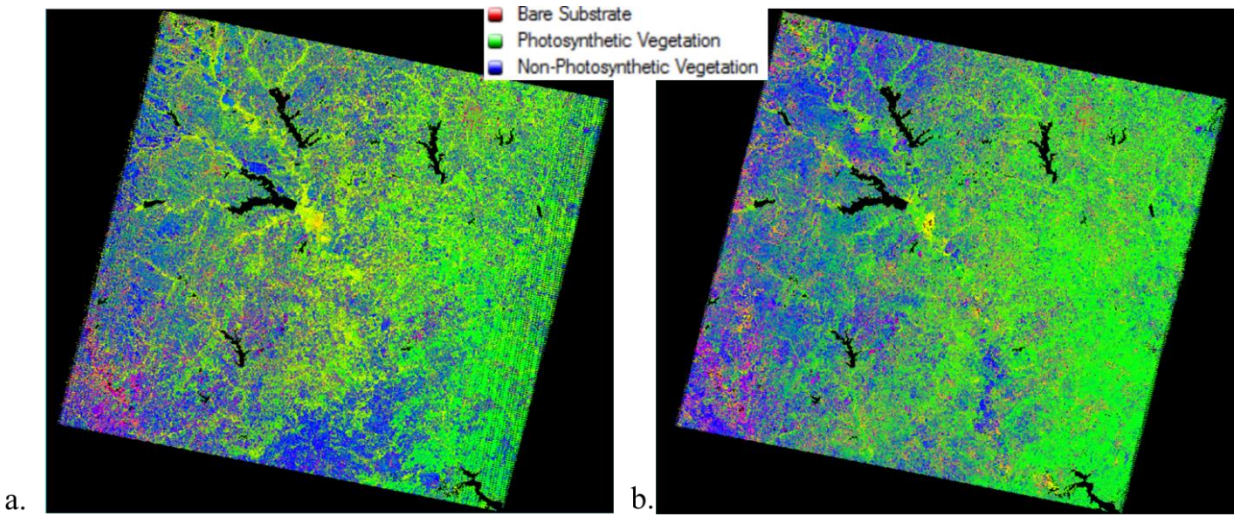

Fig. 16. Sub-pixel unmixing results of gap-filled images for a) May 2011 and b) June 2012.

tree mortality. A visual assessment showed that the area of forest classification derived using Claslite in the Landsat time series images were reasonably close to that of FIA forest proportion, with expected differences in precision due to the difference in resolution (Fig. 18). This is a rough visual assessment of the accuracy of the fractional cover and the algorithms used to produce the forest map.

The binary classification accuracies for Landsat indices were around 60% for ΔNDVI and ΔPV and 42% for NPV (Table 6). K-hats were 0.21, 0.11, and -0.06 for ΔPV, ΔNDVI, and NPV, respectively. ΔNDVI and ΔPV had high omission errors for the live class (77% and 57%) and NPV had a 81% omission error of the dead class, contributing to the low k-hat values (Table 7). The ΔNDVI index was most sensitive to dead trees, with a difference of only 2.4 dead trees between a negative and positive index value. The NPV index was reversed, with an average of 3.2 dead at the “live” side of the NPV range of less than 25% and 2.4 average dead at ≥ 25% NPV.

a.

b.

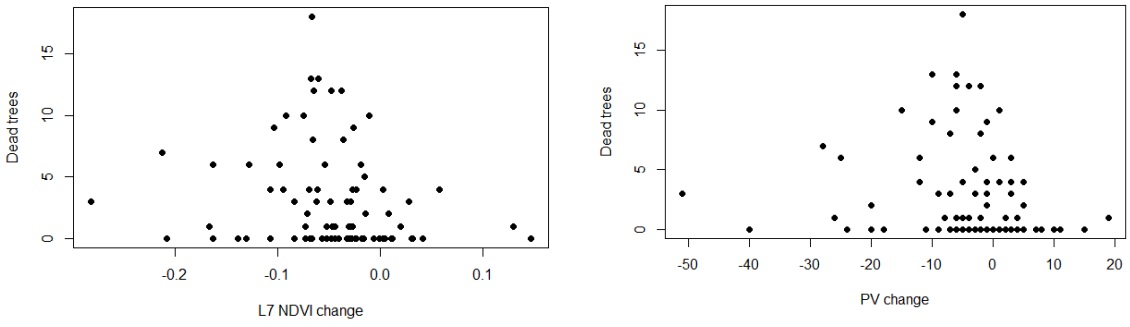

c.

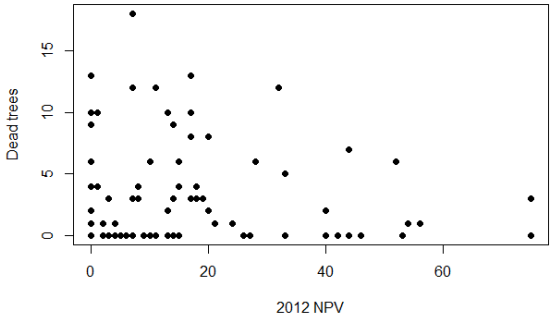

Fig. 17. Scatter plots of Landsat-derived index values with number dead in a plot.

Combined "deforestation" and "disturbance" (forest loss) pixels totaled 48,512 ha which is less than 1% of the entire scene. Only 5 of the 83 plots overlaid a forest loss pixel so these cannot be used to validate the prediction. But of these, the number dead in these plots were 10, 7, 6, 2, and 0. A visual assessment of the forest loss pixels over the All Forest model's estimated dead map found that the forest loss did pick up burned areas (which were excluded from the coarse-resolution analysis) and coincided with the

areas of high predicted dead (Fig. 19). Though promising, more processing is needed to quantify the accuracy of the forest loss pixels.

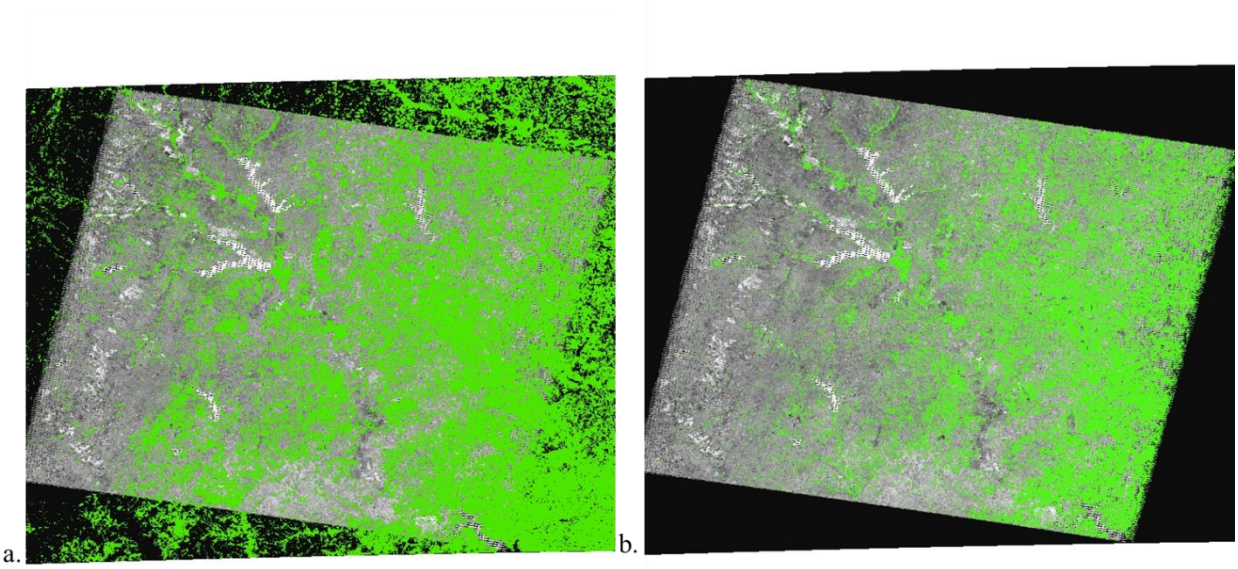

Fig. 18. Comparison of forest area distribution depicted between a) FIA forest proportion (≥50%) and b) Classification of June 2012 Landat ETM+ image using fractional cover of PV and S.

Table 6
Accuracy statistics of binary Landsat derived index-based classification, and sensitivity calculated as the average dead on the "live side" (positive NDVI & PV change or < 25% NPV) and the "dead side" (negative NDVI & PV change or ≥ 25% NPV).

	Accuracy		Sensitivity (Average % dead)	
	Overall (%)	K-hat	"live side"	"dead side"
ΔNDVI	60.24	0.11	1.07	3.48
ΔPV	62.65	0.21	1.62	3.74
NPV	42.17	-0.06	3.26	2.39

Table 7
Commission and Omission error for Landsat-derived index classifications.

Index	Class	Commission Error (%)	Omission Error (%)
ΔNDVI	live	42.86	77.14
	dead	39.13	12.50
ΔPV	live	42.31	57.14
	dead	35.09	22.92
NPV	live	60.00	25.71
	dead	50.00	81.25

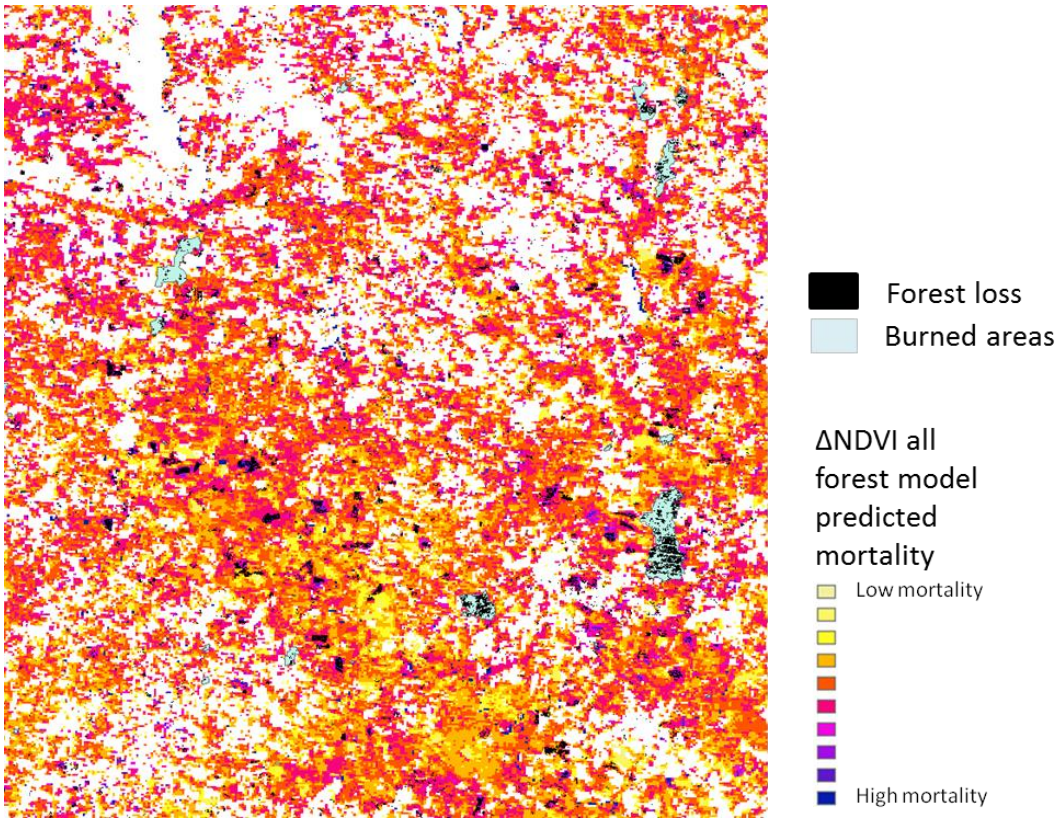

Fig. 19. Zoomed-in view of Landsat fractional cover-derived forest loss (black) overlaid on the All Forest model mortality prediction and burned areas in 2011 (light blue).

2.4. Discussion

While in most cases observed dead trees coincided with lower index values, the ability of a large pixel to precisely detect diffuse mortality is problematic and the reason few studies have attempted to use coarse resolution imagery for that purpose. A few dead trees in a 0.16 ha plot could be surrounded by green forest and vice versa. Therefore the high errors and low accuracies were expected. However by testing and comparing variations in the models it is possible to see what can be done to improve the methodology, should the use of finer resolution not be feasible. In all cases, low index values were associated with higher mortality rates and there were consistent relationships between indices and observed mortality.

The use of coarse-resolution models to estimate tree mortality requires consideration of many factors to determine the best approach for a given forest condition. Among the variations of coarse-resolution models, there were no clear "winners" or "losers", nor were there consistent rankings among evaluation criteria. The VegDRI model, as being based on the coarsest resolution, did tend to rank low on most counts where the criteria was comparable. This includes the low R2, low model-based accuracy, the high estimated percent dead, and low sensitivity. Although very low, VegDRI's detection threshold is a product of its overestimation of dead trees. The spatial application of the VegDRI model shows that VegDRI predicts an increase of mortality westward. This is likely due to the incorporation of climatic variables such as PDSI.

Among the ΔNDVI models, high proportion/density forest stands out in model and classification accuracy, sensitivity, and low detection threshold. However this model

by far overestimated percent dead. This may be related to the low number of calibration plots in the more restricted sampling area. Evidenced by this and VegDRI where calibration plots were taken only from 75% forest, restricting the calibration plots to areas of higher amounts of forest leads to overestimation, and there is a tradeoff between detection and estimation accuracy, particularly when applying the model to lower and heterogeneous forest density areas. The separation of east and West Texas was an attempt to "normalize" this phenomenon by applying more uniform forest density associated calibration models to only that area from which the calibration data was taken. For example, although East Texas calibration plots were, like the high forest model, taken from high proportion/density forest, it does not have the same level of overestimation due to its application to only highly forested areas. Intuitively, the more specialized the calibration to an area, the more accurate; the tradeoff, however, is limiting the area of analysis.

East and West Texas models did not stand out as particularly accurate or poor, although West Texas showed a markedly high dead tree sensitivity. This may be related to the overall lower tree density in this portion of the state. The All Forest model might be considered the overall winner for application to a large area. Its inclusiveness and high sample size help to moderate the estimations to realistic levels, and the accuracies were generally high relative to the others.

As seen in the map on Fig. 10, the models far over predicted the presence of one dead tree. This is reflected in the high omission errors for the live class and the commission errors for the dead class (Table 5.). In contrast, the index classifications

underpredicted pixels with at least one dead tree, indicated by the high omissions of the dead class. Raising the threshold to 6.2% dramatically increased accuracies (171% for high density/proportion forest model), as it imposes expectations that are closer to the indices' actual detection thresholds. However, these classifications also underpredicted dead, with the exception of West Texas.

It is important to note that a large amount of error was introduced by using MODIS-derived live tree density to calculate percent dead in each plot. The field data collection took place without these particular research questions in mind. Live tree data from a 250-m (6.25 ha area) pixel was used with data from a 0.16 ha plot, adding to the inherent error of a large pixel's ability to detect diffuse mortality. However it was deemed necessary to try to account for density differences in such a heterogeneous landscape.

The Landsat binary classification accuracies did not appear to stand out above the coarser-resolution classifications. Overall accuracy was slightly higher on average though k-hats remained in the 0.1 - 0.2 range (Table 6.). Compared to the MODIS ΔNDVI index-derived classification, accuracies were higher and errors were lower with the exception of the Landsat commission errors of the dead class, meaning that the Landsat classification had more incorrectly-labeled "live" pixels. However, it should be noted that these classifications are not directly comparable because the Landsat classification was based on number dead and the MODIS classifications were based on percent dead.

The ΔNDVI classification omitted 77% of live pixels and the NPV, with a negative k-hat, omitted 81% of dead pixels. The spectral unmixing-derived forest loss area totaled less than 1% of the Landsat scene which is lower than expected. Visually, this method looks promising, but at present, the field plots cannot be used to quantify its accuracy. Although there is very weak agreement with the field data, this is not dismissive of the potential of the spectral mixture analysis method for determining mortality.

For the Landsat classifications, the low numbers in the negative range of the change indices were not consistent with the understanding of how the indices pick up the dead tree signal, though may be indicative of other problems or signals. Since density was not accounted for in this analysis, these are likely to be plots where very few dead trees were found but were surrounded by dead vegetation or substrate within the 30-m pixel area. This may also be the case with NPV which showed the inverse relationship than was expected with high numbers of dead seen in the low range of NPV and low numbers of dead in the higher range (Fig. 16, Table 6). In addition to density and grain size effects, the relationship may also have to do with the endmembers used by Claslite to calculate presence of NPV which may not be calibrated well to the particular areas. The detection threshold should also be considered, though it was not calculated due to the high errors. With many possible explanations, the next recommended step would be to account for density in the plots, ideally in the field.

2.5. Conclusions

This exercise found that time-series indices work best for capturing drought-related mortality, and it worked best in areas of denser forest cover. Isolating the change in the pixels helps to reduce the signal-to-noise ratio especially in low density areas where a lot of S and NPV are present. If estimating mortality in a large heterogeneously forested area such as the state of Texas, it is recommended to have a large sample size with calibration plots that are inclusive of the various types of forested areas of estimation. However, this coarse-resolution modeling method is best for estimating mortality in large areas of relatively uniform forest density and forest type and where the estimated percent mortality is close to or greater than the index detection threshold. It is also highly recommended to record live tree estimation from the field plots along with mortality.

In order for Landsat estimations to be compared with that of MODIS and AVHRR, the next steps of the analysis are to calculate subpixel fractions for MODIS and AVHRR and/or use the Landsat-derived indices to calibrate models of mortality. Future studies can utilize US Forest Service FIA data. In the next sections, abiotic and biotic variables are assessed as drivers of drought mortality.

3. THE CONTRIBUTION OF CLIMACTIC AND DROUGHT CONDITIONS TO DROUGHT-RELATED TREE MORTALITY

3.1. Introduction

3.1.1. Ecological description of Texas

Texas has been described as a major biological crossroads of North America because it is the meeting ground of diverse flora and fauna of the eastern deciduous forest, the tall, mixed, short and desert grasslands, the southwestern deserts and the southern Tamaulipan shurblands, as well as having its own unique components (Smeins 2004). Because of its size and geographic location, Texas is unique in its variation in climate, topography, and soils; all of which influence habitat and species diversity. Climate varies from warm temperate in the north to subtropical in the south. Mean annual precipitation varies 1524 mm in the eastern Pineywoods region to less than 203 mm in the Chihuahuan Desert of West Texas, while annual temperature varies from 12°C in the northwest to 23°C in the south. The frost-free period ranges from 180 days in Amarillo to over 330 days in the Rio Grande Valley. These parameters can experience considerable intra- and interannual variation in any part of the state, particularly precipitation (Smeins 2004).

Ecoregions are defined as geographical areas of similar type, quality, and quantity of environmental resources (Griffith et al. 2004). The regions are broadly distinguished by the climate and geography of the region. Below is a brief description of

the vegetation regions as outlined by Gould et al. (1960) and their vegetation communities (Fig. 20).

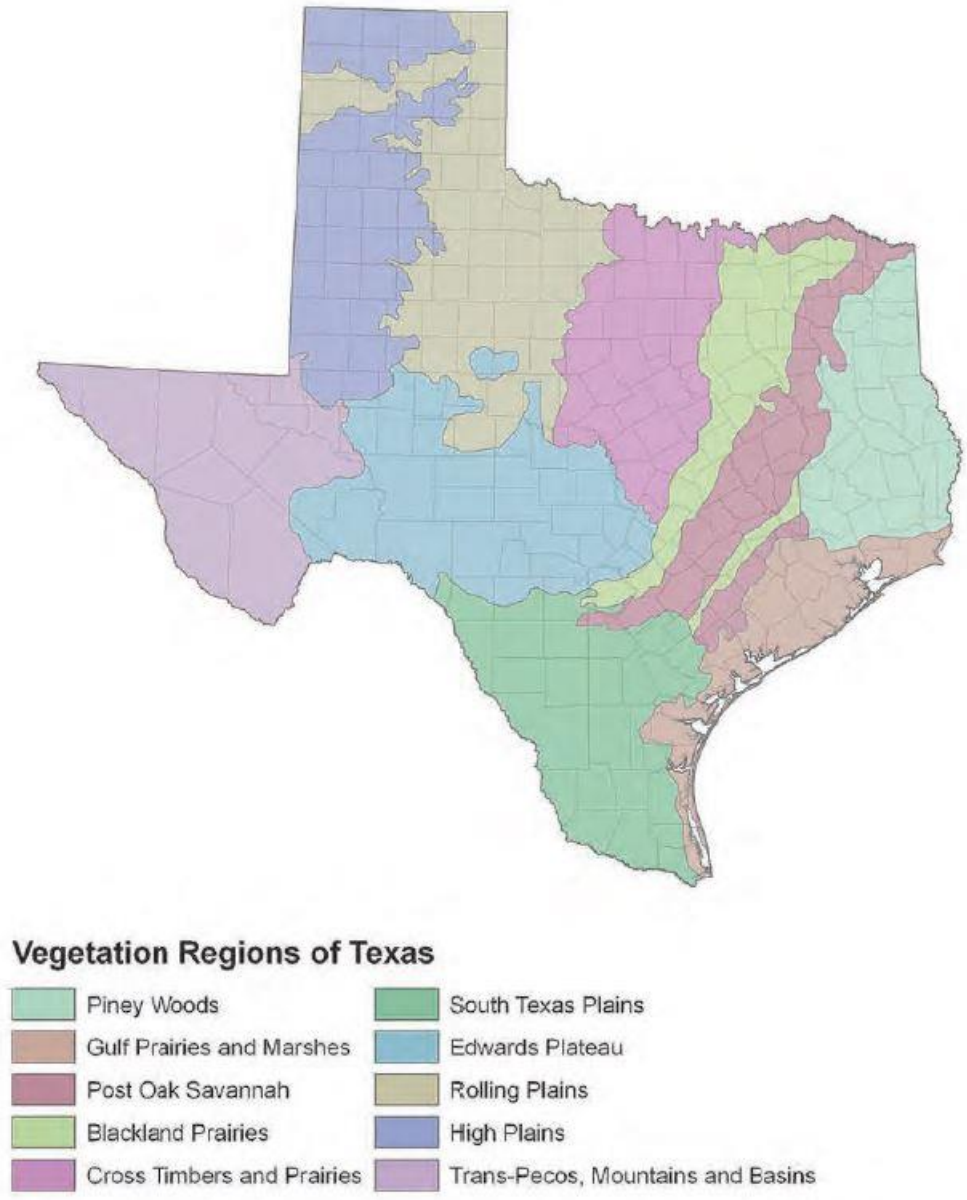

Fig. 20. Vegetation regions of Texas from Gould et al. (1960)

The Trans-Pecos in the extreme western part of the state contains diverse vegetation, due to diversity of soils and elevations. Trans-Pecos contains desert valleys, plateaus, and mountain slopes. Elevations range from 762 to over 2667 m at Guadalupe Peak. Over most of the area, average annual rainfall is less than 12 in, but with high intra-annual variability. Plant communities found here are creosote-tarbush desert scrub, desert grassland, yucca and juniper savannahs, and mountain forests of pinon pine and oak. The Sand Hills subregion consists of shin oak and mesquite. Desert Scrub has creosote bush flats with yucca, lechuguilla, and other small-leafed plants. The mountain ranges with higher rainfall contain woody vegetation such as junipers, oaks, pinon pine, ponderosa pine, and Douglas fir.

The High Plains are the southern extent of the Great Plains of the central United States. Elevation ranges from 914 to 1372 m above sea level and annual rainfall is 381 to 559 mm. Extended droughts have been common in this region in the last century. Vegetation consists of shortgrass prairie dominated by buffalo grass. Although historically a grassland, many other species have encroached in the region including mesquite, yucca, shinnery oak, sand sage, and juniper.

The Rolling Plains, so-called because of the rivers and numerous tributaries in the region which cause a rolling pattern, have canyons that create a sheltered habitat. Rainfall is 508 to 711 mm. The original prairie grasslands featured tall and mid-grasses such as bluestems and gramas, with an increase of buffalo grass and shortgrasses with heavy grazing. The most common vegetation community is described as mesquite-

shortgrass savannah. The stream floodplains feature various hardwood species and juniper.

The Edwards Plateau is characterized by springs, stony hills, and steep canyons. Annual rainfall ranges from 381 to 864 mm. The Edwards plateau contains shallow soils underlain by limestone and the Edwards Aquifer which creates unique aquatic cave habitats. Historically, vegetation was primarily open grassland and savannah, but now includes juniper/oak woodlands, plateau live oak, and mesquite savannah.

The South Texas Plains, also known as South Texas Brush Country, is known for its plains of thorny shrubs and trees with patches of palms and subtropical woodlands in the Rio Grande Valley. Historically, the area was primarily open grasslands and the valley woodlands were more extensive. Average annual rainfall is 508 to 813 mm. and summer temperatures are high. The deeper soils support taller trees such as mesquite and spiny hackberry, and the shallow caliche soils support short, dense brush. The Southern plains are a meeting point of semi-tropical species that occur in Mexico, grassland species in the north, and desert species found in the Trans-Pecos.

The Blackland Prairies are characterized by their dep, fertile soils. These soils once supported tallgrass prairie dominated by big bluestem, little bluestem, indiangrass, and switchgrass, though much of this land was converted for agriculture. Mesquite, huisache, and oaks have invaded abandoned fields and pecans, oaks, elms, and cottonwood occur in riparian areas. Average annual rainfall rangers from 711 – 1016 mm.

The Cross Timbers located in North Central Texas contains dense stands of trees and irregular plains. Savannah and woodlands are found in the east and south, and shorter mixed-grass prairie in the west. A combination of fire, topography, and drought have determined the location of grassland and woodland. Post oak and blackjack oak are the dominant woody plant species and bottomlands contain hackberry, elm, and pecan. The Post Oak Savana is a transitional area for many species ranges that move north to the Great Plains or East into the Pineywoods. Annual rainfall averages 711 to 1016 mm. The oak savannah is characterized by patches of post oak and blackjack oak interspersed with tallgrass prairie herbaceous species.

The Gulf Prairies and marshes region is a low-lying coastal plain dissected by streams and river flowing into the Gulf of Mexico and includes barrier islands along the coast, salt grass marshes surrounding bays and estuaries, remnant tallgrass prairies, oak mottes scattered along the coast, and tall woodlands in the river bottomlands. Average rainfall varies from 762 to 1270 mm. Native vegetation consists of tallgrass prairies and live oak woodlands, with more current encroachment of brush such as mesquite and acacias.

The Piney Woods ecoregion is distinguished by pines and oaks, rich bottomlands and tall hardwoods. This biome extends into Louisiana, Arkansas, and Oklahoma. Average rainfall is 914-1270 mm, distributed fairly uniformly throughout the year. The main vegetation assemblages can be described as pine and pine-hardwood forest, which now has cropland and planted pastures among native pasture. Loblolly pine is the most common species and shortleaf pine is found in drier areas. Longleaf pine is found in the

southeastern portion. Slash pine is used in pine plantations. Major hardwoods are oaks, hickories, red maple, and sweetgum. Bottomland forests contain various oaks including swamp chestnut, overcup, and water oak.

The variety of habitats and conditions has lent different types of evolutionary pressure. Some of these will be more conducive to future climate than others. With the precipitation gradient, more drought tolerant species are found as one moves west, as droughts are a regular occurrence in arid and semi-arid lands (Le Houérou 1996). As Texas is predicted to become hotter and drier, and droughts continue on a trajectory of longer duration and higher intensity, drought-tolerance will determine survivability of species and the future of the landscape (McDowell et al. 2008).

3.1.2. Drought adaptation

Climate is a driver of biotic systems, affecting individual fitness, population dynamics, distribution and abundance of species, and ecosystem structure and function. Regional variation in climate creates selective pressures for locally adapted physiologies and morphological adaptations (Parmesan et al. 2000). For instance, a known response to increases in mean temperature would be for different tree species to shift their range poleward and to higher elevations, thus affecting species composition, and therefore forest structure (Barry et al. 1995; Grabherr et al. 2009; Hersteinsson and Macdonald 1992; Parmesan 1996; Parmesan et al. 2000; Parmesan et al. 1999; Pounds et al. 1999; Sagarin et al. 1999; Thomas and Lennon 1999). However, there are more indirect effects on forest composition that could act through changes in disturbance regime. There is

evidence that extreme weather events can be implicated as mechanistic drivers of broad ecological responses to climate trends. Models by Miller and Urban (1999) suggest that there can be profound effects from small changes in temperature (2°C) and precipitation (20%) on forest structure and function. They found that depending on elevation, total woody biomass could decrease by more than an order of magnitude.

These large-scale range shifts take place because of differential survivability to drought stress caused by genetic variations between species but also within species. For example, Pines in Bastrop County located within Central Texas, considered the most arid natural loblolly pine habitat have been found to be more drought tolerant than those in eastern Texas (Van Buijtenen 1966; Van Buijtenen et al. 1976). Some of the drought tolerant strategies involved are more extensive root systems and rapid reductions in leaf conductance as soil moisture is depleted (Bilan et al. 1977; Van Buijtenen et al. 1976). In oaks (*Quercus spp*.), drought tolerance characteristics involve deep roots, effective water transport, xeromorphic leaves, and osmotic and elastic adjustments. Osmotic potentials are greater in oaks in more arid regions of North America (Abrams 1990).

Desert vegetation found in the Trans Pecos region and surrounding regions are highly adapted to high evaporation and low moisture. The general strategy of xerophytes is to promote uptake and reduce water loss. A plant can do this through drought evasion or drought resistance. The short-lived annuals are an example of evasions, where they evade drought in seed from, then emerge after precipitation and set seed quickly. These are characterized by a low root/stem ratio and short life cycle (Wu et al. 2002).

The large perennial plants, including the succulents (e.g. yucca) and non-succulents, are examples of drought resistors. Succulents are specially designed for water storage and retention. They store water in their tissues, have shallow but extensive roots systems, and engage in nighttime gas-exchange. Woody plants such as the honey mesquite and huisache have deep extensive roots systems and have high root/stem ratio. They have small leaves with waxy or pubescent cuticles which reflect heat and in the later case, hold moisture close to the plant surface to increase evaporative resistance. Deciduous xerophytes lose leaves during drought periods (Wu et al. 2002).

A conceptual diagram by Anderegg et al. (2013) (Fig. 21) shows the process by which precipitation deficit eventually leads to physiological damage and ultimately mortality. It is a good illustration of where different mortality drivers fit into the process that ultimately leads to death. This begins with drought translating to soil moisture deficit, the rate of which depends on climatic and edaphic factors that influence soil infiltration and evaporative demand and the plant characteristics that determine plant water uptake. The soil moisture deficits then leads to plant water stress, which is influenced by the plant's evaporative demands plus other physiological characteristics, processes and feedbacks that are dependent on seasonality and duration of the plant water stress. With sufficient physiological damage, the plant can no longer function and dies (Anderegg et al. 2013).

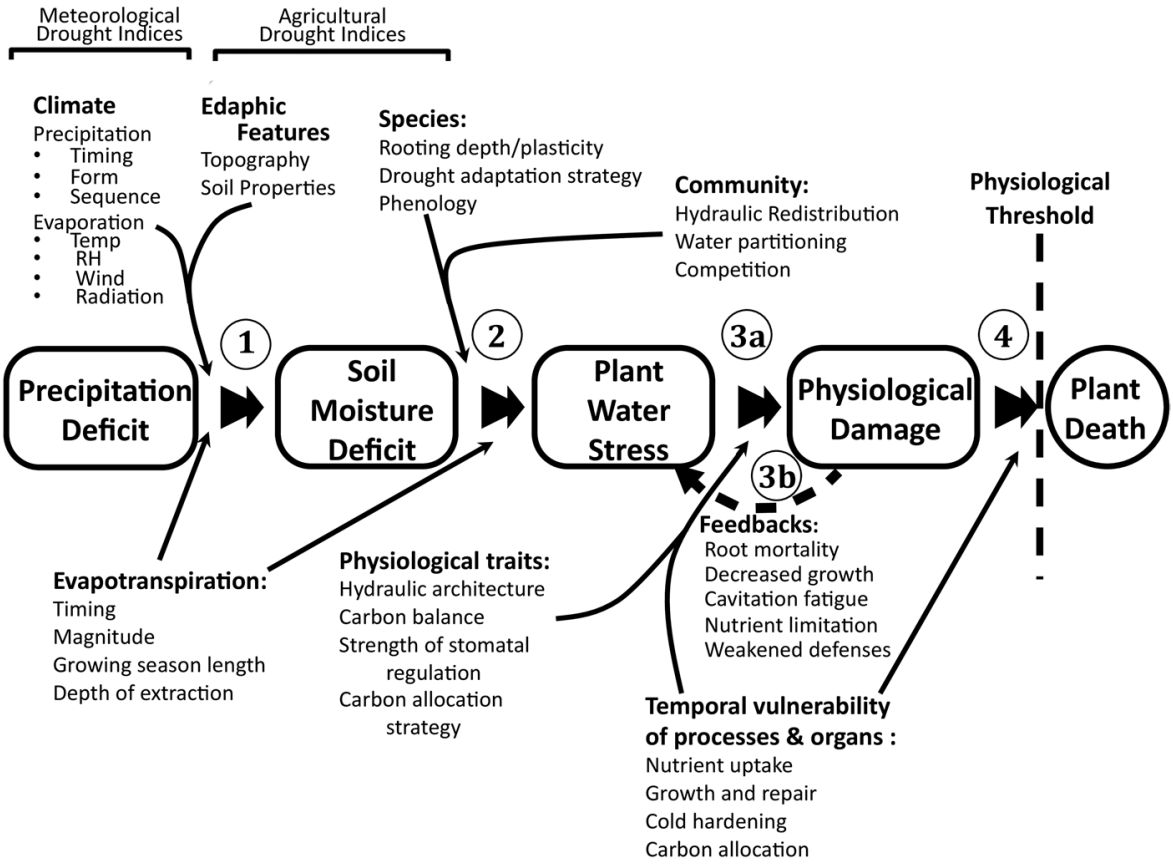

Fig. 21. Conceptual diagram by Anderegg et al. (2013) describing the process by which water deficit translates to plant mortality. Large numbered arrows represent the transition from one box to another while small arrows indicate factors that influence large arrows.

3.1.3. Species distribution models

Species distribution models (SDMs) are correlative models that use environmental and/or geographic information to explain observed patterns of species occurrences (Elith and Graham 2009) by exploiting the statistical association between spatial environmental data and the occurrences to capture processes limiting distribution (Kearney et al. 2010). They rely on a complex interdependency between theory, data,

and statistics and have been shown to perform well in characterizing natural distributions, providing useful ecological insight and strong predictive capability (Huston 2002). SDMs have been applied to a wide variety of questions, such as potential location of a known or unknown species. The answer of which is important for purposes like restoration or reintroductions. A popular use for SDMs is to determine potential climate change impacts on a particular species or on biodiversity, in which either the presently occupied area is in question or potentially suitable areas that are being predicted (Araújo and Pearson 2005; Hijmans and Graham 2006; Kearney et al. 2010; Thuiller et al. 2008).

Ranking environmental models is not usually the primary use of SDMs. However, variable importance is either built-in or can be derived from many SDMS and can be used for this purpose successfully with careful implementation and interpretation. Random forests (Breiman 2001) are the most common machine learning technique to assess variable importance. This technique is widespread in geospatial modeling and analysis in ecology, remote sensing, and carbon cycling in a number of environment types (Asner et al. 2015). For example, they have been used to determine ecological drivers of fire (Archibald et al. 2009) and treefall rate (Asner et al. 2015).

Maximum entropy modeling (Maxent) is a machine learning method that calculates the most uniform distribution with the constraint that the expected value for each variable should match the average value of a set of sample points taken from the target-species distribution (Phillips et al. 2006). One advantage of Maxent is that it is capable of dealing with continuous and categorical variables. Probability distribution is

exponential, ranging from 0 to 1. Maxent indicates probability of presence using gain, which is the average log probability of the presence samples, minus a constant that makes the uniform distribution have 0 gain. The gain indicates how closely the model is concentrated around, or a measure of likelihood of the samples. The model begins with a uniform probability distribution (gain = 0) and a weight is altered at each iteration until the probability of occurrence of the source data is maximized, increasing the gain towards an asymptote during a run. For example, a gain of 2 means the model is exp(2) or about 7.4 times higher than that of a random background pixel (Phillips et al. 2006).

Despite limitations of being a presence-only model, it has been shown to outperform established techniques such as regression-based approaches (Elith et al. 2006; Guisan et al. 2007). In a study comparing 6 different modeling techniques including random forest and boosted regression trees, Maxent performed consistently high in modeling geology, calibration, and when comparing its results to truth (Elith & Grahm 2009).

3.1.4. Climatic factors and ecological niche modeling

Maxent is often associated with climate envelope modeling. Climate envelope models are useful tools in biodiversity conservation as they can assess species vulnerability to climate change. The general approach is to circumscribe the range of climate conditions currently experienced by a species (the climate envelope) and forecast the future spatial distribution of the climate envelope according to projections of climate change, assuming the contemporary species-climate relationship will hold true (Franklin,

2009). In this study, however, we are interested only in how climate variables predict current distribution. They are constructed either from recent climate or "bioclimate variables" derived from seasonal relationships between precipitation and temperature (Table 8). Since these describe seasonal conditions and climate extremes, these are thought to be directly limiting to species, possibly more than monthly climate variables. Climate can impose physiological constraints on species and therefore helps to shape species distributions. The degree to which it does this depends on local adaptation and factors such as dispersion constraints related to habitat availability. Bioclimatic predictors are designed to better represent the types of seasonal trends pertinent to the physiological constraints of different species (Hijmans 2004; Nix 1986). For example, wettest month and seasonal anomalies will generally capture broader biological trends better than the temperature or the amount of precipitation for a given day due to the inherent variability associated with weather.

A few studies compared long-term (climate) and short-term (weather) variables in their performance in species distribution models. Watling et al. (2012) compared model performance between climate envelope models created with bioclimate variables and models created from monthly variables, finding no difference in performance. They concluded that when using a high performance algorithm such as random forests, using bioclimate or monthly variables for modeling does not significantly alter spatial predictions, Stankowski and Parker (2010), with GLMs, however, found that monthly variable- produced models outperformed those made with bioclimate variables. Similarly, Reside et al. (2010) argue that SDMs require an organism-relevant temporal

scale to optimally model the species and that weather models largely outperform climate models. Even for sedentary species which may shift due to local weather events or whose distribution may be limited by extremes, these two factors that are better explained by weather models than climate (Reside et al 2010).The conflicting results of these variables on model performance are likely due to modeling technique and parameters used for each.

Few studies have closely considered the ecological implications behind the relative importance of variables for driving distributions. Use of weather and use of climate data to model distributions, besides causing (or not causing) differences in predictive capability, answer different questions related to potential vs. realized niche. It is a premise of biogeography that climate exerts dominant control over the distribution of species, as seen in the fossil record (Davis and Shaw 2001; Huntley 1999; Woodward 1987) and observed trends (Hughes 2000; McCarty 2001; Walther et al. 2002). Therefore, long-term climate envelopes would be more descriptive of a fundamental niche, or the set of resources a population is theoretically capable of using under ideal conditions, given that the species of interest have the potential to exist at these climatic locations and given assumptions of niche conservatism. Because long-term climate is to varying degrees associated with ecoregions and species biogeography, it is somewhat descriptive of the adaptive characteristics. Modeling distributions with shorter term climate or weather conditions puts more constraining assumptions on a species distribution as it assumes that their present locations are related to relatively recent conditions. As you shorten the length of time of the average conditions, the conditions

become less descriptive of biogeography related to long-term climate and more about the weather conditions at hand. Short-term climate has also been found to be useful in determining the types of variables with which organisms associate themselves, but represent short-term conditions at the geographic locations so these may be more suited for answering question related to species responses to short-term events. When using short-term climate to model distribution, you assume the species of interest are able respond to the conditions within time interval from which the weather conditions were averaged.

If climate can be effectively used to describe the geographic limits of an organism's existence, it stands to reason that the inverse is true - that the same abiotic conditions can be used to explain where an organism *cannot* exist, the limits of mortality, when training a model with locations of dead. In fact, modeling the response of tree species to a short-term disturbance is only possible if using dead trees rather than live trees as indicators. In this study, a species distribution modeling approach was used to model drought-killed trees due to the 2011 Texas Drought throughout the state with the of aims of determining 1) which type of climatic variables are the more important drivers of mortality distribution: the extreme conditions during the year of drought, or long-term average climatic conditions; and 2) which long-term and/or immediate condition best explains mortality patterns? Answering this question should provide information on whether it was adaptive characteristics which predispose trees to mortality that better predict dead tree distribution, or whether it was the extremity of the conditions themselves that explained the distribution of mortality in this drought.

Though both are important for determining whether a plant will ultimately die from drought, I test the hypothesis that the drought conditions of 2011 were extreme enough that it was these short-term conditions that were the dominant drivers on the regional scale.

3.2. Methods

3.2.1. Occurrence data

The same field plot data described in Chapter 2 was used to train a model of dead trees based on short- and long-term climate conditions. Briefly, extensive field sampling across Texas was conducted in June of 2012, ultimately producing 599 plots which tallied trees ≥12.7 cm that died due to the drought (Moore et al. 2016). Texas was divided into 10 regions, then plots were selected within each using a two-stage unequal probability sampling with replacement (Lohr 1999). A 10 km x 10 km grid was overlaid on a forest distribution map (Wilson et al. 2012) creating a list of primary sample units (PSUs). PSUs were selected from these using an unequal probability sample design. Within each selected PSU, seven 0.16 ha circular plots were randomly selected. This data provided the occurrence locations of 1800 identified drought-killed trees used to produce the tree mortality model.

3.2.2. Bioclimate variables

The contributions of climatic variables were derived from the 30 arc-second (~1 km) WorldClim database version 1.4. These so-called “bioclimatic variables” were

derived from the monthly temperature and rainfall values (~1950-2000) in order to generate more biologically meaningful variables (Hijmans et al. 2005). Highly correlated variables can confound interpretations of contributions of individual variables. Therefore, a Pearson's correlation test was run on all 19 bioclimatic variables (Table 8) to ensure a degree of independence of each variable being used to explain dead tree distribution. Prior to the correlation test, each climate variable was checked for normality and log transformed if necessary. Variables were considered highly correlated if the coefficient was ≥ 0.65. When deciding between two correlated factors to keep in the model, variables were kept that represented different kinds of information that could

Table 8

Nineteen bioclimatic variables derived from the WorldClim database.

Bioclim abbreviation	Variable description
BIO1	Annual Mean Temp (C)
BIO2	Mean Diurnal Range (C)
BIO3	Isothermality (100 * BIO2 / BIO7)
BIO4	Temp Seasonality (100 * SD)
BIO5	Max Temp of Warmest Month (C)
BIO6	Min Temp of Coldest Month (C)
BIO7	Temp Annual Range (C) (BIO5-BIO6)
BIO8	Mean Temp of Wettest Quarter (C)
BIO9	Mean Temp of Driest Quarter (C)
BIO10	Mean Temp of Warmest Quarter (C)
BIO11	Mean Temp of Coldest Quarter (C)
BIO12	Annual Precip (mm)
BIO13	Precip of Wettest Month (mm)
BIO14	Precip of Driest Month (mm)
BIO15	Precip Seasonality (CV)
BIO16	Precip of Wettest Quarter (mm)
BIO17	Precip of Driest Quarter (mm)
BIO18	Precip of Warmest Quarter (mm)
BIO19	Precip of Coldest Quarter (mm)

explain distribution. These included: a long-term average trend, temperature "evenness", seasonal variation, an extreme, an interaction variable, and a precipitation variable.

3.2.3. 2011 variables

In order to do a direct comparison between long-term and short-term climate, the same precipitation and temperature-related variables were calculated for 2011 only, the year of the drought (also referred to here as "weather" variables). The six variables that were calculated were chosen based on the correlation results. Monthly mean, maximum, and minimum temperature values; and annual precipitation were downloaded for 2011 from the PRISM climate group website (http://prism.oregonstate.edu). These spatial climate datasets are 4-km grids. PRISM (Paratmeter-elevation Regressions on Independent Slopes Model) is a climate-mapping technology that uses point observational data, a digital elevation grid, and other spatial data sets to generate estimates of climatic variables on a grid. The model is a climate-elevation regression calculated for each DEM grid cell, and stations surrounding the grid cell are entered in the regression and are assigned weights based on the physiographic similarity of the station to the grid cell. Location, elevation, coastal proximity, topographic facet orientation, vertical atmospheric layer, topographic position, and orographic effectiveness of the terrain were among the factors considered in the weighting (Daly et al. 2008).

ArcGIS raster calculator was used to compute 2011 variables with PRISM that corresponded to the selected long-term average bioclimatic variables (Table 8). All data

were extracted within the bounds of Texas, precisely coregistered, and projected in GCS North American 1983 coordinate system. The raster data products were reprojected with nearest neighbor resampling to maintain the pixel values, and resampled to 250-m output pixel dimensions. Although the smallest pixel size in this analysis is 1 km, 250 m dimensions were used in order to match dimensions in the next analysis.

3.2.4. Analysis

Conventional statistical models cannot be used for investigating the drivers of tree mortality in the context of this study because many of the relationships were nonlinear, with non-additive predictor-response interactions. Therefore, a habitat suitability approach was used to predict areas most likely to contain drought-related tree mortality. The Maxent algorithm constructs a habitat suitability model using dead tree occurrence data and environmental variables to predict geographic areas where there are likely to be other occurrences and calculates a percent contribution for each of the variables and their percent contributions (Phillips et al. 2006).

A model was trained with 70% of the occurrences and tested with the remaining 30%, which were randomly assigned from the original plot-level observations. Background points are random samples from the environmental data that are used by Maxent as "pseudo-absences" for model evaluation. To ensure that these were taken from forested areas similar to the locations from which the samples were taken, the training area was limited to 78.5-km^2 circular areas around each of the field sampling locations. The model was then applied only to areas where values of the environmental

variables were within their respective range of values within the training area. The models were evaluated using receiver operating characteristic (ROC) analyses and binomial tests of omission. The ROC curve describes the sensitivity of the model, the increase of occurrence data that is predicted as area of prediction increases. The area under the receiver curve (AUC) is the probability that a randomly chosen presence site will be ranked above a randomly chosen background site. A perfect model would have an AUC of 1.0 and a random model would have an AUC close to 0.5 (Phillips and Dudík 2008). Models with an AUC greater than 0.75 are considered potentially useful (Elith 2000).

First, I ranked 2011 and bioclimatic variables separately to control for those factors and see how each type of variable would influence the dead tree distribution independently. Then to test the ranking between drought year conditions and bioclimatic conditions, both were put into the model and percent contribution of each variable was compared. Variable importance is calculated by adding/subtracting the increase/decrease in regularized gain to the contribution of the variable for each iteration of the training algorithm. Jacknife tests in Maxent calculate gain of the training data, gain of the held back test data, and the AUC of test data for each variable. These give the variable with the highest gain or AUC when used in isolation and which variables decrease the gain or AUC the most when omitted. All of these measures of variable importance were evaluated in the models.

One concern for including too many variables to model distributions is overfitting the model to the data; however, in this case, the data were not being used as

independent variables in a statistical model with the aim of explaining variance in the independent data. Rather, the purpose was to rank variables by using them to characterize a multivariate environmental space of high probability of dead tree occurrence. The idea is that the variables that were most closely associated with the dead tree distribution will be those that emerge as influential in the habitat suitability model, whereas the ones that were not associated with the geographic distribution will have little or no effect on the model.

Table 9
Correlations between the 19 bioclimactic variables. Highly correlated variables are in bold.

	bio1																	
bio2	-0.59	bio2																
bio3	-0.01	0.59	bio3															
bio4	-0.58	0.27	-0.51	bio4														
bio5	0.33	-0.02	-0.31	0.33	bio5													
bio6	**0.93**	**-0.74**	-0.09	**-0.67**	0.08	bio6												
bio7	**-0.68**	0.58	-0.19	**0.90**	0.30	**-0.84**	bio7											
bio8	0.44	0.07	0.43	-0.32	0.26	0.28	-0.18	bio8										
bio9	0.53	-0.58	-0.30	-0.23	0.08	0.62	-0.45	-0.12	bio9									
bio10	**0.69**	-0.49	-0.42	-0.02	**0.79**	0.54	-0.17	0.36	0.31	bio10								
bio11	**0.96**	-0.53	0.16	**-0.72**	0.15	**0.94**	**-0.78**	0.46	0.50	0.52	bio11							
bio12	0.34	**-0.70**	-0.44	-0.16	-0.26	0.57	-0.48	-0.29	0.63	0.04	0.35	bio12						
bio13	0.39	**-0.74**	-0.48	-0.17	-0.15	0.58	-0.47	-0.22	0.56	0.17	0.37	**0.91**	bio13					
bio14	0.40	**-0.71**	-0.40	-0.20	-0.23	0.62	-0.53	-0.26	**0.65**	0.09	0.42	**0.99**	**0.89**	bio14				
bio15	-0.35	**0.65**	0.41	0.14	0.21	-0.57	0.45	0.32	**-0.71**	-0.05	-0.37	**-0.97**	**-0.84**	**-0.97**	bio15			
bio16	0.28	**-0.72**	-0.47	-0.16	-0.31	0.52	-0.49	-0.32	0.57	0.02	0.28	**0.98**	**0.93**	**0.95**	**-0.91**	bio16		
bio17	0.39	**-0.69**	-0.40	-0.20	-0.22	0.61	-0.51	-0.27	**0.66**	0.07	0.41	**0.99**	**0.90**	**0.99**	**-0.98**	**0.95**	bio17	
bio18	0.27	-0.62	-0.23	-0.33	-0.45	0.53	-0.60	-0.21	0.43	-0.10	0.33	**0.89**	**0.81**	**0.87**	**-0.82**	**0.91**	**0.86**	bio18
bio19	0.38	**-0.68**	-0.40	-0.19	-0.23	0.60	-0.50	-0.29	**0.70**	0.06	0.40	**0.99**	**0.88**	**0.98**	**-0.98**	**0.95**	**0.99**	**0.85**

3.3. Results

3.3.1. Correlation results and variables used

Based on the correlation results (Table 9) and hypotheses on what climate factors would influence drought-related tree mortality, the model was reduced to 6 relatively uncorrelated climate variables. These included mean average temperature, isothermality, temperature seasonality, maximum temperature of warmest month, mean temperature of wettest quarter, and annual precipitation. Mean average temperature represented a long-term average trend. Isothermality is the average monthly diurnal range divided by the mean annual temperature range (O'Donnell and Ignizio 2012). This can be thought of as temperature evenness or variability over the course of a year. It quantifies how large the day-to-night temperatures oscillate relative to summer-to-winter (annual) oscillations. An isothermal value of 100% indicates that the diurnal temperature range is equivalent to the annual temperature range. Including this variable in the model will see if the dead tree distribution was influenced by larger or smaller temperature fluctuations within a month relative to the year. Temperature seasonality is calculated as the standard deviation of the mean monthly temperatures over the year and represents average seasonal variation. Isothermality and temperature seasonality are measures of weather variation. The amount of temperature variability in a location, assuming that the trees present within those locations are adapted to the temperature variability at the location, may play a role in vulnerability of some tree species to drought. For example,

trees that are adapted to more variable environments may be better equipped to deal with the extreme conditions of a drought.

Maximum temperature of warmest month represents an extreme environmental factor. This variable in a model would tell us whether species distributions are affected by ranges of extreme temperature conditions. Extreme variables are often found to be the limiting factors for species ranges (Oliver et al. 2009). The mean temperature of wettest quarter is the calculated average temperature for the three months with the highest cumulative precipitation total. This variable is a combination or interaction between temperature and precipitation, which could potentially offer an element of variability not found in temperature and precipitation variables in isolation. Annual precipitation was included as the representative precipitation variable.

3.3.2. Bioclimate and 2011 variables modeled in isolation

The 2011 variables model had a test AUC of 0.86. Annual precipitation contributed the most (26%) followed by isothermality (23%) and temperature seasonality (Table 10). Probability of dead tree presence generally declined with increasing precipitation (Fig. 22) and increasing isothermality (Fig. 23). The bioclimate variables model had a test AUC of 0.79. The top three variables were annual precipitation, temperature seasonality, and mean temperature of wettest quarter. Here, dead tree probability also showed a general decline with increasing annual precipitation.

3.3.3. Relative contributions of bioclimate and 2011 variables

The resulting model with all twelve (climate and temperature) variables had an AUC of 0.84. Variable rankings found that 17% of the variability of dead tree

Table 10
Contribution rankings of models separated by variable type.

2011 variables	% contribution	Bioclimatic variables	% contribution
Annual precip	26.1	Annual precip	47.5
Isothermality	22.6	Temp seasonality	17.9
Temp seasonality	16.1	Mean temp of wettest quarter	17.2
Max temp of warmest month	14.4	Max temp of warmest month	8.1
Annual mean temp	12.1	Annual mean temp	5.3
Mean temp of wettest quarter	8.7	Isothermality	4.0

occurrence could be explained by long-term annual precipitation (Table 11). 2011 isothermality was the next most important variable, contributing 16%. This was followed by two more short-term variables: 2011 annual precipitation and 2011 temperature seasonality, which contributed between 13 and 11%, respectively. Altogether, climatic variables explained 43% and 2011 variables explained 57% of dead tree distribution. Long-term averages of isothermality and annual mean temperature ranked the lowest (<3%). The probability of dead tree occurrences generally declined with annual precipitation, which follows a strong east-to-west gradient in Texas (Fig. 24). The highest ranking 2011 variable, isothermality, showed a general decline with increasing seasonality (Fig. 25).

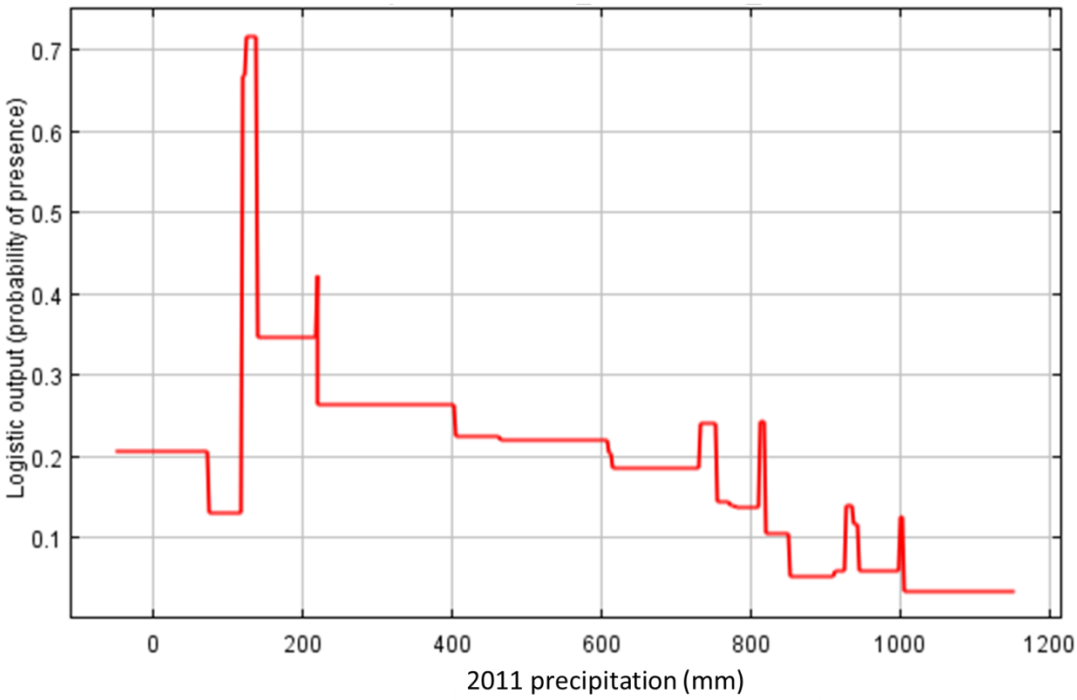

Fig. 22. The 2011 climate variables model prediction probability response of dead trees as function of 2011 precipitation when keeping other variables at average value.

A comparison of each variable between long-term average and 2011 revealed that isothermality had the highest discrepancy between the two conditions in predictive ability (14%, Table 12), followed by annual mean temperature (6%). The map shown in Fig. 26 shows the spatial prediction of dead tree probability of occurrence. White indicates areas where no prediction occurred, due to being defined as non-forest, an area of 2011 fire occurrence, or an area that was masked out because of the presence of one or more variables with values outside of those within the model training range and

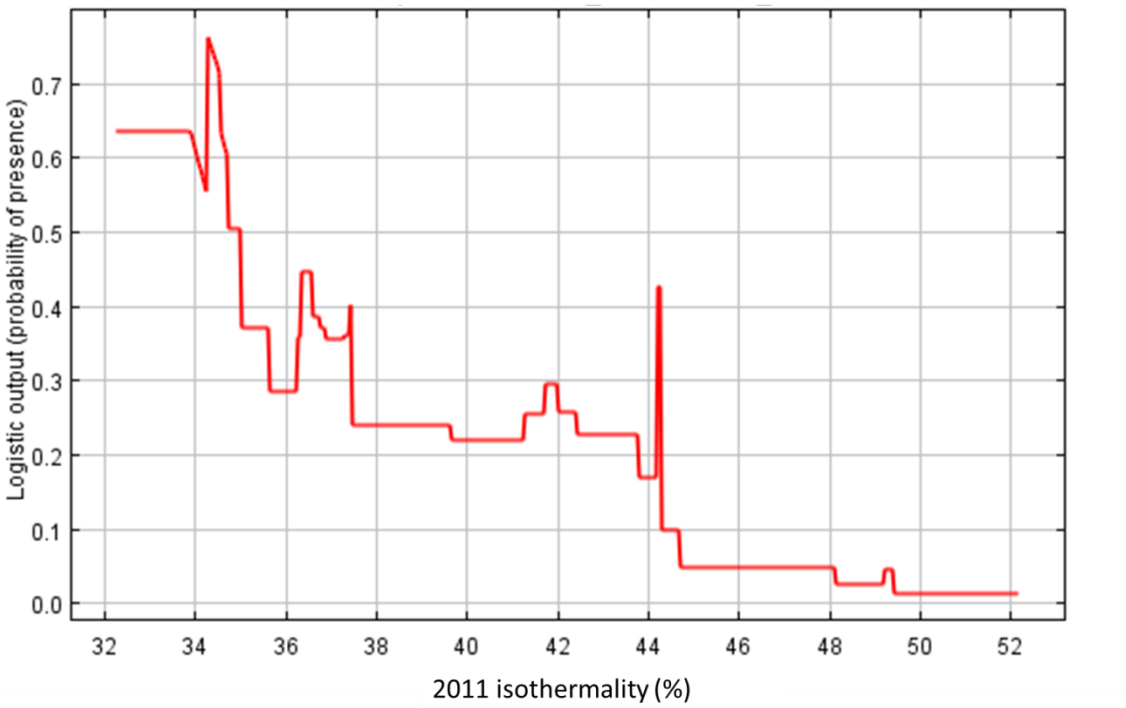

Fig. 23. The 2011 climate variables model prediction probability response of dead trees as function of 2011 isothermality when keeping other variables at average value.

therefore would be an unreliable prediction. The prediction map shows high probability throughout the eastern regions of Texas, the Brazos Valley, and hotspots located in the Panhandle and eastern and western portions of Central Texas (Figs. 26 and 27). The model predicts the highest mean probability of occurrence in the Southeast-west region and lowest probability in the neighboring Southeast-East region (Fig. 27).

Table 11
An estimate of relative contributions of environmental variables to the Maxent model.

Variable	Percent contribution
Annual precip	17.1
2011 isothermality	16.3
2011 annual precip	13.0
2011 temp seasonality	11.2
Temp seasonality	10.2
Mean temp wettest quarter	9.1
2011 mean temp	7.3
2011 mean temp wettest quarter	4.6
2011 max temp warmest month	4.3
Max temp warmest month	3.3
Isothermality	2.7
Annual mean temp	1.0

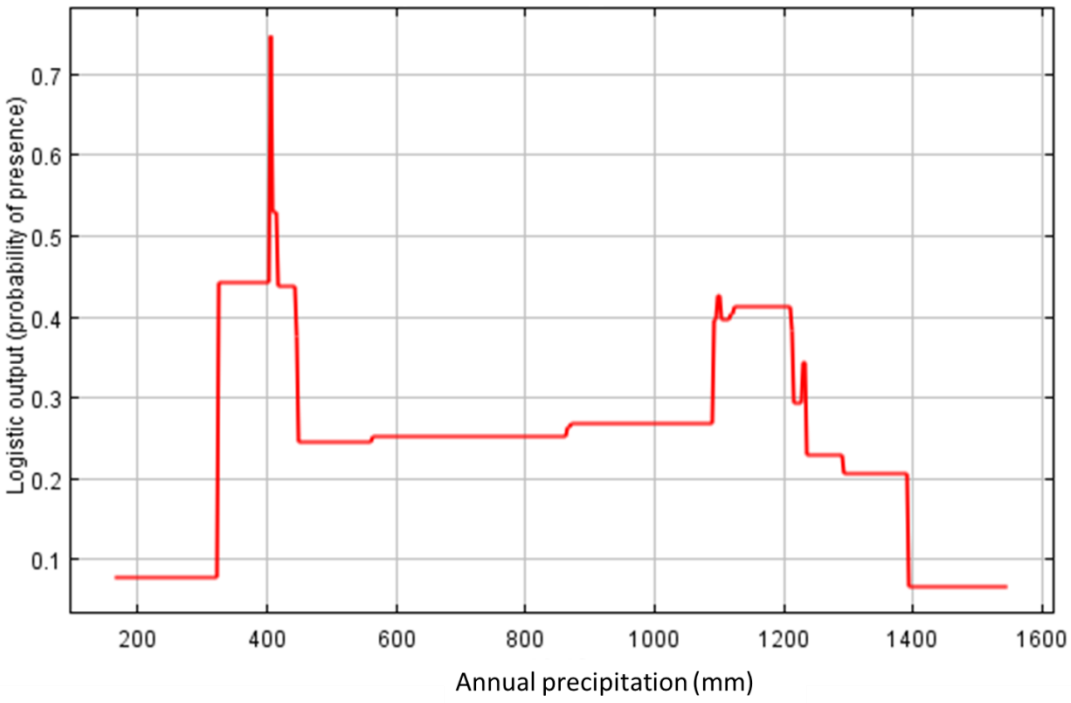

Fig. 24. The combined model prediction probability response of dead trees as function of annual precipitation when keeping all other variables at their average value.

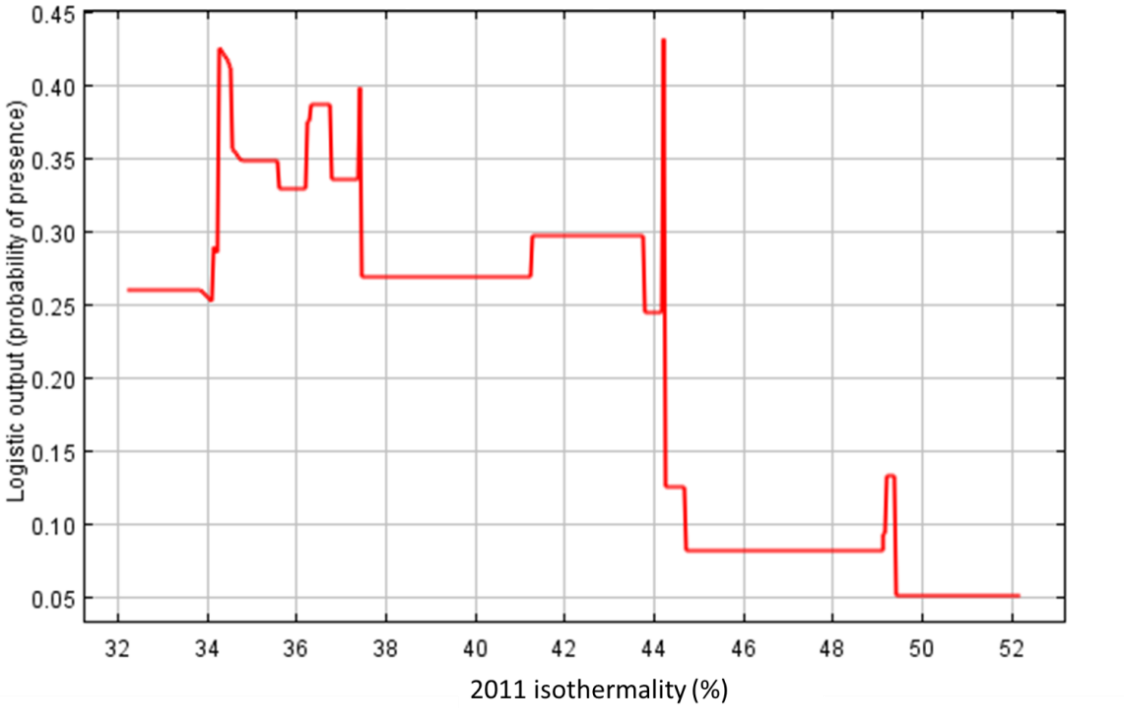

Fig. 25. The combined model prediction probability response of dead trees as function of 2011 isothermality when keeping other variables at average value.

Table 12
Difference in percent contribution between the bioclimatic variable and corresponding 2011 variable. Negative values indicate that the 2011 variable contribution was higher.

Variable	Percent difference
Annual precipitation	4.2
Isothermality	-13.6
Temperature seasonality	-1.0
Mean temp of wettest quarter	4.5
Annual mean temperature	-6.4
Max temperature of warmest month	-1.0

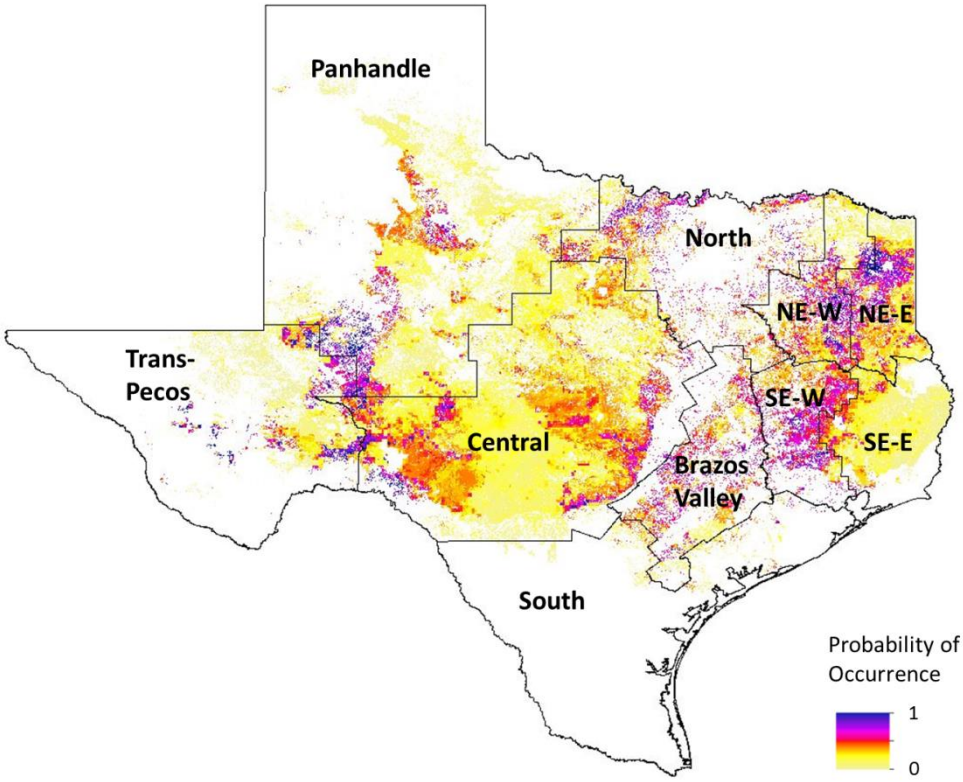

Fig. 26. Spatial representation of Maxent model prediction of dead tree occurrence using bioclimatic and 2011 weather conditions.

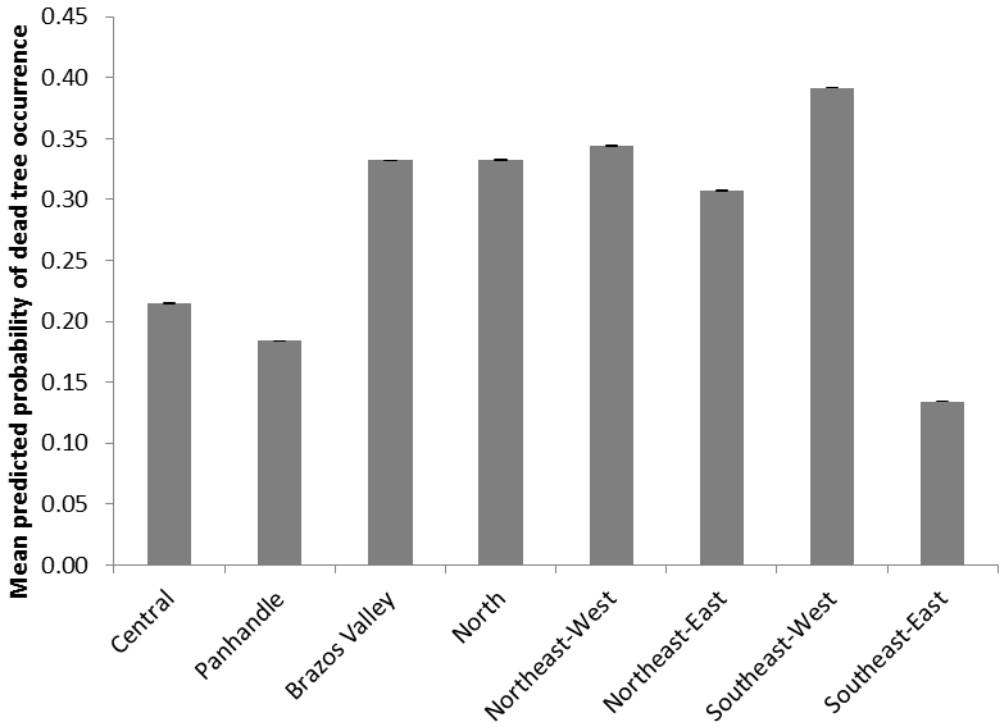

Fig. 27. Mean predicted probability of dead tree occurrence by FIA region.

3.4. Discussion

By separating the variable types into different models, a few insights were gained prior to directly comparing one variable type against the other. The model using only 2011 variables explains which drought factors play a role in mortality distribution if there were no long-term climate effect, i.e., all vegetation in Texas had the same characteristics and life histories. In this hypothetical scenario, not surprisingly precipitation had the greatest contribution to drought mortality. When examining the relationship of dead tree occurrence probability with 2011 precipitation, there is a

general downward trend indicating that drought-killed trees were more likely to be in areas that received less precipitation, which leads to the natural assumption that water deficiency leads to evaporative stress, ultimately leading to mortality. Isothermality, or daily temperature oscillation relative to annual temperature oscillation, was the second highest contributor at 23%. The relationship of probability dead tree presence with isothermality shows a steep downward trend, indicating that, in a uniform climate environment, trees in regions that had average daily temperature isolation that were much different from the average temperature range of 2011, were more likely to be killed by drought. Put another way, trees that experienced erratic fluctuations throughout the year as opposed to those in regions where fluctuation was more even, were more susceptible to drought. As a measure of variability, it is not surprising that this may play a role in drought mortality. More studies would be needed to firmly place a link between isothermality and drought vulnerability.

Modeling the bioclimate variables in isolation gave information on which climate variables are most important in determining dead tree distribution in the absence of any short-term climate variability. Here, annual precipitation was the highest contributor to the model, but by a much wider margin than in the 2011 model. Though less of a clear pattern, the relationship is also generally negative, showing higher probability of mortality in regions with less precipitation. Isothermality had a notable difference in percent contribution between the 2011 and long-term versions (14%, Table 12). 2011 isothermality ranked second, and long-term isothermality ranked last. This discrepancy

may be a result of the departure from average temperature oscillations of 2011, which would have exposed trees to temperature oscillations outside of their normal range.

The combined model allowed the comparison of long-term variables and corresponding drought variables. Two out of the six different climate variables had their long-term version out-contribute the short-term version, including annual precipitation and mean temperature of wettest quarter (Table 12). That the long-term climate rather than the condition during the time of drought was more dominant in the model may be an indication that for these variables, it was the response of the species of those particular climate regions to extreme conditions, rather than the intensity of the conditions themselves, that indicated risk. The dominance of annual precipitation is a possible indication that trees adapted to high rainfall are more vulnerable to drought, up to a particular threshold.

The combined model predicted areas of high mortality in both wet and dry areas of the state and areas in-between (Fig. 26). One reason for this is differential survival of tree species within their communities. A genus-level evaluation of tree mortality from the 2011 Texas Drought using all of the same plot data used in this modeling exercise found that different types of genera from different areas of the state suffered disproportionately from others (Moore et al. 2016). They also found apparent spatial thresholds of survival of genera associated with the dominant species of the genera in the area. Oaks suffered high mortality overall, but particularly in the eastern regions, where the dominant species is *Quercus nigra*, compared to the Brazos Valley to west where the dominant species are *Q. fusiformis* and *Q. Stellata*. Elm mortality was much higher in

the Brazos Valley compared to Central Texas, where the dominant species shifts to *Ulmus crassifolia*. For junipers, survival was high in North Texas and Panhandle regions where *Juniperus pinchotii* dominates, but disproportionately high in Central Texas where most are *J. ashei*.

Overall, Moore et al. (2016) found a generally uniform rate of mortality across the regions. This agrees with the Maxent results when looking at how the bioclimatic variables predicted spatial mortality, and the fact that these variables were less dominant drivers than the 2011 drivers. Despite the fact that Texas has such a pronounced precipitation gradient, it could be the adaptations of the taxa to their environment that produced an equalizing effect on the distribution of mortality caused by this drought.

Contribution of both variable types came out to be roughly even, showing that both are important for predicting dead tree distribution. Likely, it is the severity of the drought at hand that would influence predictive contribution. In the case of the 2011 drought, precipitation deficits were so high that it is not surprising that these variables contributed more to the model. However, bioclimatic variables played a significant role as well, meaning that the local adaptation of the trees was important in determining if and where they died. In a hypothetical situation where species distributions were uniform across the state, it would be easier to get a clear picture of where the drought had the most effect. This not being the case, the bioclimatic variables give us general vegetation zones that tell us where some species can survive well in one region versus another, and see how these adaptations play a role in drought mortality. It is this type of differential survival probability to varying conditions that drives range shifts (Davis and

Shaw 2001) and extreme events or conditions, such that the 2011 variables represent, drive these changes, putting vegetation in an immediate "live or die" situation.

Movement of ranges with climate change has always occurred and is evident in the fossil record. For example, through radiocarbon dating, scientists have reconstructed the northern tree line shifts in Russia that correspond with climate changes in the region (Kremenetski et al. 1998). In North America, there is paleoecological evidence for changes in terrestrial vegetation during an episode of climate warming between 5,000 and 4,000 years ago at the boreal treeline in central Canada as the tundra transformed to forest-tundra (MacDonald et al. 1993). What is less understood is how climate extremes and their increasing frequency affects range shifts. In the quaternary, there is evidence that adaptation and migration have played important roles in how species respond to climate change, however, rapid climate change can interrupt this process by not allowing for adaptation. Instead of steady migrations of woody species as were observed as climate warmed at the end of the last glacial interval (Davis and Shaw 2001), extreme events cause massive die-offs (Allen et al. 2010), which can cause extirpation, extinction, and an uncertain future for the landscape.

Range limits are often determined using mean values of climatic variables, however, with increasing frequency of climate extremes, it is important to further investigate the role these play in influencing range limits. Species distribution models were found to improve with the inclusion of measures of extremes (Zimmermann et al. 2009). By looking at mortality from a specific event, this study was able to, to some degree, determine how range limits were enforced by this particular extreme event and

determine the relative role of long-term factors vs. the extreme event factors. The finding that the contribution of bioclimate and 2011 variables were roughly even, but 2011 variables came out slightly ahead (57% vs. 43%), confirms the hypothesis that, although species distributions play a significant role, it was the 2011 departures from normal conditions put trees under extreme conditions outside their tolerance for drought, ultimately driving the distribution of mortality.

4. THE RELATIVE CONTRIBUTION OF CLIMATIC, EDAPHIC, AND BIOTIC DRIVERS TO RISK OF TREE MORTALITY FROM DROUGHT

4.1. Introduction

It is well known that species responses to drought differ (Engelbrecht et al. 2007; Lei et al. 2006; Peñuelas et al. 2007), the duration and severity of drought impacts plant survival (Adams et al. 2009; Mafakheri et al. 2010; McDowell et al. 2008), and edaphic conditions control the relative amount of water available to plants during drought (Baldocchi and Xu 2007; Seyfried et al. 2005; Svenning and Skov 2005). However, models that incorporate biotic, climatic, and edaphic drivers have not been extensively tested. As discussed in the previous section, long-term average climate defines general vegetation boundaries. However, edaphic factors likely influence tree range limits in a way that imposes even sharper gradients and boundaries than those imposed by climate alone because of the scale at which these factors are distributed in the landscape; for example, soil composition and source and sink zones which directly control water availability. Lastly, biotic factors determine how the plants deal with soil water deficit and in the case of forest density, water availability.

Actual drought mortality events are the ideal testbed for better understanding the relative contribution of known drivers of mortality. The 2011 drought may show that widespread drought has varying effects of tree mortality across the landscape. Understanding the cause of this variation is not simple because tree mortality is influenced by multiple factors including long-term climate trends (Luo and Chen 2013),

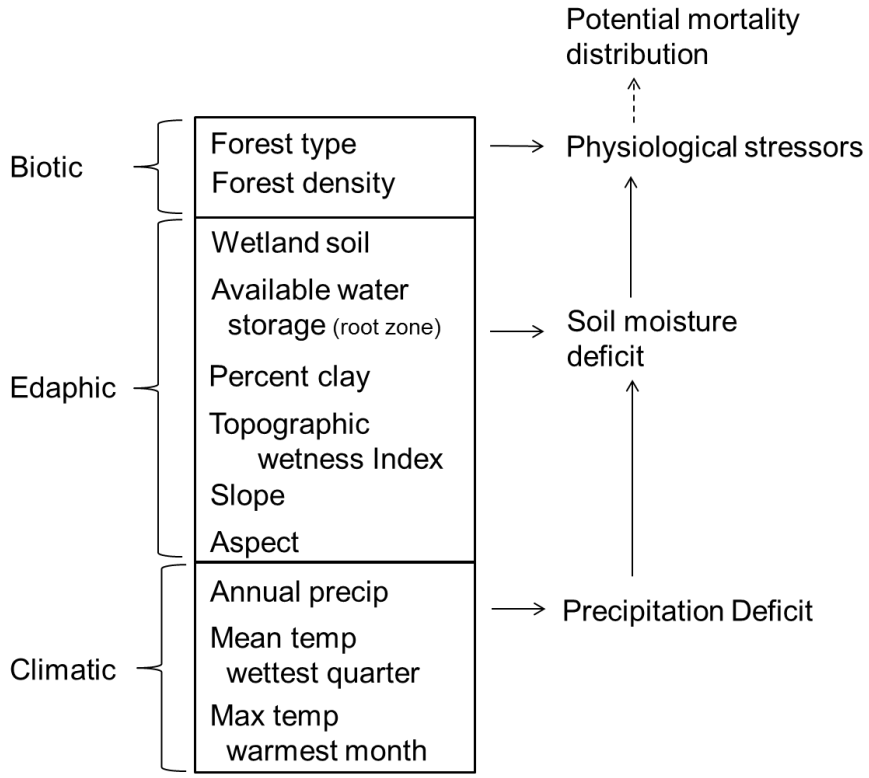

Fig. 28. Theoretical model of the biotic, edaphic, and climatic factors affecting tree mortality. Items in boxes are indirect factors that can be measured. Items on the right are direct drivers of drought-related mortality.

timing and duration of local drought conditions, functional type, position on the landscape, predation, and competition with other vegetation among other possibilities. Additionally, the importance of these factors is dependent on the scale of observation. Quantitative methods can now be applied to address these questions that previously relied on anecdotal information or local studies.

For this study, I tested known drivers of drought stress that could lead to mortality. In the precipitation deficit to plant death continuum (Fig. 21), the test variables fall under climate and edaphic features, which drive soil moisture deficit; and

species factors, which influence plant water stress. Selection of appropriate environmental factors was based on a conceptualization of the drivers of mortality from drought (Fig. 28). The biotic factors selected for the model were forest type and density. The edaphic factors selected for the model were wetland soil, topographic wetness index, available water storage in the root zone, percent clay content, slope, and aspect. The climatic factors selected for the model were long-term annual total precipitation, average temperature of the wettest quarter, and maximum temperature of the warmest month. The following section provides further justification for the use of these variables in the model.

4.1.1. Forest density and forest type

Forest density is widely associated with risk of mortality from competition for resources. Areas with denser vegetation have higher soil water depletion rates due to increased competition for the resource. In oak forests it has been shown that thinning stands lead to higher predawn leaf water potential; and decreases in interception and transpiration leading to increased water availability (Bréda et al. 1995). However, there is threshold for which low density leads to greater water availability. In an experiment using tree density gradients, it was found that the least dense stand was not the most ideal due to low water retention (Gouveia and Freitas 2008).

Species composition differs greatly with ecoregion and management regime, which is represented by the variable “forest type”. A species may have a competitive advantage over another for water by 1) acquiring a greater proportion of available soil

water, 2) using water and nutrients more efficiently in producing biomass, or 3) allocating in ways that maximize survival and growth (Nambiar and Sands 1993). In the face of water limitation, plants have developed different physiological strategies for coping. For example, two widespread species in central Texas, live oak and Ashe juniper, have contrasting strategies. Isohydric species close stomata to reduce risk of catastrophic hydraulic failure, but in doing so risk the consequences of carbon starvation which ultimately causes mortality (McDowell et al 2008). Anisohydric species in contrast do not risk carbon uptake with stomatal closure, making them more prone to mortality via hydraulic failure.

4.1.2. Soils

During the 2011 drought, it was observed that deeper-rooted trees on deep soils were experiencing relatively higher mortalities than those constrained by shallow soil. One localized investigation following the 2011 Texas Drought found significantly higher tree mortality in deep soils than in shallow soils or rock draws (Twidwell et al. 2013). Deeper – rooted plants that are dependent on groundwater during season drought are more able to tolerate moderate drought but are likely more vulnerable to extreme or sustained drought as their groundwater source is depleted (Froend and Drake 2006). Visual evidence for this has been observed throughout the state, but a large scale study is needed to test whether trends are widespread. Since 2010 was a wet year for Texas, this may have contributed to the high mortality response to the 2011 drought as some plants

in may have responded to the wet year with increased aboveground biomass disproportionately to belowground root growth (Lytle et al. 2004).

Available water storage at the root zone (AWS_{rz}) is hypothesized to be a dominant factor that determines the survivability of trees during drought. Low soil water potential can kill or weaken a plant by constraining carbon assimilation, causing desiccation to the point of catastrophic cavitation, or both (McDowell et al. 2010). AWS_{rz} is controlled by soil texture and rooting depth. More AWS_{rz} give plants an advantage during light to moderate dry periods; e.g., trees in topographic sinks are relatively protected from stress and mortality (Breshears and Barnes 1999). However, in prolonged or severe drought, plants adapted to grow in high AWS_{rz} conditions may be more vulnerable as water availability declines to unprecedented levels or as water tables fall below root zones (Breshears et al. 2005). Clay is also thought to play a role in plant survivability. It is shown to be important for plant function during drought because of its water retention properties (Cosby et al. 1984; Williams et al. 1983).

4.1.3. Topography

Across the landscape, topography defines the pattern, number, and frequency of source and sink zones, which in turn, control the spatial distribution of vegetation and water availability (Ludwig et al. 1995; Thompson et al. 2011). In terms of the influence of slope on tree mortality, it has been hypothesized that soil moisture is higher in flat benches and bottom slopes during normal years; therefore, rooting is relatively shallow and clones are more susceptible to drought mortality (Worrall et al. 2008). Aspect has

direct and indirect influence on solar radiation, surface temperature, evaporation, soil moisture, and precipitation of an area. North-facing aspects are generally considered to generate wetter and cooler micro-climates in the northern hemisphere and south-facing aspects form drier and hotter climates with higher soil water depletion rates. The topographic wetness index quantifies topographic control on hydrological processes an indicates water availability as a function of upstream contributing area and slope (Sörensen et al. 2006).

4.1.4. Possible effects of scale and location

This study will look at the effects of both scale and location. Climate is more likely to drive mortality on a regional scale because climate determines broad ecological regions which in turn define general vegetation zones. Studies have found that ecotones separating vegetation zones are sensitive to climatic conditions (Brubaker 1986; Houle and Filion 1993; Loehle 2000; Schwarz 1997). However, on a finer scale, within climate zones, edaphic factors are likely to play an important role because within climate zones or ecoregions, soil composition and topography will ultimately determine available water storage at the community and individual level, which determines plant water deficit then death. This is why I hypothesize that AWSrz which should be a direct determinant of that would be a driving variable. When it comes to location, it is likely that mortality in mesic areas more driven by biotic factors. If the mesic regions have more water storage and water than the xeric regions, it may be that the biotic, or physical characteristics of the trees and the way in which they deal with water scarcity, may be

what drives mortality. Conversely, xeric regions were influenced by edaphic factors. In dry regions, where water limitation is more of a problem compared to East Texas, it may be edaphic factors such as soil capacity and topography - that control water storage that make a difference in which trees survive.

The objectives of this study were to 1) determine the relative contribution of edaphic, climatic, and biotic variables to drought-related mortality, and 2) examine the relationship of each important driver to mortality prediction. Additionally, I look at how these contributions differ with scale, and how they differ by region. Specific hypotheses tested were 1) At the state scale, climate is the dominant driver of mortality, 2) At a smaller scale, edaphic factors drive mortality, particularly available water storage, 3) Mortality in mesic areas are more driven by biotic factors, and 4) Xeric regions are more influenced by edaphic factors.

4.2. Methods

4.2.1 Data

Potential wetlands soil landscape (PWSL) and available water storage at root zone (AWSrz) are "ready to map" attributes that are part of the National Value Added Look Up Table database (Soil Survey Staff 2012) available from the USDA Natural Resource Conservation (NRCS) Gridded Soil Survey Geographic (gSSURGO) database (Table 13). AWSrz is based on soil layering, soil texture, and the root limiting horizon. PWSL is expressed as the percentage of the map unit that meets PWSL criteria. Hydric

Table 13
Spatial data on environmental drivers used as inputs to the Maxent model.

Variables	Units	original resolution (m)	source/attributes
forest type	Categorical	250	FIA (Wilson et al. 2012)
forest density	live trees > 5 in DBH/acre	250	FIA
AWSrz	Mm	10	NRCS SSURGO
PSWL	% of soil map unit that meets PSWL criteria	10	NRCS SSURGO
Percent clay	% average value for the soil range in clay content	10	NRCS STATSGO
Slope	unitless (m/m)	30/250	NED/GMTED DEM from USGS. Converted in ArcMap
Topographic wetness index	unitless	30/250	NED/GMTED DEM from USGS. Converted in ArcMap
Aspect	categorical (N, NE, E, SE, S, SW, W, NW)	30/250	NED/GMTED DEM from USGS. Converted in ArcMap
2011 temp/precip	°C/mm	4000	PRISM Climate Group
bioclim variables	°C/mm	1000	WorldClim (Highmans et al 2005)

soils were considered PWSL, as well as those considered as “poorly drained”, “undrained”, or other descriptive words indicating a current or originally wet soil. Percent clay was obtained as a shapefile form the NRCS State Soil Geographic (STATSGO) data base (Soil Survey Staff). Average percent clay was calculated and the layer was rasterized in ArcGIS. The topographic variables of aspect, slope, and topographic wetness index (TWI) were calculated from the 2010 USGS Global Multi-resolution Terrain Elevation Data (GMTED) digital elevation model (DEM) Resolution was 250-m (7.5 arc seconds at equator). Aspect degree values were reclassified into 8 categories representing each cardinal direction and resulting layer was input into Maxent

as a categorical variable. For the smaller scale models, the same topographic variables were calculated using elevation data from the USGS National Elevation Dataset (NED) with a resolution of 30-m.

4.2.1.1. Climatic variables

Bioclimatic variables from the WorldClim database version 1.4 are derived from the monthly temperature and rainfall values (~1950-2000) in order to generate more biologically meaningful variables (Hijmans et al. 2005). The top 3 bioclimatic variables, determined from Ch. 3 analysis, were used as input to represent long-term average conditions that are most likely to be important drivers of mortality. As long-term variables, these were included to see how they ranked in comparison to the biological and edaphic factors. The 2011 variables from the previous analysis were not included because unlike all of the other variables, these represent more temporary conditions.

4.2.2. Analysis

As with Chapter 3, analyses were performed using Maxent, a habitat suitability approach that predicts areas most likely to contain drought-related tree mortality. Briefly, Maxent is a machine learning method that calculates the most uniform distribution with the constraint that the expected value for each variable should match the average value of a set of sample points taken from the target distribution (Phillips et al. 2006). The Maxent algorithm constructs a habitat suitability model using dead tree occurrence data and environmental variables to predict geographic areas where there are

likely to be other occurrences and calculates a percent contribution for each of the variables and their percent contributions. All data were extracted within the bounds of Texas, precisely coregistered, and projected in GCS North American 1983 coordinate system. The raster data products were reprojected with nearest neighbor resampling to maintain the pixel values, and resampled to 250-m output pixel dimensions. As with the previous analysis, the training area was limited to 78.5-km^2 circular areas around each of the field sampling locations then applied only to areas where values of the environmental variables were within their respective range of values within the training area.

Although Maxent is generally stable with correlated variables (Elith et al. 2011), highly correlated variables can confound the percent contributions of individual variables and interpretations of how each variable affects the model prediction. All variables that were run in the same model were transformed if necessary and run through a Pearson's correlation test. Variables were removed if highly correlated using threshold coefficient of 0.65. First, only edaphic variables were run through the Maxent model, then biotic factors (forest density and forest type), and lastly, the 3 top bioclimatic variables were added (total of 11 variables). Improvement to the model and relative contributions were compared.

This process was repeated for two smaller areas in Texas, one in the East and another in Central Texas (Fig 29). Each area is a Landsat footprint - path 26 row 38 in the east, path 29 row 39 in the west – measuring 170 x 185 km; though no reflectance data was used in this analysis. The East Texas area is located southwest of Dallas and

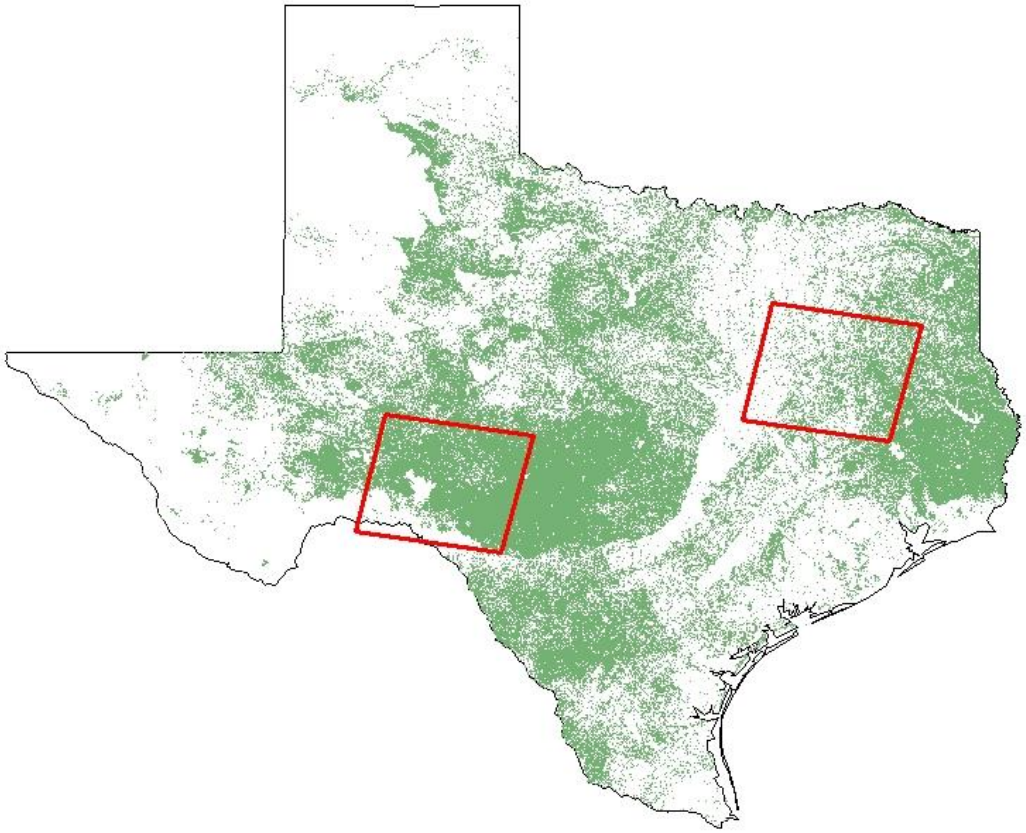

Fig. 29. Study area: forested non-burned areas of the state and two Landsat footprints in East and Central Texas.

traverses the Piney Woods, Post Oak Savanah, and Blackland prairie vegetation regions.

The Central Texas area includes the Edwards Plateau and the southeastern section of the

Trans Pecos region and includes the city of Sonora. A small part of this scene in the southwest corner is not within the state and was not analyzed.

The data used for the statewide analysis was also used for the smaller areas, with the exception of the DEMs used to derive slope, aspect and TWI. The elevation data used were 30-m DEMs from the USGS 3D Elevation Program (3DEP), downloaded from the National Map Viewer (Dollison 2010). All data were extracted within the respective footprint, precisely coregistered, and projected in GCS North American 1983 coordinate system. The raster data products were reprojected with nearest neighbor resampling to maintain the pixel values, and resampled to 30-m output pixel dimensions.

4.3. Results

4.3.1. Statewide models

Model accuracy as measured by the AUC increased incrementally with the addition of more variables (Fig. 30). The model containing all three variable types had an AUC of 0.86. The edaphic model (AUC = 0.74) had AWSrz as the highest contributor (26%) followed by slope (22%, table 14). With the addition of biotic variables, forest density was most important (39%), followed by an edaphic factor, slope (15%). After adding the climatic variables, annual precipitation contributed the most (29%), then forest density (27%). Considering relative contributions of the variable types grouped together (Fig. 31), the edaphic and biotic factors model showed a close to equal contribution to explaining mortality distribution, with edaphic factors explaining only

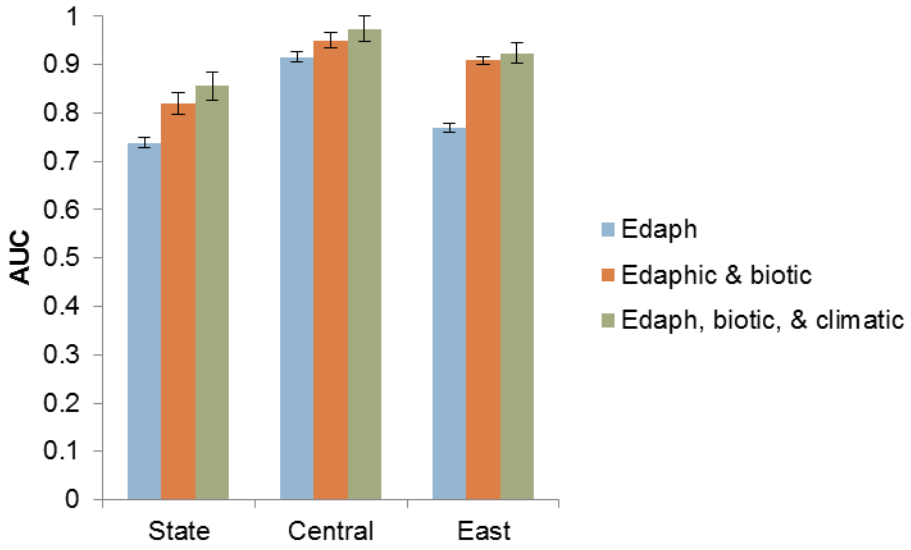

Fig. 30. AUC of test data for Maxent models created with different variables.

10% more than biotic variables. When combining all three variable types, climatic factors drive the model, contributing 42%.

Next the relationships of predicted dead tree occurrence with the top contributing variable in the model were examined. Within the edaphic model, probability of dead trees showed a few peaks of occurrence at low water storage (0 – 25mm), and peaks at high water storage (around 200 and 275 mm, Fig. 32). In the edaphic and biotic model, occurrence probability in relation to forest density was high between 25 – 150 trees/acre (Fig. 33). In the edaphic, biotic, and climatic model where annual precipitation was the top contributor, mortality occurrence probability generally decreased with increasing precipitation. This is seen particularly between precipitation levels between 1100 and 1400 mm, where probability drops from 0.33 to 0.02% (Fig. 34).

Table 14
An estimate of relative contributions of environmental variables to the statewide Maxent models. Top 2 contributing variables are in bold.

	Percent contribution		
Variable	Edaph, biotic, & climatic	Edaph & biotic	Edaphic
Annual precip	**29.5**	-	-
Forest density	**27.3**	**39.1**	-
Mean temp of wettest quarter	8.7	-	-
Available water storage	7.9	9.9	**26.3**
Slope	6.7	**14.6**	**21.5**
Topographic wetness index	6.4	10.0	18.7
Potential wetland	4.0	7.5	10.5
Max temp of warmest month	3.4	-	-
Forest type	3.3	6.1	-
Aspect	2.6	3.5	5.0
Clay	0.3	9.2	18.0

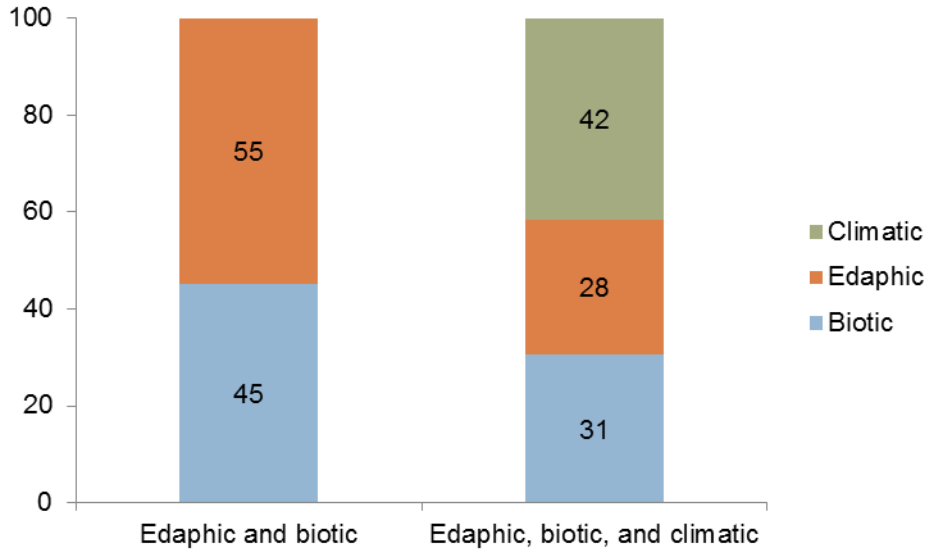

Fig. 31. Percent contributions of edaphic, biotic, and climatic variables to statewide Maxent models created using varying combinations of each.

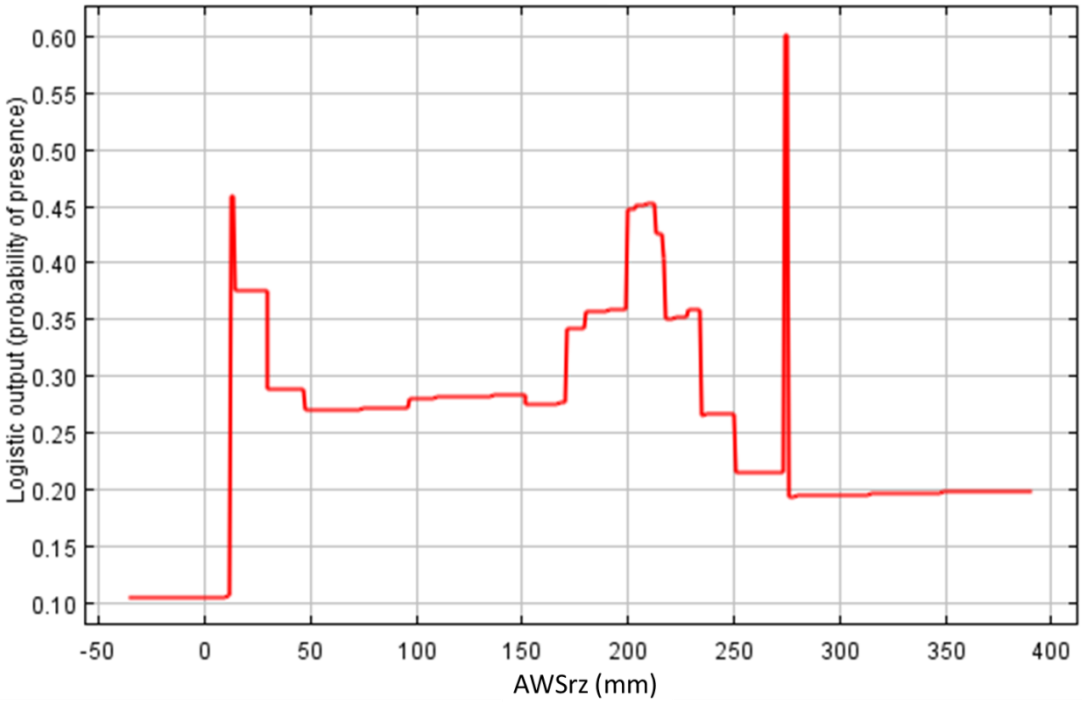

Fig. 32. Response of dead tree probability of occurrence to AWSrz in edaphic variable model when all other variables are held constant.

The results reported involving individual strata comparisons do not include the Trans-Pecos or the South FIA regions because of sparse plot coverage in these areas. Also, very little of the Trans-Pecos was defined as forested area. In all cases, the variation of the models using only edaphic variables predicted the most mortality (Fig. 35). This can be seen in the maps of the statewide model by the lighter colors that progressively dominate from the edaphic to the "full" model (Figs. 36 - 38). There are only two regions within the statewide model in which the edaphic, biotic, and climatic model predicted a slightly higher mean mortality than the edaphic and biotic model: the North and Northeast-West regions (Fig. 35). The all-inclusive model showed the highest mean mortality in the Northeast-West and the Brazos Valley regions

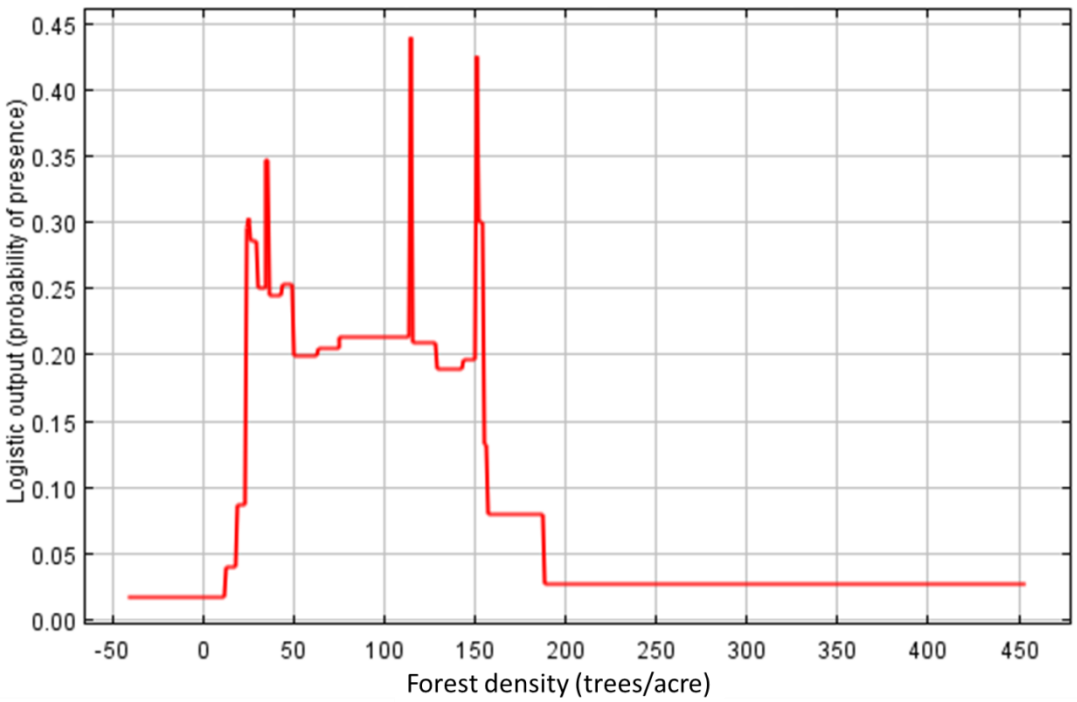

Fig. 33. Response of dead tree probability of occurrence to forest density in edaphic and biotic variables model when all other variables are held constant.

(34 and 33%, respectively), followed by the Southeast-West region (Figs. 35 and 38). The Southeast-East region averaged the least predicted mortality (10%). The edaphic and biotic model showed the highest mean mortality in the Northeast-West and Southeast-West regions (33%) and lowest in the Panhandle (17%). The edaphic only model had the same regions with highest mortality but both averaged 42%. The region with the lowest mortality was the Southeast-East at 32%.

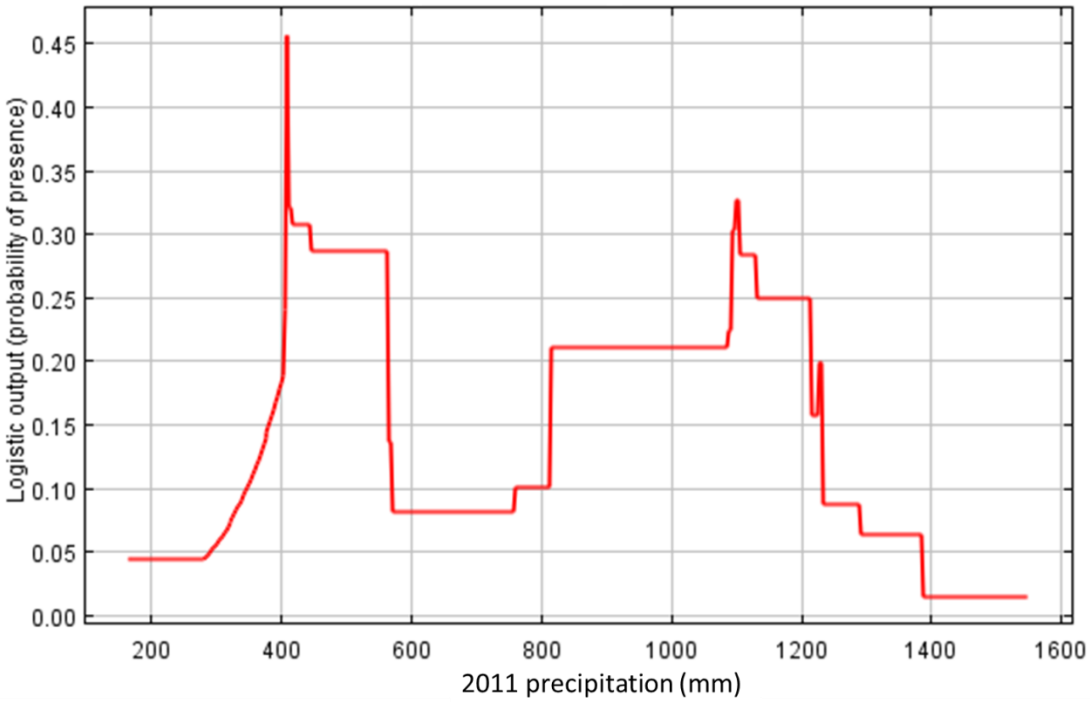

Fig. 34. Response of dead tree probability of occurrence to annual precipitation in the edaphic, biotic, and climatic model when all other variables are held constant.

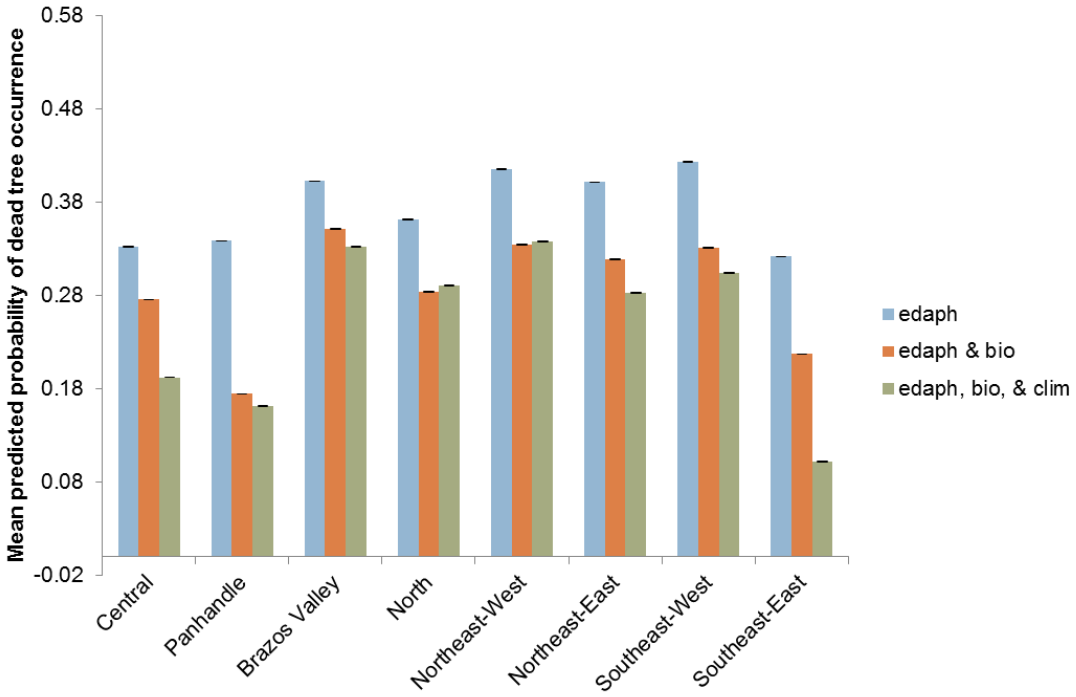

Fig. 35. Mean predicted probability of dead tree occurrence by FIA region for all three models.

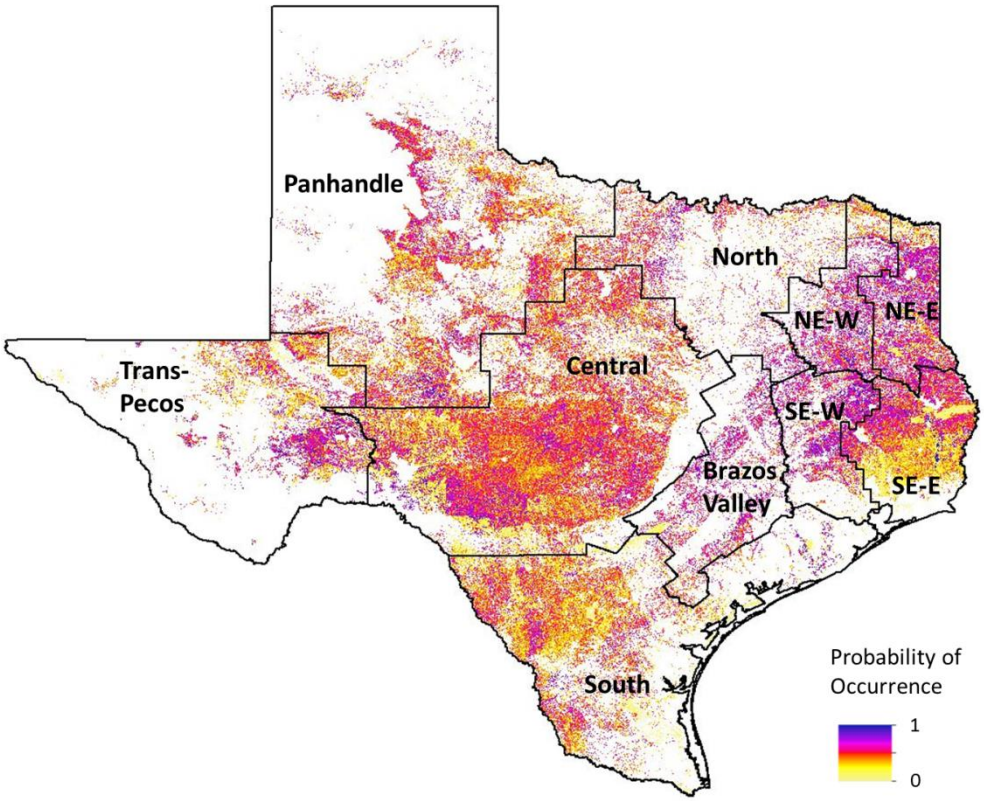

Fig. 36. Predicted probability of dead tree occurrence with Maxent model using only edaphic variables.

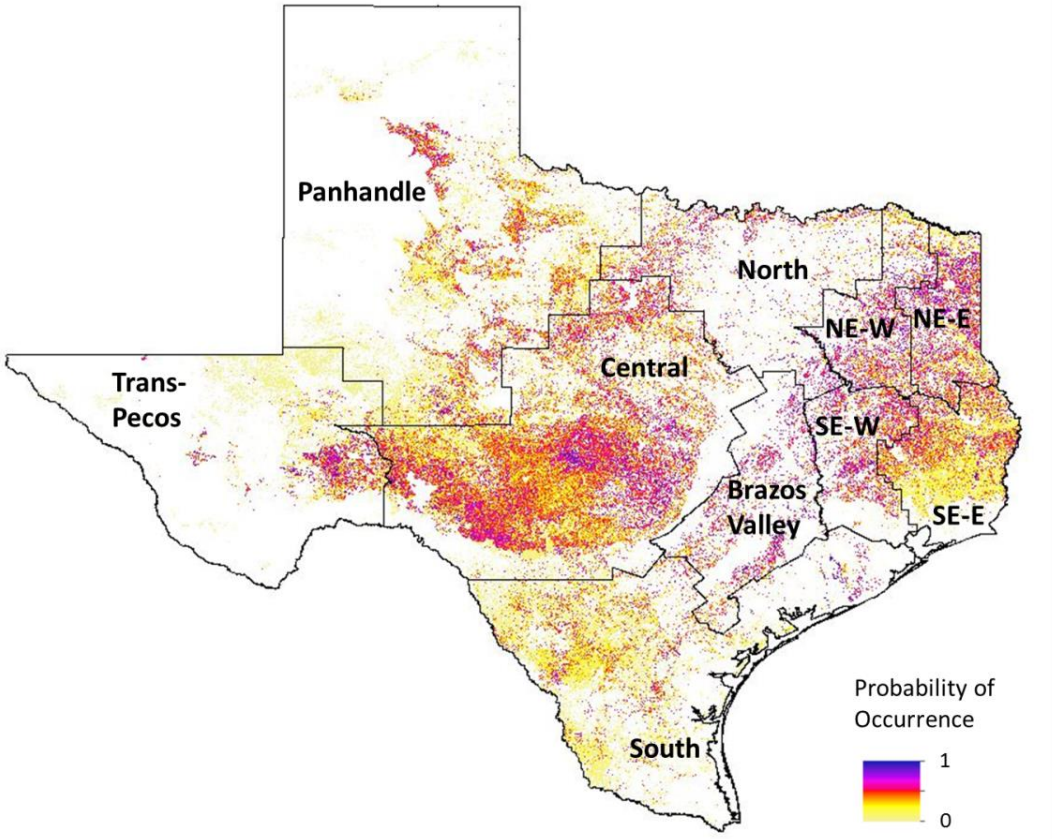

Fig. 37. Predicted probability of dead tree occurrence with Maxent model using edaphic and biotic variables.

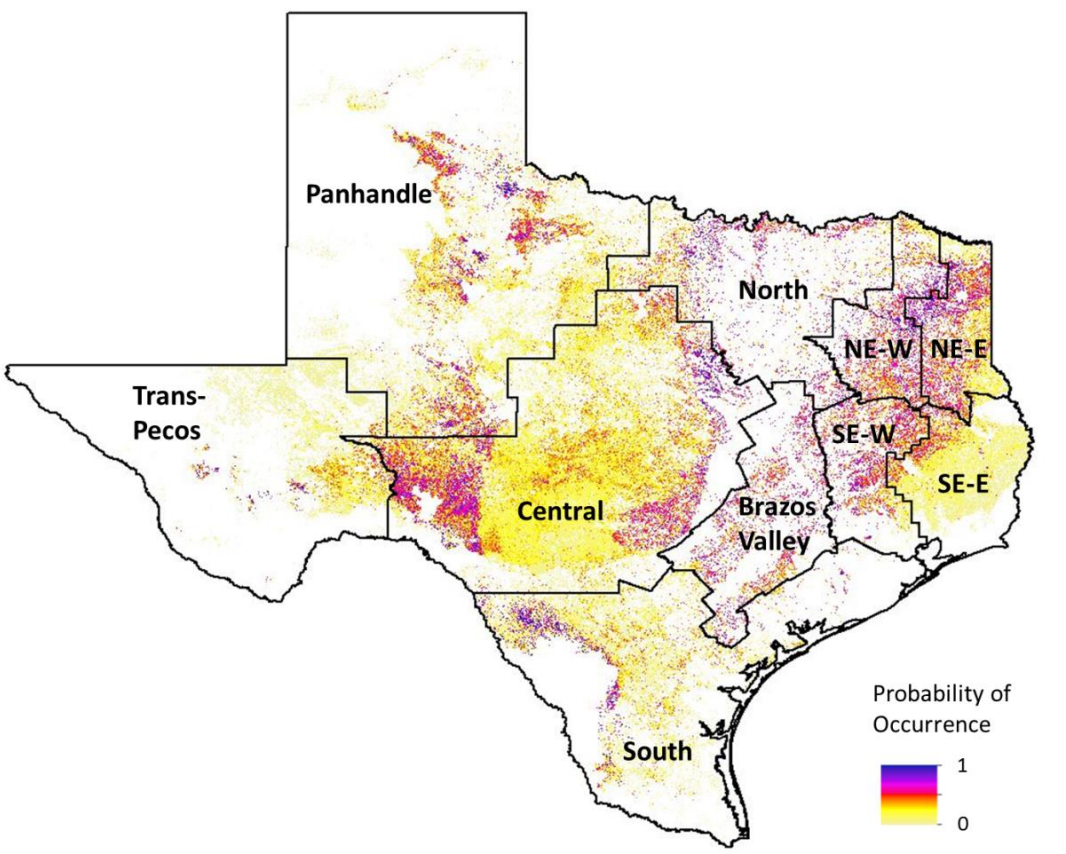

Fig. 38. Predicted probability of dead tree occurrence with Maxent model using edaphic, biotic, and climatic variables.

4.3.2. Local models

As with the statewide models, the local models' AUCs increased as variables were added (Fig. 30). Starting with Central Texas and the edaphic only model (AUC = 0.92), AWSrz contributed overwhelmingly at 44% followed by slope (Table 15). In the edaphic and biotic model (AUC = 0.95), forest density and AWSrz contributed over 60%. When adding bioclimatic variables (AUC = 0.97), annual precipitation contributed

the most at 31% followed by forest density. In East Texas, the edaphic only model and the edaphic and biotic models (AUC = 0.77 and 0.91, respectively) were also driven by

Table 15
An estimate of relative contributions of environmental variables to the Maxent models in Central Texas. Top 2 contributing variables are in bold.

	Percent contribution		
Variable	Edaph, biotic, & climatic	Edaph & biotic	Edaphic
Annual precip	**30.6**	-	-
Forest density	**22.5**	**33.4**	-
Max temp of warmest month	11.3	-	-
Available water storage	10.7	**31.3**	**43.6**
Aspect	8.3	10.7	17.5
Slope	8.1	14.6	**28.3**
Mean temp of wettest quarter	5.7	-	-
Topographic wetness index	1.5	4.7	10.4
Potential wetland	0.7	0.1	0.1
Forest type	0.5	5.1	-
Clay	0.0	0.0	0.1

AWSrz and slope (Table 16). The all-inclusive model (AUC = 0.92) is different than Central Texas in that it was driven most by forest density then mean temperature of wettest quarter. Annual precipitation, which dominated every other model in which it was included, contributed only 4% in East Texas.

With variable types grouped together, the edaphic and biotic models in Central and East Texas contributed similar proportions: 60% edaphic, 40% biotic. The addition of the climate variables causes the proportions to differ much more from each other. In Central Texas, bioclimatic variables as a whole contributed 48%, followed by edaphic

(29%), then biotic (23%). Edaphic variables contributed the most in East Texas (47%), followed by biotic (32%), and lastly climatic variables (21%, Fig. 39).

Table 16
An estimate of relative contributions of environmental variables to the Maxent models in East Texas. Top 2 contributing variables are in bold.

	Percent contribution		
Variable	Edaph, biotic, & climatic	Edaph & biotic	Edaphic
Forest density	**22.3**	**29.4**	-
Mean temp of wettest quarter	**15.1**	-	-
Clay	12.8	12.4	6.4
Available water storage	11.7	**17.6**	**33.3**
Slope	10.8	14.8	**29.8**
Forest type	9.9	10.5	-
Aspect	5.4	6.8	10.9
Annual precip	4.2	-	-
Topographic wetness index	3.4	4.7	19.4
Potential wetland	3.1	3.8	0.2
Max temp of warmest month	1.3	-	-

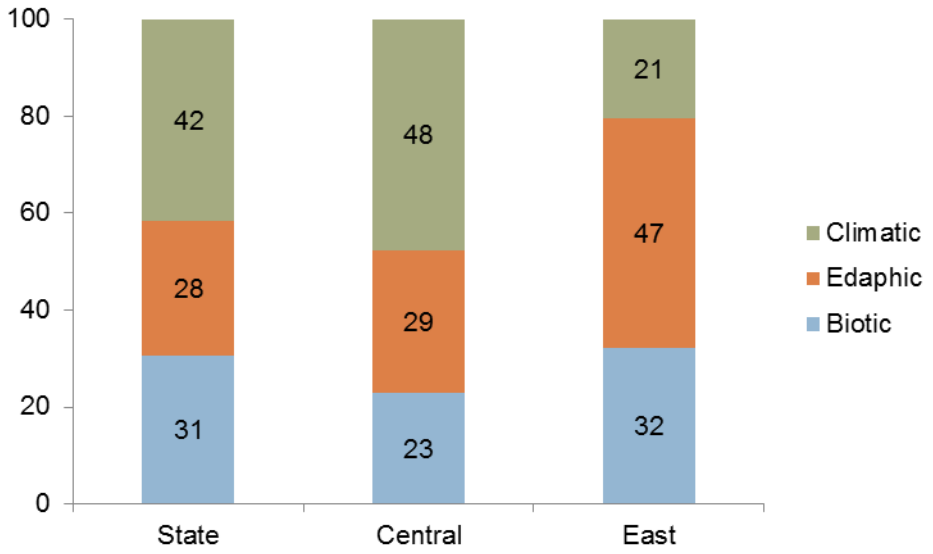

Fig. 39. Percent contributions of edaphic, biotic, and climatic variables to the all-inclusive statewide, Central, and East Texas Maxent models.

The Central Texas edaphic model showed a few high peaks of dead tree occurrence with low AWSrz, between approximately 10 and 30 mm (Fig. 40). In the East Texas edaphic model where AWSrz is also the top driver, probability of dead trees is high at low AWSrz values, but the decline with increasing water storage is much more gradual and a consistent decline in dead tree probability is not seen until 225 mm (Fig 41). In the Central Texas edaphic and biotic model, mortality prediction generally rose with forest density, with a peak at about 70 trees/acre and probability remains at about 11% throughout the high densities (Fig. 42). The corresponding model in East Texas also show peaks between 10 – 130 trees/acre, but thereafter gradually declines to zero probability with increasing density (Fig. 43). In the all-inclusive model of Central Texas, the relationship of mortality to annual precipitation is less clear, but there is a peak of dead tree occurrence at 440 mm, a gradual increase in mortality to 560 mm, and a

subsequent sharp decrease (Fig. 44). The all-inclusive model for East Texas was driven by density, which shows the same pattern seen in the edaphic and biotic model (Fig 45).

As with the statewide models, the edaphic models predict the highest mortality, followed by the edaphic and biotic models, and then the all-inclusive model (Fig. 46 – 49). Note that the maps depict different areas with white indicating no prediction, because different areas were masked with each model depending on the presence of any variable values outside of those within the training range. In all variations, East Texas averaged higher mortality than Central Texas, particularly in the edaphic models where the difference is 21%.

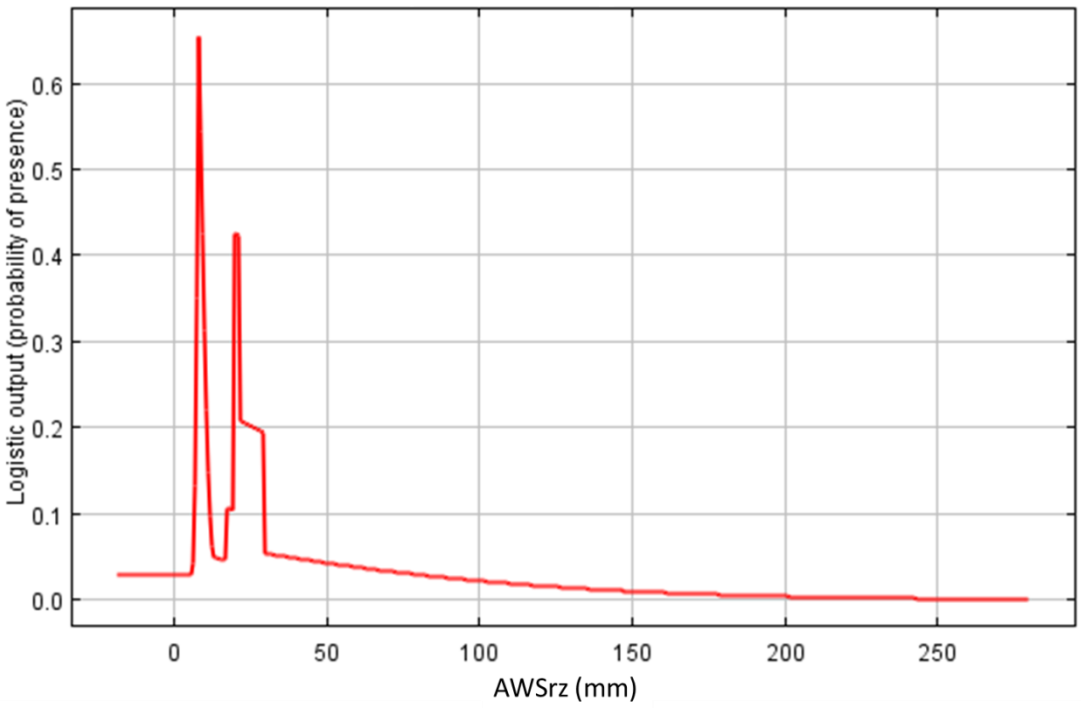

Fig. 40. Central Texas response of dead tree probability of occurrence to AWSrz in edaphic variable model when all other variables are held constant.

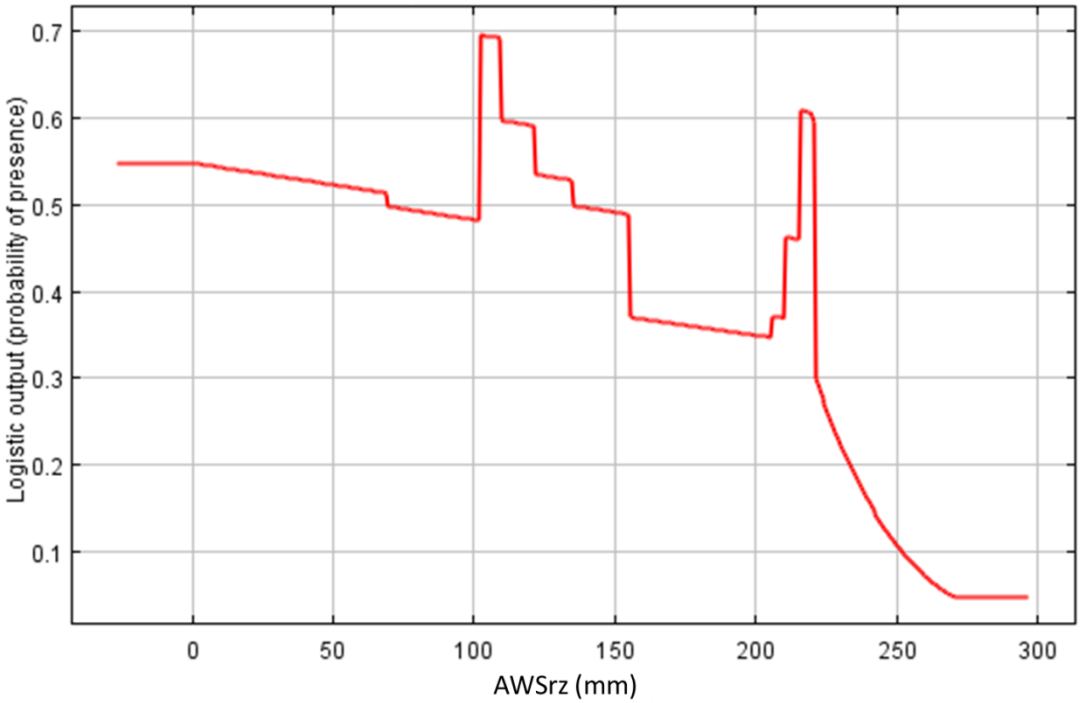

Fig. 41. East Texas response of dead tree probability of occurrence to AWSrz in edaphic variable model when all other variables are held constant.

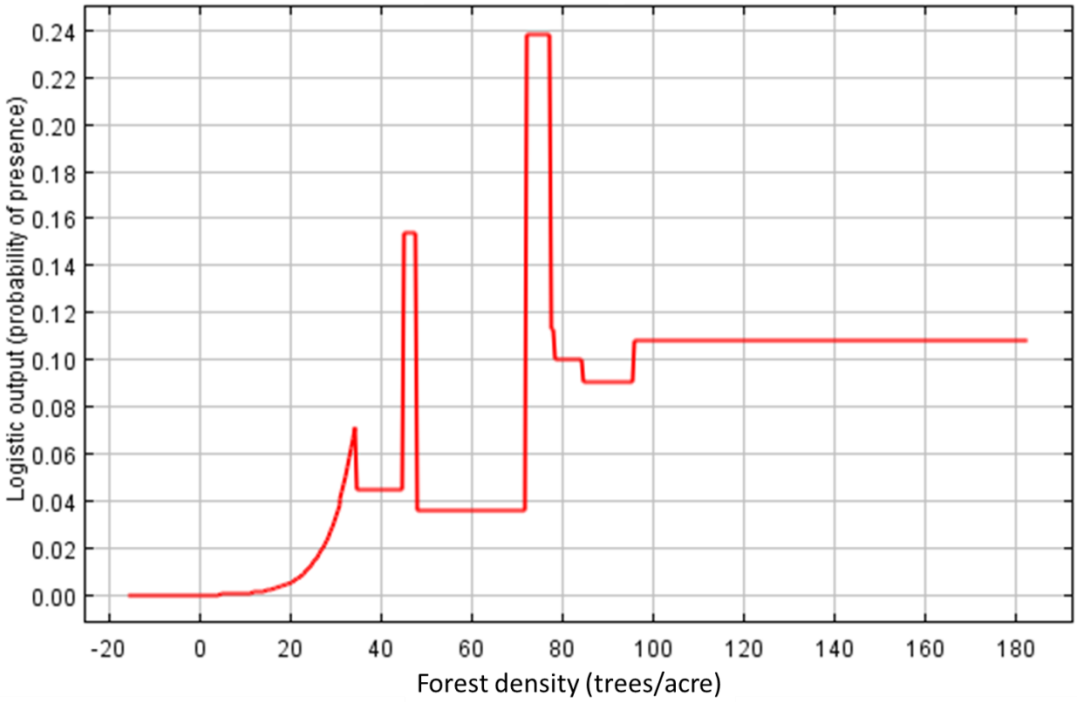

Fig. 42. Central Texas response of dead tree probability of occurrence to forest density in edaphic and biotic variables model when all other variables are held constant.

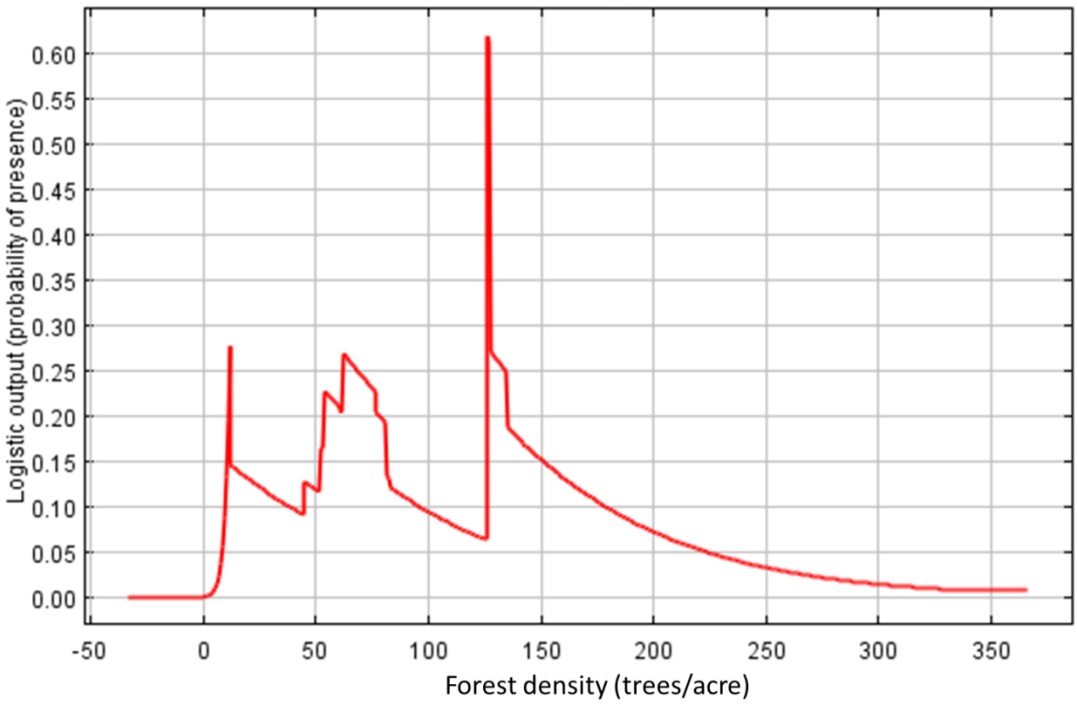

Fig. 43. East Texas response of dead tree probability of occurrence to forest density in edaphic and biotic variables model when all other variables are held constant.

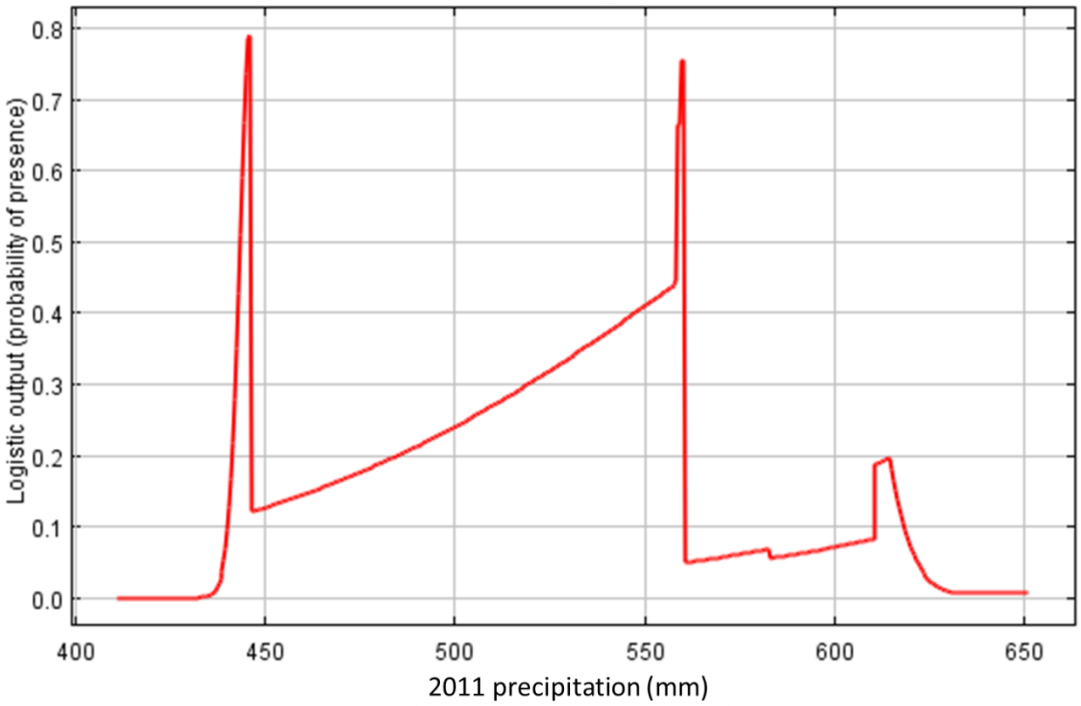

Fig. 44. Central Texas response of dead tree probability of occurrence to 2011 precipitation in edaphic, biotic, and climatic variables model when all other variables are held constant.

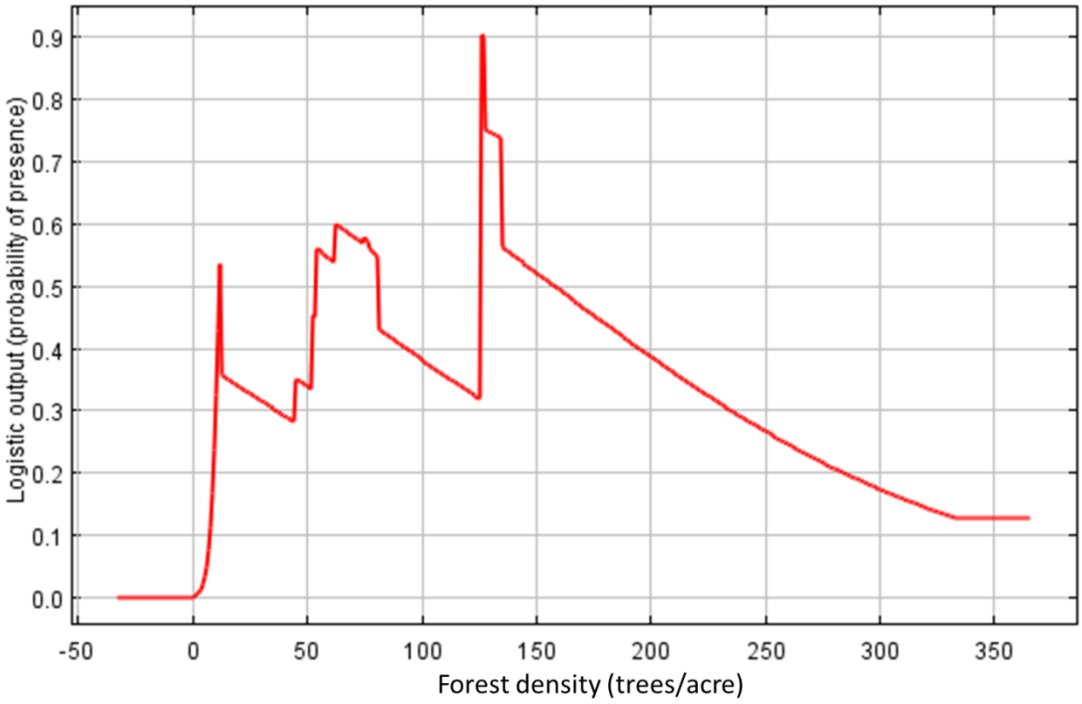

Fig. 45. East Texas response of dead tree probability of occurrence to forest density in edaphic, biotic, and climatic variables model when all other variables are held constant.

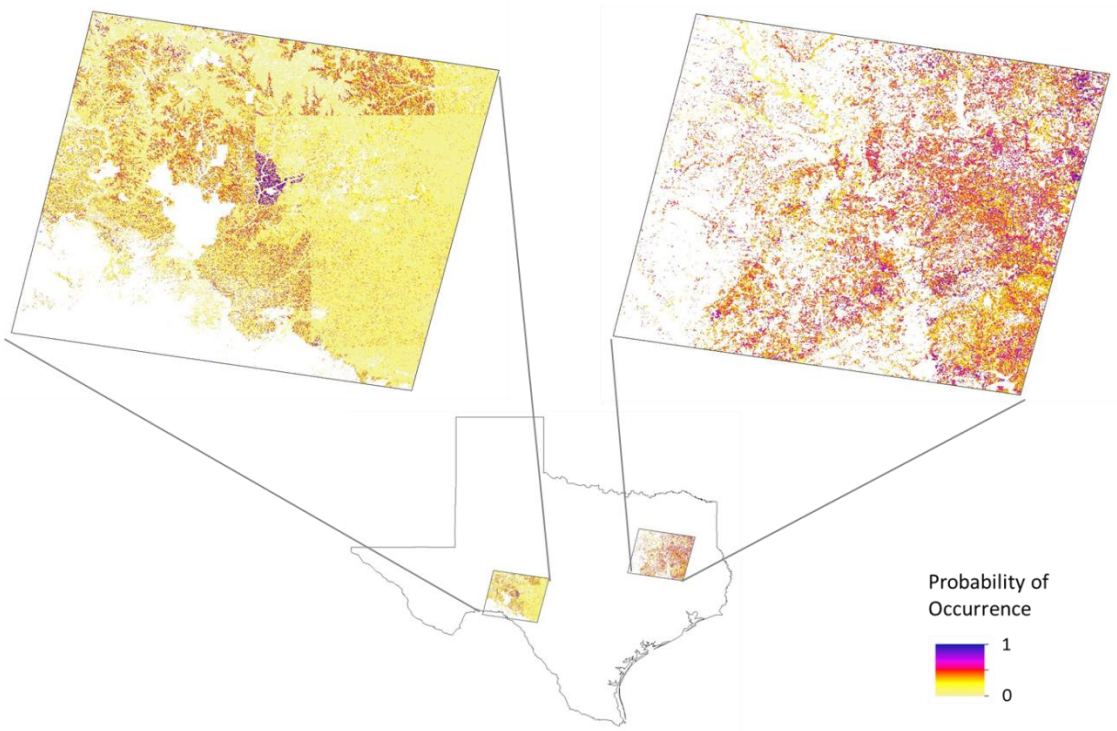

Fig. 46. Maxent-predicted probability of dead tree occurrence in Central TX (left) and East TX (right) using only edaphic variables.

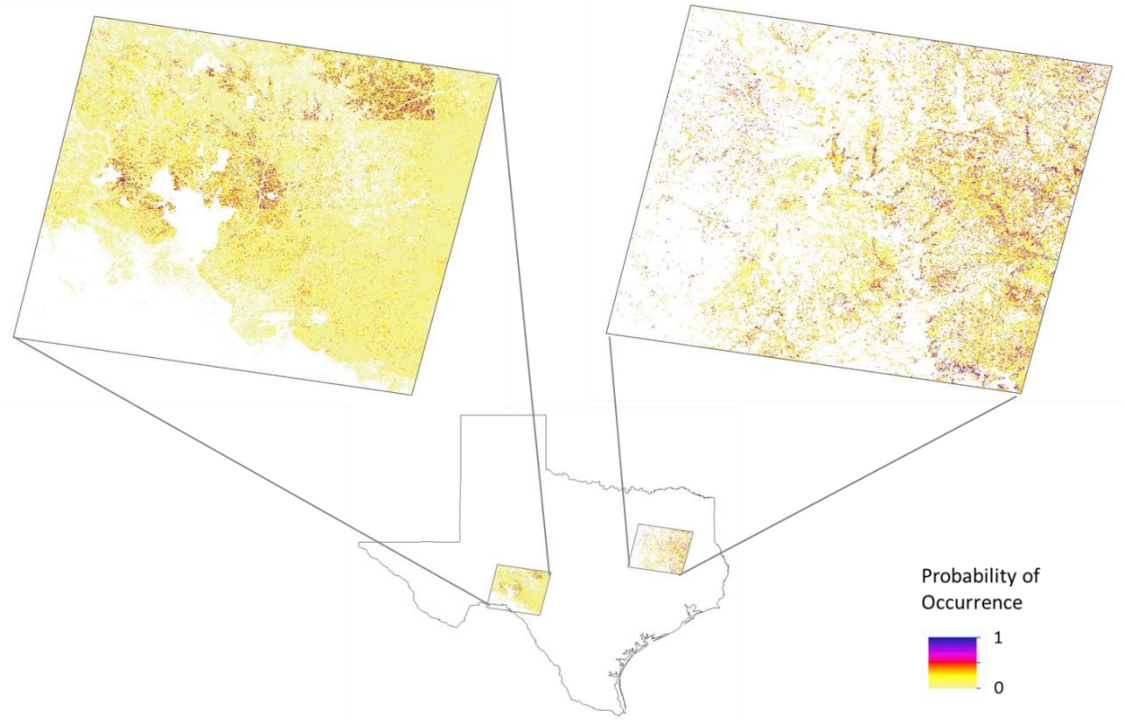

Fig. 47. Maxent-predicted probability of dead tree occurrence in Central TX (left) and East TX (right) using edaphic and biotic variables.

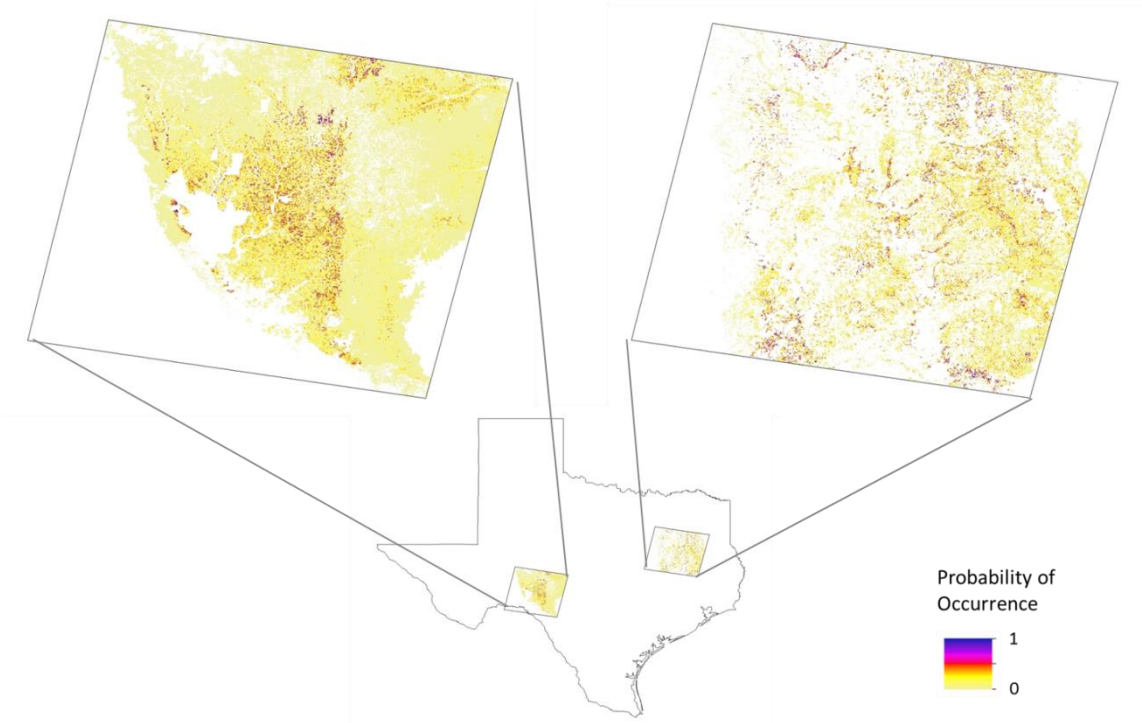

Fig. 48. Maxent-predicted probability of dead tree occurrence in Central TX (left) and East TX (right) using edaphic, biotic, and climatic variables.

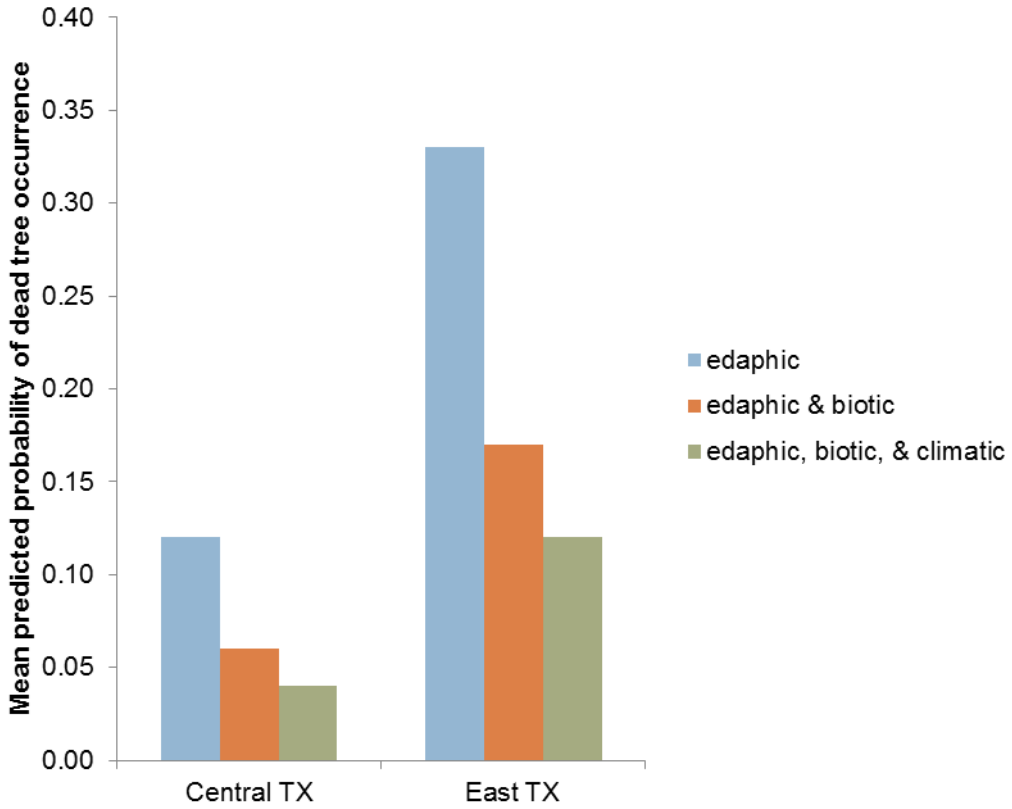

Fig. 49. Mean predicted probability of dead tree occurrence in Central and East TX for all three models.

4.4. Discussion

Maxent was able to identify and rank important drivers of tree mortality at two different spatial scales and ecosystem types. Large proportions of the spatial variation in tree mortality could be explained using a combination of biotic, edaphic, and climate drivers. When combined, the rank order of variables shifted and adjusted to the addition of new variables, which produces a set of probable models that can be used to predict mortality in future droughts. The addition of environmental variables increased the

prediction accuracy, which is normally the case. This means that each type of variable had explanatory power not present in the other variable types.

In the statewide edaphic model, the dominance of AWSrz confirms its importance in plant survivability. It's direct relationship to water avaialability makes the relationship intuitive. Forest density being a dominant driver in both the edaphic & biotic model as well as the all-inclusive model may be related to sample bias in dense forests. However, at least part of this result may be due to the fact that there are more dead trees where there are more trees. In addition, trees in dense forests have increased competition for resources including water. It may also be an indication of adaptation, as dense forests are found in mesic areas where trees are less likely to be adapted to water limitation. The importance of slope is also intuitive, ranking high in all of the statewide models. Probability of dead trees increased with increasing slope, which may indicate that gravitational runoff on high slopes caused increased water stress in plants (Burt and Butcher 1985).

After adding the three climatic variables annual precipitation comes out on top as forest density remains close behind. While it is not surprising that precipitation would be a driver of mortality, the relationship is not entirely consistent – presence of mortality was seen in many ranges of annual precipitation. The general trend, however, was a decrease of mortality with precipitation, after a sharp rise between 200 and 400 mm. The downward trend may indicate that water availability for the state, while record low in all areas, may have been spatially in proportion to the average annual rainfall in those areas;

i.e. mesic areas still received relatively more rainfall than dry areas, making survival higher in those regions. Inspection of 2011 precipitation shows that this is the case.

Potential wetland soils landscape showed minimal contribution in all models. This may imply that the potential presence of wetlands might not be an adequate predictor of dead trees or this may be a scaling issue, and the phenomena may not be well detected at coarse resolution if the wetland units were too few, small, or otherwise isolated from the occurrence data. One way a model may better account for this variable is through plant characteristics like root depth and plasticity of root depth which are likely important predictors of drought vulnerability (Jackson et al. 1996; Rodríguez-Iturbe and Porporato 2004).

As the models increase in variables and accuracy, mortality prediction decreases, showing more "realistic" probabilities. Spatially, they all show high mortality in the Eastern regions, the Brazos Valley, the North, and hot spots in the panhandle. There are some regions that show some variation between models. The Central region shows high mortality throughout the entire region in the edaphic model, likely driven by the low AWSrz in these shallow, rocky soils. Adding the biotic factors decreased prediction of mortality which is likely due to forest density variable and the fact that most of the ground data had dead trees found in high density areas, thereby lowering the prediction in Central Texas where density is low. Adding the bioclimatic factors caused prediction to decline further, but there are hot spots in the east and west. The high mortality in the eastern part of the region appears to be mostly caused by annual precipitation. The cause of mortality in the east is less clear by viewing spatial overlays, but seems to be a

combination of the annual precipitation and density. The fluctuating predictions in the southeast-east region seemed influenced primarily by forest density. Though these models are useful, it is important to keep in mind the spatial bias of this particular field data, because the clustering of plots affects the spatial prediction.

Another notable spatial observation is that mortality seems to be concentrated on the western edge of some major forest types groups: The Loblolly/shortleaf pine group to the east, the Pinyon/Juniper group, and the Oak/hickory group in the west. These areas can also be considered the eastern pine-deciduous forest and the oak-juniper savanna. It is likely that the western edge will be the trailing edge of range migrations, if this were to take place. As climate becomes hotter a drier, ecotones in Texas are likely to move eastward if given the ability to migrate and edaphic characteristics allow. This drought and the subsequent mortality show how extreme events can lead to range shifts in in relatively short time scales.

The high importance of the bioclimatic variables seen in the statewide and Central Texas models show that for the variables considered presently, bioclimate can be as useful for predicting mortality as biophysical variables. Knowing that they can predict present mortality is useful because they represent average conditions over approximately 50 years not including the decade in which the drought took place. This means that to a certain degree, probability of mortality can be predicted without having to wait for data from the year of the onset of the drought.

In Central Texas, the 44% of the edaphic model is explained by AWSrz, which shows the expected relationship with spikes of mortality probability where storage is

low. The map shows sharp transitions in mortality that coincide with county lines. This is a common problem in using NRCS SSURGO data, which was collected by individual counties and many counties list different soil types and characteristics that are different than that of a neighboring county. The hot spot of mortality seen in the middle of the study area shows a relatively straight boundary to the west which is a result of this county data discrepancy - particularly that of the driving factor, AWSrz. The graph showing East Texas mortality with AWSrz shows sustained high mortality at low AWSrz with a more gradual decline. This contrast compared to West Texas is likely due to the few numbers of trees found at all at higher AWSrz values.

In the edaphic and biotic model, Central Texas shows peaks at mid-densities and a sustained mortality probability at high densities, which is in contrast to East Texas which shows a decline at high densities. Since East Texas has uniformly dense forests, the decline may simply represent all those trees that did survive (non-presence, according to the model); whereas in Central Texas, where high densities are scarce, the model predicted about 10% chance of mortality in all dense stands above 90 trees/acre. The maps show that the predictions are generally decreased and the sharp discrepancies across county lines are smoothed out. In the East, the effect of density can be seen in the high mortality predictions along water ways with presence of dense riparian and bottomland forests.

In the all-inclusive models for East and West Texas, different top contributing variables emerge. In the east, density remained at the top and showed an almost identical pattern with mortality, except for the probability numbers themselves, where in the all-

inclusive models, the values were about 3% higher than that of the edaphic and biotic model corresponding to the same density value. Even though density contributed less to the all-inclusive model, the model predicted higher mortality with density. The spatial distribution appears similar with both maps, but more concentrated in the all-inclusive model. This implies that the bioclimatic variables predict similar distributions as the other variables, showing the coupling of climate with biotic and edaphic factors (Van der Putten et al. 2010).

In Central Texas where climatic factors dominate, annual precipitation is again the driving factor. The relationship is not a clear positive or negative; like the statewide model, high mortality was found in a range precipitation levels. In this case, however, there is 100-mm range of precipitation values that show a gradual incline. If not purely random, this could again be representative of trees in higher precipitation zones being more susceptible to mortality. Overlays show that high mortality was seen in the pinyon/juniper forest type group. There is also anecdotal evidence that many junipers were affected during this drought. As mentioned in the previous chapter, Moore et al. (2016) found disproportionately high mortality of *J. asheii* in Central Texas. This was unexpected because they are considered drought-resistant species. Although additional studies are needed to confirm that trees have not resprouted, it's possible that this that the drought conditions exceeded a particular threshold for this species, especially in the western part of its range.

The first hypothesis stated that climate was a more dominant driver at the regional compared to local scale. This was found to be true only in comparison to East Texas (Fig. 39). The bioclimate variables contributed a slightly larger proportion to dead tree distribution in Central Texas (48 vs. 42%). Climate may have played an unexpectedly large role in Central Texas because of annual precipitation, which explained 31% of the model, had a large precipitation gradient in the area, a range of about 365 mm. Maximum temperature of warmest month contributed 11%, a variable that ranked low in the East Texas and statewide models, showing the high maximum temperatures may have played more of a role in determining mortality in the drier regions..

The second hypothesis, that edaphic factors drive mortality more at a local scale relative to the statewide scale, was certainly more clearly confirmed in East Texas than in Central Texas where edaphic variables explained close to half of the mortality model. Clay, AWSrz, and slope explained over 35%. In Central Texas, however, edaphic factors contributed only 1% more than they did in the statewide model because of the dominance of climatic variables discussed earlier. The importance of AWSrz was also confirmed. It was the top driver in all edaphic models, second in both of the local edaphic and biotic models, and fourth in all of the all-inclusive models. With the exception of the all-inclusive model for East Texas where AWSrz contributed 1% less than percent clay, it was the top edaphic variable in every other model.

In comparing the two smaller-scale models, I hypothesized that mortality in mesic areas were driven most by biotic factors and mortality in xeric regions would be

driven most by edaphic factors. The former was somewhat confirmed in this analysis in that in the East Texas model, the biotic contribution was greater than that of the climate contribution as well as the biotic contribution in Central Texas. However, the biotic contribution was less than edaphic in the East. With regards to Central Texas, the results lead to the rejection of the hypothesis that edaphic factors drive mortality in this region. These variables contributed slightly more than biotic, but clearly not as important as the climatic variables.

As a whole, Central Texas relative contributions by variable type more closely mirror that of the statewide model. The East and West Texas areas examined represent very different environments and ecological profiles. Interestingly, the edaphic and biotic models of both areas show almost identical contribution proportions of both variables types: 60% edaphic and 40% biotic. It is the addition of the biolimate variables that caused the proportions to vary vastly from each other.

There are many other drought mortality factors that should be considered in future studies. All of the variables listed in Anderegg's plant death continuum (Fig. 21) could be tested and each could have multiple indices that represent them. For example, there are a number other edaphic variables to consider. Although in no way exhaustive, this exercise was useful in that it allowed us to rank variables in relation to each other. It has also generated many hypotheses regarding the specific relationships of the tested variables to tree mortality.

5. CONCLUSIONS

This study has shown how much information can be gleaned from coarse-resolution satellite detection, drought indices, and environmental factors in their ability to detect and predict drought-related tree mortality. Given that these resolutions cannot detect individual trees, indices at this level still give us useful estimations of location, magnitude, and quantification of mortality. By separating calibration data, it is seen that uniform tree density plays a large role in prediction accuracy and that calibration data should be representative of the area of prediction application. For future applications, it is important to be mindful of detection threshold. By raising the threshold from 1 to 6% mortality, below which there are no expectations for the indices to accurately quantify mortality, model accuracy increased dramatically. Therefore, when deciding on a modeling strategy, it is helpful to have an initial estimation of the mortality to determine a model's potential utility. There were not clear advantages or large increases in accuracy when going from 250- to 30-m resolution to derive indices. Although moderate resolution can detect finer detail, it is still susceptible to the effects of tree density and other signal noise.

In this study, drought-mortality was modeled using current and time-series biophysical indicators; 2011 weather conditions; climate, biotic, and edaphic variables, each offering very different but useful information for prediction. Ranking environmental factors gives information on how they might contribute to mortality relative to each other in a given drought. In the 2011 Texas Drought, it was seen that the

climate variables for that year were more instrumental in driving mortality than long-term climate, likely because they were severe enough to push many trees beyond their drought adaptation limits. Differences were seen when comparing mortality drivers between different regions where climate contributed to half of the model prediction in Central Texas and edaphic variables also contributed nearly half in the East Texas model. This highlights the fact that there are major differences between how these regions will react to drought and climate change.

Although modeling and extrapolation from models is risky, it is up to the ecologist and the question at hand to decide how to choose and "design" the seemingly endless amounts of relevant information, modeling techniques, resolutions, etc. to answer questions about complex processes. It is because of this necessary creativity that modeling is sometimes called an "art" (Elith et al. 2010).

Drought is certainly one of those complex processes that spans multiple time scales, spatial scales (molecular to regional), and disciplines. Anderegg et al. (2013) laid out a useful conceptual framework of drought mortality that can help piece together past work and inform future studies of drought mortality and where information fits within the precipitation deficit - to- plant death continuum (Fig. 25). For example, in this study our look into meteorological indices (chapter 3) and edaphic features (chapter 4) goes into explaining how precipitation deficit leads to soil moisture deficit. The examination of biotic variables (chapter 4) goes into explaining how soil moisture deficit translates to plant water stress. When that stress leads to physiological damage, the changes in

biophysical properties can be picked up by remote sensors and incorporated into indices that detect mortality (chapter 2).

Future research should go into synthesizing what is already known about drought-mortality in order to set recommendations for managing forest ecosystems in the face of climate change. This research also generated hypotheses that can be further investigated. For example, the role of isothermality has brought up the question of whether trees more adapted to variable environments are better equipped to deal with drought. Other questions raised were whether adaptation of taxa to their environments helps to produce an equalizing effect on the distribution of mortality, and whether tree ranges in Texas and the Southwest are likely to move eastward with climate change. It is also interesting that the VegDRI performed poorly in predicting mortality according to accuracy assessments, when many of the variables that contribute to this index successfully predicted mortality within Maxent. This may reflect inherent differences in the techniques used to assess accuracy. However, if possible it would be worthwhile to calculate the VegDRI index for the state at a finer resolution in order to have a fair comparison with the predictive power of ΔNDVI.

Ecologists are still uncovering of the drivers of drought-related tree mortality at the precipitation deficit-to-mortality continuum and these can be represented by a number of spatial datasets that either already exist or are yet to be created. As more years of drought mortality data become available and with continual testing of models, variables, and combinations of variables, the ability to predict vulnerable landscapes will be further refined. As catastrophic events like the 2011 Texas Drought continue to

increase in frequency, being able to detect and predict forest die-offs can help mitigate the consequences.

REFERENCES

Abrams, M.D. (1990). Adaptations and responses to drought in Quercus species of North America. *Tree Physiology, 7,* 227-238

Adams, H.D., Guardiola-Claramonte, M., Barron-Gafford, G.A., Villegas, J.C., Breshears, D.D., Zou, C.B., Troch, P.A., & Huxman, T.E. (2009). Temperature sensitivity of drought-induced tree mortality portends increased regional die-off under global-change-type drought. *Proceedings of the National Academy of Sciences, 106,* 7063-7066

Adams, J.B., Sabol, D.E., Kapos, V., Almeida Filho, R., Roberts, D.A., Smith, M.O., & Gillespie, A.R. (1995). Classification of multispectral images based on fractions of endmembers: Application to land-cover change in the Brazilian Amazon. *Remote Sensing of Environment, 52*, 137-154

Allen, C.D., Macalady, A.K., Chenchouni, H., Bachelet, D., McDowell, N., Vennetier, M., Kitzberger, T., Rigling, A., Breshears, D.D., Hogg, E.H., Gonzalez, P., Fensham, R., Zhang, Z., Castro, J., Demidova, N., Lim, J.-H., Allard, G., Running, S.W., Semerci, A., & Cobb, N. (2010). A global overview of drought and heat-induced tree mortality reveals emerging climate change risks for forests. *Forest Ecology and Management, 259,* 660-684

Alley, W.M. (1984). The Palmer drought severity index: Limitations and assumptions. *Journal of Climate and Applied Meteorology, 23*, 1100-1109

Anderegg, L.D., Anderegg, W.R., & Berry, J.A. (2013). Not all droughts are created equal: Translating meteorological drought into woody plant mortality. *Tree Physiology, 33,* 672-683

Araújo, M.B., & Pearson, R.G. (2005). Equilibrium of species' distributions with climate. *Ecography, 28,* 693-695

Archibald, S., Roy, D.P., Van Wilgen, B.W., & Scholes, R.J. (2009). What limits fire? An examination of drivers of burnt area in Southern Africa. *Global Change Biology, 15,* 613-630

Asner, G.P., D.E. Knapp, A. Balaji, and G. Paez-Acosta (2009). Automated mapping of tropical deforestation and forest degradation: CLASlite. *Journal of Applied Remote Sensing, 3*, 033543

Asner, G.P., & Heidebrecht, K.B. (2002). Spectral unmixing of vegetation, soil and dry carbon cover in arid regions: Comparing multispectral and hyperspectral observations. *International Journal of Remote Sensing, 23*, 3939-3958

Asner, G.P., Knapp, D.E., Broadbent, E.N., Oliveira, P.J., Keller, M., & Silva, J.N. (2005). Selective logging in the Brazilian Amazon. *Science, 310,* 480-482

Asner, G.P., & Lobell, D.B. (2000). A biogeophysical approach for automated SWIR unmixing of soils and vegetation. *Remote Sensing of Environment, 74*, 99-112

Asner, G.P., Vaughn, N., Smit, I.P., & Levick, S. (2015). Ecosystem-scale effects of megafauna in African savannas. *Ecography, 39*, 240-252

Asner, G.P., Wessman, C.A., Bateson, C.A., & Privette, J.L. (2000). Impact of tissue, canopy, and landscape factors on the hyperspectral reflectance variability of arid ecosystems. *Remote Sensing of Environment, 74*, 69-84

Baldocchi, D.D., & Xu, L. (2007). What limits evaporation from Mediterranean oak woodlands–The supply of moisture in the soil, physiological control by plants or the demand by the atmosphere? *Advances in Water Resources, 30*, 2113-2122

Barry, J.P., Baxter, C.H., Sagarin, R.D., & Gilman, S.E. (1995). Climate-related, long-term faunal changes in a California rocky intertidal community. *Science, 267*, 672

Bateson, C.A., Asner, G.P., & Wessman, C.A. (2000). Endmember bundles: A new approach to incorporating endmember variability into spectral mixture analysis. *IEEE Transactions on Geoscience and Remote Sensing, 38*, 1083-1094

Bernstein, L., Bosch, P., Canziani, O., Chen, Z., Christ, R., Davidson, O., Hare, W., Huq, S., Karoly, D., Kattsov, V., Kundzewicz, Z., Liu, J., Lohmann, U., Manning, M., Matsuno, T., Menne, B., Metz, B., Mirza, M., Nicholls, N., Nurse, L., Pachauri, R., Palutikof, J., Parry, M., Qin, D., Ravindranath, N., Reisinger, A., Ren, J., Riahi, K., Rosenzweig, C., Rusticucci, M., Schneider, S., Sokona, Y., Solomon, S., Stott, P., Stouffer, R., Sugiyama, T., Swart, R., Tirpak, D., Vogel, C., & Yohe, G. (2007). Climate Change 2007: Synthesis Report. In R.K. Pachauri, & A. Reisinger (Eds.), *Contribution of working groups I, II and III to the Fourth Assessment Report of the Intergovernmental Panel on Climate Change* (p. 104). Geneva, Switzerland: IPCC

Bigler, C., Gavin, D.G., Gunning, C., & Veblen, T.T. (2007). Drought induces lagged tree mortality in a subalpine forest in the Rocky Mountains. *Oikos, 116,* 1983-1994

Bilan, M.V., Hogan, C.T., & Carter, H.B. (1977). Stomatal opening, transpiration, and needle moisture in loblolly pine seedlings from two Texas seed sources. *Forest Science, 23*, 457-462

Boisvenue, C., & Running, S.W. (2006). Impacts of climate change on natural forest productivity–evidence since the middle of the 20th century. *Global Change Biology, 12*, 862-882

Bonan, G.B. (2008). Forests and climate change: Forcings, feedbacks, and the climate benefits of forests. *Science, 320,* 1444-1449

Borak, J.S., & Strahler, A.H. (1996). Feature selection using decision trees-an application for the MODIS land cover algorithm. *Geoscience and Remote Sensing Symposium, 1*, 243-245

Bréda, N., Granier, A., & Aussenac, G. (1995). Effects of thinning on soil and tree water relations, transpiration and growth in an oak forest (Quercus petraea (Matt.) Liebl.). *Tree Physiology, 15*, 295-306

Breiman, L. (2001). Random forests. *Machine Learning, 45*, 5-32

Breshears, D., & Barnes, F. (1999). Interrelationships between plant functional types and soil moisture heterogeneity for semiarid landscapes within the grassland/forest continuum: A unified conceptual model. *Landscape Ecology, 14*, 465-478

Breshears, D.D., Cobb, N.S., Rich, P.M., Price, K.P., Allen, C.D., Balice, R.G., Romme, W.H., Kastens, J.H., Floyd, M.L., Belnap, J., Anderson, J.J., Myers, O.B., & Meyer, C.W. (2005). Regional vegetation die-off in response to global-change-type drought. *Proceedings of the National Academy of Sciences of the United States of America, 102*, 15144-15148

Brown, J., Wardlow, B., Tadesse, T., Hayes, M., & Reed, B. (2008). The Vegetation Drought Response Index (VegDRI): A new integrated approach for monitoring drought stress in vegetation. *GIScience & Remote Sensing, 45*, 16-46

Brubaker, L.B. (1986). Responses of tree populations to climatic change. *Vegetation, 67*, 119-130

Burt, T., & Butcher, D. (1985). Topographic controls of soil moisture distributions. *Journal of Soil Science, 36*, 469-486

Chambers, J.Q., Asner, G.P., Morton, D.C., Anderson, L.O., Saatchi, S.S., Espírito-Santo, F.D.B., Palace, M., & Souza Jr, C. (2007). Regional ecosystem structure and function: Ecological insights from remote sensing of tropical forests. *Trends in Ecology & Evolution, 22*, 414-423

CLASlite Team (2013). *CLASlite Forest Monitoring Technology: Version 3.1 User Guide*. Washington, DC.: Carnegie Institution for Science

Coppin, P., Jonckheere, I., Nackaerts, K., Muys, B., & Lambin, E. (2004). Digital change detection methods in ecosystem monitoring: A review. *International Journal of Remote Sensing, 25*, 1565-1596

Cosby, B., Hornberger, G., Clapp, R., & Ginn, T. (1984). A statistical exploration of the relationships of soil moisture characteristics to the physical properties of soils. *Water Resources, 20*, 682-690

Daly, C., Halbleib, M., Smith, J.I., Gibson, W.P., Doggett, M.K., Taylor, G.H., Curtis, J., & Pasteris, P.P. (2008). Physiographically sensitive mapping of climatological temperature and precipitation across the conterminous United States. *International Journal of Climatology, 28*, 2031

Davis, M.B., & Shaw, R.G. (2001). Range shifts and adaptive responses to quaternary climate change. *Science, 292*, 673-679

Dawson, B. (2011). A drought for the centuries: It hasn't been this dry in Texas since 1789. In B. Dawson, J. Simmon, R.L. Loftis, & G. Harman (Eds.), *Texas Climate News*. Houston, Texas: Houston Advanced Research Center

Dollison, R.M. (2010). *The National Map: New viewer, services, and data download: U.S. Geological Survey Fact Sheet 2010–3055, 2p. (Also available at http://pubs.usgs.gov/fs/2010/3055/)*.

Eastman, J., & Fulk, M. (1993). Time series analysis of remotely sensed data using standardized Principal Components Analysis. *Proceedings of 25th International Symposium on Remote Sensing and Global Environmental Change, 1*, 4-8

Elith, J. (2000). Quantitative methods for modeling species habitat: Comparative performance and an application to Australian plants. *Quantitative Methods for Conservation Biology* (pp. 39-58): Springer

Elith, J., & Graham, C.H. (2009). Do they? How do they? WHY do they differ? On finding reasons for differing performances of species distribution models. *Ecography, 32,* 66-77

Elith, J., Graham, C.H., Anderson, R.P., Dudík, M., Ferrier, S., Guisan, A., Hijmans, R.J., Huettmann, F., Leathwick, J.R., Lehmann, A., Li, J., Lohmann, L.G., Loiselle, B.A., Manion, G., Moritz, C., Nakamura, M., Nakazawa, Y., McOverton, J., Peterson, A.T., Phillips, S.J., Richardson, K., Scachetti-Pereira, R., Schapire, R.E., Soberón, J., Williams, S., Wisz, M.S., Zimmermann, N.E., & Araujo, M. (2006). Novel methods improve prediction of species' distributions from occurrence data. *Ecography, 29,* 129-151

Elith, J., Kearney, M., & Phillips, S. (2010). The art of modelling range-shifting species. *Methods in Ecology and Evolution, 1,* 330-342

Elith, J., Phillips, S.J., Hastie, T., Dudík, M., Chee, Y.E., & Yates, C.J. (2011). A statistical explanation of MaxEnt for ecologists. *Diversity and Distributions, 17,* 43-57

Engelbrecht, B.M., Comita, L.S., Condit, R., Kursar, T.A., Tyree, M.T., Turner, B.L., & Hubbell, S.P. (2007). Drought sensitivity shapes species distribution patterns in tropical forests. *Nature, 447,* 80-82

Fensham, R., & Holman, J. (1999). Temporal and spatial patterns in drought-related tree dieback in Australian savanna. *Journal of Applied Ecology, 36,* 1035-1050

Floyd, M.L., Clifford, M., Cobb, N.S., Hanna, D., Delph, R., Ford, P., & Turner, D. (2009). Relationship of stand characteristics to drought-induced mortality in

three Southwestern pinon-juniper woodlands. *Ecological Applications, 19*, 1223-1230

Froend, R., & Drake, P. (2006). Defining phreatophyte response to reduced water availability: Preliminary investigations on the use of xylem cavitation vulnerability in Banksia woodland species. *Australian Journal of Botany, 54*, 173-179

Gould, F.W., Hoffman, G., & Rechenthin, C.A. (1960). Vegetational areas of Texas. *Texas A&M University Texas Agricultural Experiment Station, Leaflet, 492*, 1-4

Gouveia, A.C., & Freitas, H. (2008). Intraspecific competition and water use efficiency in Quercus suber: Evidence of an optimum tree density? *Trees, 22*, 521-530

Grabherr, G., Gottfried, M., & Pauli, H. (2009). Climate effects on mountain plants. *Nature, 369*, 448; 448

Griffith, G.E., Bryce, S.A., Omernik, J.M., Comstock, J.A., Rogers, A.C., Harrison, B., Hatch, S.L., & Bezanson, D. (2004). Ecoregions of Texas (color poster with map, descriptive text, and photographs). *US Geological Survey, Reston, Virginia, USA*

Guisan, A., Zimmermann, N.E., Elith, J., Graham, C.H., Phillips, S., & Peterson, A.T. (2007). What matters for predicting the occurences of trees: Techniques, data, or species' characteristics? *Ecological Monographs, 77*, 615-630

Hansen, M.C., Potapov, P.V., Moore, R., Hancher, M., Turubanova, S.A., Tyukavina, A., Thau, D., Stehman, S.V., Goetz, S.J., Loveland, T.R., Kommareddy, A., Egorov, A., Chini, L., Justice, C.O., & Townshend, J.R.G. (2013). High-

resolution global maps of 21st-century forest cover change. *Science, 342*, 850-853

Hargrove Jr, W.W., Spruce, J., Gasser, G., & Hoffman, F.M. (2009). Toward a national early warning system for forest disturbances using remotely sensed canopy phenology. *Photogrammetric Engineering & Remote Sensing, 75*, 1150-1156

Hersteinsson, P., & Macdonald, D.W. (1992). Interspecific competition and the geographical distribution of red and arctic foxes Vulpes vulpes and Alopex lagopus. *Oikos*, 505-515

Hijmans, R.J. (2004). *Arc Macro Language (AML®) version 2.1 for calculating 19 bioclimatic predictors*. Berkeley, CA: Museum of Vertebrate Zoology, University of California at Berkeley

Hijmans, R.J., Cameron, S.E., Parra, J.L., Jones, P.G., & Jarvis, A. (2005). Very high resolution interpolated climate surfaces for global land areas. *International Journal of Climatology, 25*, 1965-1978

Hijmans, R.J., & Graham, C.H. (2006). The ability of climate envelope models to predict the effect of climate change on species distributions. *Global change biology, 12*, 2272-2281

Hoerling, M., Kumar, A., Dole, R., Nielsen-Gammon, J.W., Eischeid, J., Perlwitz, J., Quan, X.-W., Zhang, T., Pegion, P., & Chen, M. (2013). Anatomy of an extreme event. *Journal of Climate, 26*, 2811-2832

Houle, G., & Filion, L. (1993). Interannual variations in the seed production of Pinus banksiana at the limit of the species distribution in northern Quebec, Canada. *American Journal of Botany*, 1242-1250

Huang, C., & Anderegg, W.R.L. (2012). Large drought-induced aboveground live biomass losses in southern Rocky Mountain aspen forests. *Global Change Biology, 18*, 1016-1027

Huang, C., Asner, G.P., Barger, N.N., Neff, J.C., & Floyd, M.L. (2010). Regional aboveground live carbon losses due to drought-induced tree dieback in piñon–juniper ecosystems. *Remote Sensing of Environment, 114*, 1471-1479

Huete, A., Didan, K., Miura, T., Rodriguez, E.P., Gao, X., & Ferreira, L.G. (2002). Overview of the radiometric and biophysical performance of the MODIS vegetation indices. *Remote Sensing of Environment, 83*, 195-213

Hughes, L. (2000). Biological consequences of global warming: Is the signal already apparent? *Trends in Ecology & Evolution, 15*, 56-61

Huntley, B. (1999). Species distribution and environmental change: Considerations from the site to the landscape scale. In E. Maltby, M. Holdgate, M. Acreman, & A. Weir (Eds.), *Ecosystem Management: Questions for Science and Society* (pp. 115-130). University of London, Egham: Royal Holloway Institute for Environmental Research

Huston, M.A. (2002). Introductory essay: Critical issues for improving predictions. In J.M. Scott, P.J. Heglund, M.L. Morrison, J.B. Haufler, M.G. Raphael, W.A.

Wall, & F.B. Samson (Eds.), *Predicting Species Occurrences: Issues of Accuracy and Scale* (pp. 7-21). Washington: Island Press

Jackson, R., Canadell, J., Ehleringer, J., Mooney, H., Sala, O., & Schulze, E. (1996). A global analysis of root distributions for terrestrial biomes. *Oecologia, 108,* 389-411

Kasischke, E.S., & French, N.H. (1995). Locating and estimating the areal extent of wildfires in Alaskan boreal forests using multiple-season AVHRR NDVI composite data. *Remote Sensing of Environment, 51*, 263-275

Kearney, M.R., Wintle, B.A., & Porter, W.P. (2010). Correlative and mechanistic models of species distribution provide congruent forecasts under climate change. *Conservation Letters, 3,* 203-213

Kremenetski, C.V., Sulerzhitsky, L.D., & Hantemirov, R. (1998). Holocene history of the northern range limits of some trees and shrubs in Russia. *Arctic and Alpine Research*, 317-333

Lambin, E.F., & Strahlers, A.H. (1994). Change-vector analysis in multitemporal space: A tool to detect and categorize land-cover change processes using high temporal-resolution satellite data. *Remote Sensing of Environment, 48,* 231-244

Le Houérou, H.N. (1996). Climate change, drought and desertification. *Journal of Arid Environments, 34,* 133-185

Lei, Y., Yin, C., & Li, C. (2006). Differences in some morphological, physiological, and biochemical responses to drought stress in two contrasting populations of Populus przewalskii. *Physiologia Plantarum, 127,* 182-191

Lloret, F., Siscart, D., & Dalmases, C. (2004). Canopy recovery after drought dieback in holm-oak Mediterranean forests of Catalonia (NE Spain). *Global Change Biology, 10*, 2092-2099

Loehle, C. (2000). Forest ecotone response to climate change: Sensitivity to temperature response functional forms. *Canadian Journal of Forest Research, 30*, 1632-1645

Lohr, S. (1999). *Sampling: Design and Analysis* New York: Duxbury Press

Ludwig, J., Ludwig, D., & Tongway (1995). Spatial organisation of landscapes and its function in semi-arid woodlands, Australia. *Landscape Ecology, 10*, 51-63

Luo, Y., & Chen, H.Y. (2013). Observations from old forests underestimate climate change effects on tree mortality. *Nature Communications, 4*, 1655

Lutz, D.A., Washington-Allen, R.A., & Shugart, H.H. (2008). Remote sensing of boreal forest biophysical and inventory parameters: A review. *Canadian Journal of Remote Sensing, 34*, S286-S313

Lytle, D., Lytle, N.L., & Poff (2004). Adaptation to natural flow regimes. *Trends in Ecology & Evolution, 19*, 94-100

MacDonald, G.M., Edwards, T.W., Moser, K.A., Pienitz, R., & Smol, J.P. (1993). Rapid response of treeline vegetation and lakes to past climate warming. *Nature, 361*, 243-246

Macomber, S.A., & Woodcock, C.E. (1994). Mapping and monitoring conifer mortality using remote sensing in the Lake Tahoe Basin. *Remote Sensing of Environment, 50*, 255-266

Mafakheri, A., Siosemardeh, A., Bahramnejad, B., Struik, P., & Sohrabi, Y. (2010). Effect of drought stress on yield, proline and chlorophyll contents in three chickpea cultivars. *Australian Journal of Crop Science, 4*, 580-585

Malingreau, J., Tucker, C., & Laporte, N. (1989). AVHRR for monitoring global tropical deforestation. *International Journal of Remote Sensing, 10*, 855-867

McCarty, J.P. (2001). Ecological consequences of recent climate change. *Conservation Biology, 15*, 320-331

McDowell, N., Allen, C.D., & Marshall, L. (2010). Growth, carbon-isotope discrimination, and drought-associated mortality across a Pinus ponderosa elevational transect. *Global Change Biology, 16*, 399-415

McDowell, N., Pockman, W.T., Allen, C.D., Breshears, D.D., Cobb, N., Kolb, T., Plaut, J., Sperry, J., West, A., & Williams, D.G. (2008). Mechanisms of plant survival and mortality during drought: Why do some plants survive while others succumb to drought? *New Phytologist, 178*, 719-739

McDowell, N.G., Coops, N.C., Beck, P.S., Chambers, J.Q., Gangodagamage, C., Hicke, J.A., Huang, C.-y., Kennedy, R., Krofcheck, D.J., & Litvak, M. (2014). Global satellite monitoring of climate-induced vegetation disturbances. *Trends in Plant Science*

McKinley, D.C., Ryan, M.G., Birdsey, R.A., Giardina, C.P., Harmon, M.E., Heath, L.S., Houghton, R.A., Jackson, R.B., Morrison, J.F., & Murray, B.C. (2011). A synthesis of current knowledge on forests and carbon storage in the United States. *Ecological Applications, 21*, 1902-1924

Miao, S., Zou, C.B., & Breshears, D.D. (2009). Vegetation responses to extreme hydrological events: Sequence matters. *The American Naturalist, 173*, 113-118

Mildrexler, D.J., Zhao, M., Heinsch, F.A., & Running, S.W. (2007). A new satellite-based methodology for continental-scale disturbance detection. *Ecological Applications, 17*, 235-250

Miller, C., & Urban, D.L. (1999). A model of surface fire, climate and forest pattern in the Sierra Nevada, California. *Ecological Modelling, 114*, 113-135

Moody, A., & Johnson, D.M. (2001). Land-surface phenologies from AVHRR using the discrete Fourier transform. *Remote Sensing of Environment, 75*, 305-323

Moore, G.W., Edgar, C.B., Vogel, J., Washington-Allen, R.A., March, R.G., & Zehnder, R. (2016). Tree mortality from an exceptional drought spanning mesic to semiarid ecoregions. *Ecological Applications, 26*, 602-611

Mueller, R.C., Scudder, C.M., Porter, M.E., Talbot Trotter, R., Gehring, C.A., & Whitham, T.G. (2005). Differential tree mortality in response to severe drought: Evidence for long-term vegetation shifts. *Journal of Ecology, 93*, 1085-1093

Nambiar, E.S., & Sands, R. (1993). Competition for water and nutrients in forests. *Canadian Journal of Forest Research, 23*, 1955-1968

Nemani, R., White, M., Thornton, P., Nishida, K., Reddy, S., Jenkins, J., & Running, S. (2002). Recent trends in hydrologic balance have enhanced the terrestrial carbon sink in the United States. *Geophysical Research Letters, 29*, 106-101-106-104

Nepstad, D.C., Tohver, I.M., Ray, D., Moutinho, P., & Cardinot, G. (2007). Mortality of large trees and lianas following experimental drought in an Amazon forest. *Ecology, 88*, 2259-2269

Nix, H.A. (1986). A biogeographic analysis of Australian elapid snakes. In R. Longmore (Ed.), *Snakes: Atlas of elapid snakes of Australia* (pp. 4-15). Canberra: Australian Government Publishing Service

NOAA National Centers for Environmental Information (2011). *State of the Climate: Drought for August 2011*. Published online September 2011, retrieved on February 3, 2012 from http://www.ncdc.noaa.gov/sotc/drought/201108

O'Donnell, M.S., & Ignizio, D.A. (2012). Bioclimatic predictors for supporting ecological applications in the conterminous United States. *US Geological Survey Data Series, 691*, 10 p.

Oliveira, P.J., Asner, G.P., Knapp, D.E., Almeyda, A., Galván-Gildemeister, R., Keene, S., Raybin, R.F., & Smith, R.C. (2007). Land-use allocation protects the Peruvian Amazon. *Science, 317*, 1233-1236

Oliver, T., Hill, J.K., Thomas, C.D., Brereton, T., & Roy, D.B. (2009). Changes in habitat specificity of species at their climatic range boundaries. *Ecology Letters, 12*, 1091-1102

Overpeck, J., & Udall, B. (2010). Dry times ahead. *Science, 328*, 1642-1643

Palmer, W.C. (1965). *Meteorological Drought*. Washington, D.C.: U.S. Department of Commerce

Parmesan, C. (1996). Climate and species' range. *Nature, 382*, 765; 766

Parmesan, C., Root, T.L., & Willig, M.R. (2000). Impacts of extreme weather and climate on terrestrial biota. *Bulletin of the American Meteorological Society, 81*, 443-450

Parmesan, C., Ryrholm, N., Stefanescu, C., Hill, J.K., Thomas, C.D., Descimon, H., Huntley, B., Kaila, L., Kullberg, J., Tammaru, T., Tennent, W.J., Thomas, J.A., & Warren, M. (1999). Poleward shifts in geographical ranges of butterfly species associated with regional warming. *Nature, 399*, 579-583

Parmesan, C., & Yohe, G. (2003). A globally coherent fingerprint of climate change impacts across natural systems. *Nature, 421*, 37-42

Pedersen, B.S. (1998). Modeling tree mortality in response to short-and long-term environmental stresses. *Ecological Modelling, 105*, 347-351

Pedersen, B.S. (1999). The mortality of midwestern overstory oaks as a bioindicator of environmental stress. *Ecological Applications, 9*, 1017-1027

Peñuelas, J., Prieto, P., Beier, C., Cesaraccio, C., De Angelis, P., de Dato, G., Emmett, B.A., Estiarte, M., Garadnai, J., & Gorissen, A. (2007). Response of plant species richness and primary productivity in shrublands along a north–south gradient in Europe to seven years of experimental warming and drought: Reductions in primary productivity in the heat and drought year of 2003. *Global Change Biology, 13*, 2563-2581

Phillips, S.J., Anderson, R.P., & Schapire, R.E. (2006). Maximum entropy modeling of species geographic distributions. *Ecological Modelling, 190*, 231-259

Phillips, S.J., & Dudík, M. (2008). Modeling of species distributions with Maxent: New extensions and a comprehensive evaluation. *Ecography, 31*, 161-175

Pinzon, J.E., & Tucker, C.J. (2014). A Non-Stationary 1981-2012 AVHRR NDVI (sub 3g) Time Series. *Remote Sensing, 6*, 6929-6960

Pounds, J.A., Fogden, M.P., & Campbell, J.H. (1999). Biological response to climate change on a tropical mountain. *Nature, 398*, 611-615

Reichmann, L.G., & Sala, O.E. (2014). Differential sensitivities of grassland structural components to changes in precipitation mediate productivity response in a desert ecosystem. *Functional Ecology, 28*, 1292-1298

Reside, A.E., VanDerWal, J.J., Kutt, A.S., & Perkins, G.C. (2010). Weather, not climate, defines distributions of vagile bird species. *Plos One, 5*, e13569

Rodríguez-Iturbe, I., & Porporato, A. (2004). *Ecohydrology of Water-controlled Ecosystems: Soil Moisture and Plant Dynamics*. New York: Cambridge University Press

Rouse Jr, J.W., Haas, R., Schell, J., & Deering, D. (1974). Monitoring vegetation systems in the Great Plains with ERTS. *NASA Special Publication, 351*, 309

Royer, P.D., Cobb, N.S., Clifford, M.J., Huang, C.Y., Breshears, D.D., Adams, H.D., & Villegas, J.C. (2011). Extreme climatic event-triggered overstorey vegetation loss increases understorey solar input regionally: Primary and secondary ecological implications. *Journal of Ecology, 99*, 714-723

Running, S.W., Nemani, R.R., Heinsch, F.A., Zhao, M., Reeves, M., & Hashimoto, H. (2004). A continuous satellite-derived measure of global terrestrial primary production. *Bioscience, 54*, 547-560

Running, S.W., & Zhao, M. (2015). *User's Guide: Daily GPP and Annual NPP (MOD17A2/A3) Products NASA Earth Observing System MODIS Land Algorithm*. MODIS Land Team, U.S. National Aeronautics and Space Administration

Sagarin, R.D., Barry, J.P., Gilman, S.E., & Baxter, C.H. (1999). Climate-related change in an intertidal community over short and long time scales. *Ecological Monographs, 69*, 465-490

Scaramuzza, P., Micijevic, E., & Chander, G. (2004). SLC gap-filled products phase one methodology. *Landsat Technical Notes*: U.S. Geological Survey

Schwarz, A. (1997). Regeneration of planted conifers across climatic moisture gradients on the Canadian prairies: Implications for distribution and climate change. *Journal of Biogeography, 24*, 527-534

Seyfried, M., Schwinning, S., Walvoord, M., Pockman, W., Newman, B., Jackson, R., & Phillips, F. (2005). Ecohydrological control of deep drainage in arid and semiarid regions. *Ecology, 86*, 277-287

Smeins, F.E. (2004). Echoes of the Chisholm Trail: Texas: A Biological Crossroads. *Rangelands, 26*, 15-21

Soil Survey Staff, Natural Resources Conservation Service, General Soil Map (STATSGO2). *Web Soil Survey*. Available online, retrieved on February 15, 2012 from http://websoilsurvey.nrcs.usda.gov/

Sörensen, R., Zinko, U., & Seibert, J. (2006). On the calculation of the topographic wetness index: Evaluation of different methods based on field observations. *Hydrology and Earth System Sciences Discussions, 10*, 101-112

Stankowski, P.A., & Parker, W.H. (2010). Species distribution modelling: Does one size fit all? A phytogeographic analysis of Salix in Ontario. *Ecological Modelling, 221*, 1655-1664

Stehman, S.V. (1997). Selecting and interpreting measures of thematic classification accuracy. *Remote Sensing of Environment, 62*, 77-89

Sterl, A., Severijns, C., Dijkstra, H., Hazeleger, W., Jan van Oldenborgh, G., van den Broeke, M., Burgers, G., van den Hurk, B., Jan van Leeuwen, P., & van Velthoven, P. (2008). When can we expect extremely high surface temperatures? *Geophysical Research Letters, 35*

Svenning, J.C., & Skov, F. (2005). The relative roles of environment and history as controls of tree species composition and richness in Europe. *Journal of Biogeography, 32*, 1019-1033

Swetnam, T.W., & Betancourt, J.L. (2010). Mesoscale disturbance and ecological response to decadal climatic variability in the American Southwest. In M. Beniston (Ed.), *Tree Rings and Natural Hazards* (pp. 329-359). New York: Springer Science+Business Media

Tansey, K., Gregoire, J.-M., Binaghi, E., Boschetti, L., Brivio, P.A., Ershov, D., Flasse, S., Fraser, R., Graetz, D., & Maggi, M. (2004). A global inventory of burned areas at 1 km resolution for the year 2000 derived from SPOT VEGETATION data. *Climatic Change, 67*, 345-377

Thomas, C.D., & Lennon, J.J. (1999). Birds extend their ranges northwards. *Nature, 399*, 213-213

Thompson, S.E., Harman, C.J., Troch, P.A., Brooks, P.D., & Sivapalan, M. (2011). Spatial scale dependence of ecohydrologically mediated water balance partitioning: A synthesis framework for catchment ecohydrology. *Water Resources Research, 47*, W00J03

Thuiller, W., Albert, C., Araújo, M.B., Berry, P.M., Cabeza, M., Guisan, A., Hickler, T., Midgley, G.F., Paterson, J., & Schurr, F.M. (2008). Predicting global change impacts on plant species' distributions: Future challenges. *Perspectives in Plant Ecology, Evolution and Systematics, 9*, 137-152

Twidwell, D., Wonkka, C.L., Taylor, C.A., Zou, C.B., Twidwell, J.J., & Rogers, W.E. (2013). Drought-induced woody plant mortality in an encroached semi-arid savanna depends on topoedaphic factors and land management. *Applied Vegetation Science, 17*, 42–52

Van Buijtenen, J. (1966). Testing loblolly pines (Pinus taeda) for drought resistance. *Technical Report 13*: Texas Forest Service

Van Buijtenen, J., Bilan, M.V., & Zimmerman, R.H. (1976). Morpho physiological characteristics, related to drought resistance in Pinus taeda. In M.G.R. Cannell, &

F.T. Last (Eds.), *Tree Physiology and Yield Improvement* (pp. 349-359). New York: Academic Press

Van der Putten, W.H., Macel, M., & Visser, M.E. (2010). Predicting species distribution and abundance responses to climate change: Why it is essential to include biotic interactions across trophic levels. *Philosophical Transactions of the Royal Society of London B: Biological Sciences, 365*, 2025-2034

van Mantgem, P.J., Stephenson, N.L., Byrne, J.C., Daniels, L.D., Franklin, J.F., Fule, P.Z., Harmon, M.E., Larson, A.J., Smith, J.M., Taylor, A.H., & Veblen, T.T. (2009). Widespread Increase of tree mortality rates in the western United States. *Science, 323*, 521-524

Vose, J.C., J.S.; Luce, Charlie; Patel-Weynand, Toral (2016). Effects of drought on forests and rangelands in the United States: A comprehensive science synthesis. In J.C. Vose, J.S.; Luce, Charlie; Patel-Weynand, Toral (Ed.), *General Technical Report* (p. 302). Washington, DC: U.S. Department of Agriculture, Forest Service, Washington Office

Walther, G.-R., Post, E., Convey, P., Menzel, A., Parmesan, C., Beebee, T.J., Fromentin, J.-M., Hoegh-Guldberg, O., & Bairlein, F. (2002). Ecological responses to recent climate change. *Nature, 416*, 389-395

Washington-Allen, R.A., West, N.E., Ramsey, R.D., & Efroymson, R.A. (2006). A protocol for retrospective remote sensing-based ecological monitoring of rangelands. *Rangeland Ecology & Management, 59*, 19-29

Watling, J.I., Romañach, S.S., Bucklin, D.N., Speroterra, C., Brandt, L.A., Pearlstine, L.G., & Mazzotti, F.J. (2012). Do bioclimate variables improve performance of climate envelope models? *Ecological Modelling, 246*, 79-85

Williams, J., Prebble, R., Williams, W., & Hignett, C. (1983). The influence of texture, structure and clay mineralogy on the soil moisture characteristic. *Soil Research, 21*, 15-32

Wilson, B.T., Lister, A.J., & Riemann, R.I. (2012). A nearest-neighbor imputation approach to mapping tree species over large areas using forest inventory plots and moderate resolution raster data. *Forest Ecology and Management, 271*, 182-198

Woodward, F.I. (1987). *Climate and Plant Distribution*. New York: Cambridge University Press

Worrall, J.J., Egeland, L., Eager, T., Mask, R.A., Johnson, E.W., Kemp, P.A., & Shepperd, W.D. (2008). Rapid mortality of Populus tremuloides in southwestern Colorado, USA. *Forest Ecology and Management, 255*, 686-696

Wu, X.B., Smeins, F.E., & Slack, R.D. (2002). *Fundamentals of Ecology Laboratory Manual, Third Edition*. Dubuque, Iowa: Kendall/Hunt Publishing Company

Young, S., & Wang, C. (2001). Land-cover change analysis of China using global-scale Pathfinder AVHRR Landcover (PAL) data, 1982-92. *International Journal of Remote Sensing, 22*, 1457-1477

Zhan, X., Defries, R., Townshend, J., Dimiceli, C., Hansen, M., Huang, C., & Sohlberg, R. (2000). The 250 m global land cover change product from the Moderate

Resolution Imaging Spectroradiometer of NASA's Earth Observing System. *International Journal of Remote Sensing, 21*, 1433-1460

Zhan, X., Sohlberg, R., Townshend, J., DiMiceli, C., Carroll, M., Eastman, J., Hansen, M., & DeFries, R. (2002). Detection of land cover changes using MODIS 250 m data. *Remote Sensing of Environment, 83*, 336-350

Zhao, M., & Running, S.W. (2010). Drought-induced reduction in global terrestrial net primary production from 2000 through 2009. *Science, 329*, 940-943

Zimmermann, N.E., Yoccoz, N.G., Edwards, T.C., Meier, E.S., Thuiller, W., Guisan, A., Schmatz, D.R., & Pearman, P.B. (2009). Climatic extremes improve predictions of spatial patterns of tree species. *Proceedings of the National Academy of Sciences, 106*, 19723-19728